KINETICS AND STRUCTURAL CHARACTERIZATION OF LIPOLYTIC ENZYMES FOR HYDROLYZING POULTRY FEATHERS

A Dissertation

Presented to the Faculty of the Graduate School

of Cornell University

In Partial Fulfillment of the Requirements for the Degree of

Doctor of Philosophy

by

Matthew Barcus

August 2017

KINETICS AND STRUCTURAL CHARACTERIZATION OF LIPOLYTIC ENZYMES FOR HYDROLYZING POULTRY FEATHERS

Matthew Barcus, Ph. D.

Cornell University 2017

The processing of chicken feathers poses a challenge for the poultry industry. In the USA, near 9 billion chickens are slaughtered annually, which generates 5 million tons of recalcitrant feathers to manage. Enzymatic processing of feathers has promise to increase economic potential of the feathers, however, the abundant presence of lipids on feathers serve as a likely barrier. The genomes of a feather-degrading actinomycete and related microorganisms were mined for lipolytic genes candidates, which resulted in the identification of 16 active enzymes. SFK3309 from *Streptomyces fradiae* var. k11 was the top performing enzyme when tested against the synthetic lipase substrate p-nitrophenyl palmitate (pNPP). SFK3309 also displayed activity against feather lipids. Wax esters are the most abundant lipid class in feather lipids and a colorimetric assay was modified to perform kinetics experiments of SFK3309 against cetyl-palmitate. The K_m and K_{cat} were calculated to be 850 μM and 11.63 s^{-1}, respectively. Structural studies were undertaken for SFK3309, though diffracting protein crystals were unable to be produced. Thermal-shift assays suggest the presence of a hydrophobic patch on the protein surface that may interfere with protein being monodispersed in solution. Yet, some additives hold promise at

stabilizing the enzyme in solution. A different lipase from *S. fradiae* var. k11, SFK3087, which lacked wax ester hydrolase activity, was explored using protein engineering to improve industrial characteristics of the enzyme and initiate work in expanding the substrate specificity and performance towards wax esters. The mutation Y83A increased the thermostability of SFK3087 by 3.76℃, but enzyme activity against pNPP dropped sharply. Saturation mutagenesis was performed on the serine at residue 119 and only large, aromatic residues maintained the same stability seen in wild type. The S119F mutation had a slight increase of thermostability (0.31℃), and an overall improvement in enzyme performance against pNPP, as represented by a K_{cat}/K_m increase of 47%. A more drastic protein engineering scheme may be necessary to incorporate wax ester specificity in an enzyme. However, our work establishes feather-degrading microorganisms produce lipolytic enzymes capable of hydrolyzing wax esters and lays the foundation for further investigation on economic impact lipids have in feather processing.

BIOGRAPHICAL SKETCH

Matthew Barcus attended high school at Mountain View High School, in Mesa, AZ. Upon graduating, Matthew began taking undergraduate coursework at Brigham Young University – Idaho for one semester. Matthew then served a church service mission in Sydney, Australia for two years. Upon returning from Australia, Matthew continued his undergraduate studies at Arizona State University majoring in chemical engineering. After one semester Matthew changed his major to molecular biosciences and biotechnology. In early 2011 Matthew began working in Dr. Tsafrir Mor's Lab as an undergraduate researcher. In September of that same year Matthew married Qin Chen. Matthew graduated from ASU in 2012 and interned at Matrix Nutrition over the summer before beginning graduate school at Cornell University under the mentorship of Dr. Xin Gen Lei. Matthew and Qin's first daughter, Miya, was born on November 28, 2012. On March 13, 2016, Matthew and Qin welcomed the birth of their second daughter, Kaiya. In the summer of 2016 Matthew participated in a summer research program in the Lab of Dr. Shinya Fushinobu in Tokyo, Japan.

I dedicate this dissertation to Qin, Miya, and Kaiya.

ACKNOWLEDGMENTS

My peregrination through graduate school has benefitted from the interaction with many great people who have played important roles in my development and successes. As an undergraduate student at Arizona State University, I am grateful for Dr. Tsafrir Mor who invited me to work in his lab. It was then that I was able to experience firsthand the joys of academic research. I had the honor of working with Dr. Kathy Larrimore, who was a graduate student at the time. Her professionalism and love for research was a powerful example to me. And from my work with Kathy and conversations with Dr. Mor, I became inspired to pursue a Ph.D., something I never would have thought about achieving before. The belief Dr. Mor had in me helped me believe in myself and lead to me applying for graduate school.

At Cornell, I am forever grateful to Dr. Xin Gen Lei, who accepted me into his lab and surrounded me with many great people to work with. Krystal Lum was a tremendous help as I adjusted into the lab and quickly got my research project started. Day in and day out Carol Roneker kept the operations of the lab running and more importantly, she brought the family feel to the lab. Dr. Yi Xuan Zhu provided her expertise in *E. coli* expression and insight on improving protein yields. Ze Ping Zhao was a major help in setting up some of my experiments and also shared in the hardships of being faced as graduate students. I also really appreciate my time with Dr. Jay (JonGun) Kim, where we spent many long hours working on the HPLC together. He provided me with invaluable training on fixing different instruments and insight on how to be resourceful. Most importantly, Jay was a role model for his work

ethic and commitment to scientific integrity. In the lab, I also had the opportunity to work closely with Tess Allan and participate in the development of her research project. I was also able to be a part of Kaitlyn Yong's research training and enjoyed her excitement about research. And most of all, in the Lei lab I was able to be mentored by Dr. Xin Gen Lei, who was patient in my training and development as a scientist. Dr. Lei was able to help me refocus my sometimes-crazy ideas and challenged me to be explorative in completing my research tasks. He was always a forward thinker and provided much needed acuity at times. He also was so kind to my daughters when they would visit the lab.

My graduate committee has also played an intricate role in my graduate school experience. Dr. Jean Hunter, Dr. Matthew DeLisa, and Dr. Kimberly O'Brien all contributed to selecting meaningful coursework, designing experiments, writing grant applications, and providing resources for me to complete my work. Their guidance and advice was always worth its weight in gold.

The Cornell community has been extremely supportive of my research project and has lead me to work with many great people. I met Dr. Dario Mizrachi while trying to purify one of my proteins and in addition to getting purified protein, I was provided with great mentorship. Discussions with Dario on experiment design, data analysis, and career planning played heavily in my maturation as an independent scientist. Dr. Irina Kriksunov provided me with many resources from MacCHESS and trained me to confidently operate different beamlines independently at the Cornell High Energy Synchrotron Source in only a short period of time. Dr. Qing Qiu Huang, also from MacCHESS, was helpful in purifying my proteins for crystallography

experiments. Then, Dr. Chris Fromme, and his student Steve Halaby, contributed their time and reagents for conducting a few experiments in their lab. In designing an assay for the hydrolysis of wax esters, Dr. Jeremy Baskin was a major help, as was Dr. Robert Moreau from the USDA. I also received valuable insight from Dr. Ailong Ke in designing suitable protein variants and from Dr. John Brady in analyzing protein structures.

Much of my research would not have been possible without the financial support from multiple groups. The department of animal science at Cornell provided me with a teaching assistant position for much of my time in graduate school. The Northeast Sustainable Agriculture Research and Education (NE SARE) provided early support through their graduate student grant to support initial efforts on screening for active lipolytic enzymes. Through the National Science Foundation's East Asia and pacific Summer Institutes (EAPSI) program jointly funded by the Japan Society for the Promotion of Science, I was given an opportunity to engage in structural biology studies. During a summer, I worked in Dr. Shinya Fushinobu's lab at the University of Tokyo studying protein crystallography. Dr. Fushinobu and Dr. Takatoshi Arakawa were very helpful in my first exposure with crystallography experiments and my enjoyable experience has left me with a determination to engage further in structural biology research.

Most importantly, I must acknowledge my wife, Qin, for all her support during my Ph.D. studies. She has been with me through the highs and lows that research life brings, providing encouragement and motivation when needed and sharing in the excitement when warranted. Our two lovely daughters were born while I have been in

graduate school and Qin has undertaken much of the parental responsibilities by herself so that I could complete my work. Much of her daily sacrifices go unnoticed, and I am forever appreciative for her selflessness, patience, and support so that I can accomplish my dreams. May I return the favor and together, we can share in the successes of each other.

TABLE OF CONTENTS

LIST OF FIGURES

LIST OF TABLES

LIST OF ABBREVIATIONS

A	Alanine or Adenine
ApE	A Plasmid Editor
AT	Studier's Autoinduction Media
ATCC	American Type Culture Collection
BLAST	Basic Local Alignment Search Tool
C	Cysteine or Cytosine
$CaCl_2$	Calcium Chloride
CoA	Coenzyme A
D	Aspartate
DNA	Deoxyribonucleic Acid
EC	Enzyme Commission
F	Phenylalanine
G	Glycine or Guanine
H	Histidine
HEPES	4-(2-hydroxyethyl)-1-piperazineethanesulfonic Acid
IPTG	Isopropyl ß-D-1-thiogalactopyranoside
K	Lysine
L	Leucine
LB	Luria Broth
LED	Lipase Engineering Database

N	Asparagine
NaCl	Sodium Chloride
Ni-NTA	Nickel-Nitrilotriacetic Acid
P	Proline
pNPA	p-Nitrophenyl Acetate
pNPP	p-Nitrophenyl Palmitate
R	Arginine
RAST	Rapid Annotation using Subsystem Technology
S	Serine
SAXS	Small angle X-ray scattering
SDS-PAGE	Sodium Dodecyl Sulfate Polyacrylamide Gel Electrophoresis
T	Thymine or Threonine
TB	Terrific Broth
TLC	Thin Layer Chromatography
V	Valine
wt	Wild-type
Y	Tyrosine

CHAPTER ONE

INTRODUCTION

1.1 Poultry industry in the USA

Americans consume a considerable amount of chicken and produce more chicken than any other meat by a wide margin, as seen in Figure 1.1 [1]. High chicken consumption is largely due to a highly efficient production process. The US poultry industry has benefited from intense breeding programs, where layer breeds were selected for egg production and broiler chickens were selected for growth and meat production.

Commercial broiler chickens have an average feed conversion ratio (FCR) or feed-to-gain ratio of 1.89 [2]. For perspective, beef cows in the US can have an FCR between 4.5 and 7.5 [3]. In 2014, commercial broiler chickens would reach an average market weight of 6.12 pounds after only 47 days [2]. Moreover, the number of broiler chickens produced in the US continues to climb. In 2016 just shy of 9 billion broiler chickens were slaughtered (Table 1.1) [4]. Total US broiler industry production for 2015 was valued at $48.7 billion [5].

Table 1.1 – US annual slaughter of poultry by species.

Commodity	**2012**	**2013**	**2014**	**2015**	**2016**
Chickens	8,576,195	8,648,756	8,666,662	8,822,692	8,909,014
Turkeys	250,192	239,386	236,617	232,389	243,255
Ducks	24,183	24,575	26,368	27,749	27,268

*Data sourced from the USDA (2017).

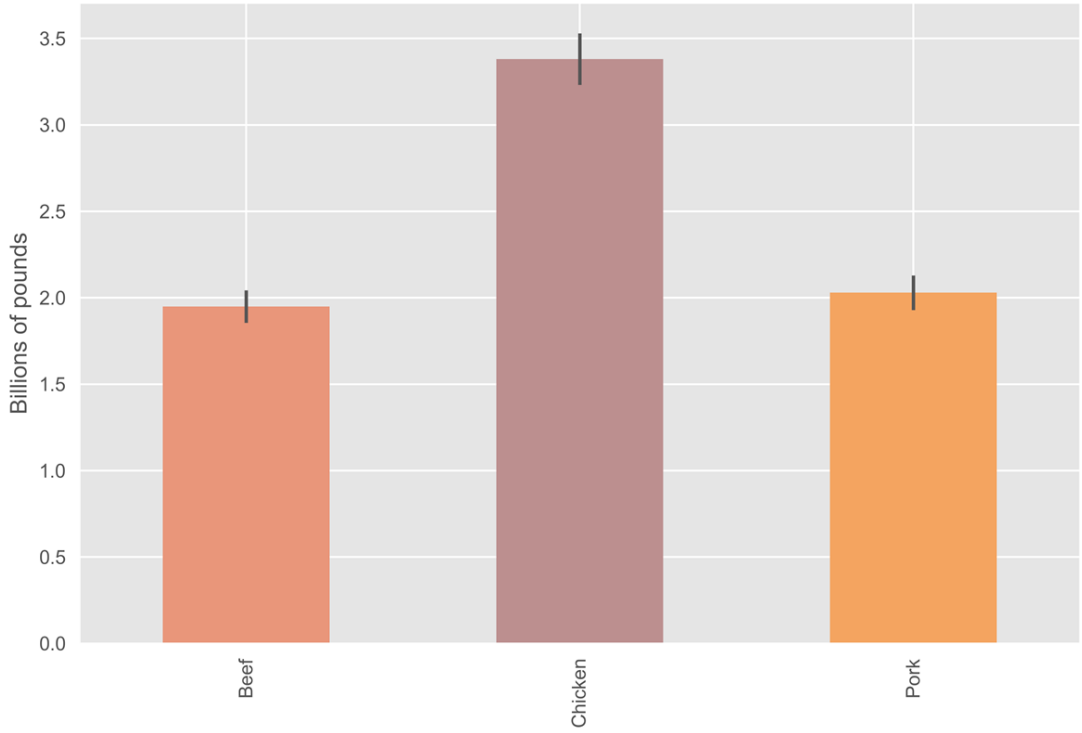

Figure 1.1 – USA average monthly meat production. Values are from 2015 and were collected from the United States Department of Agriculture - Agriculture Research Service (2016). Numbers correspond to average monthly production of federally inspected beef, pork, and chicken. Error bars represent the standard deviation from the 12-month sample space.

1.2 The Feather Problem

About 5-7% of a chicken's body weight is attributed to feathers, equating to 2 billion kg of feathers that amass annually in the USA [6-8]. Feathers offer unique properties for commercialization and are a major co-product of the poultry industry. Feathers are high in protein (~90%) and as a result are an attractive candidate as a protein source in animal feeds [9]. The high nitrogen of the feathers also makes for a good organic fertilizer in plant cultivation [10]. In 2012, 608 million kg of feather meal was used in feeds and fertilizers [11].

Yet, the full economic potential of the feathers is not realized from current feather meal processing practices. The majority of the feather protein is keratin, which arrange into antiparallel pleated β-sheets with interlocking disulfide bonds and hydrophobic interactions [12, 13]. The rigid structure of the keratin attributes to the recalcitrant nature of the chicken feathers and limits the protein bioavailability [14]. Current rendering practices are reliant on economically and environmentally taxing processes. High pressure and steam are required to break down the keratin into a usable product [15]. However, the resulting product is often of low quality [16] and leads to the destruction of some amino acids [17, 18].

1.3 Biotechnology Approach to Feather Rendering

The use of biotechnology to render chicken feathers with biocatalysts is a viable alternative to current feather rendering methodologies to reduce processing energy and

create a better product. Like many biotechnological applications, the origins for enzymatic feather hydrolysis emerged from the identification of keratinolytic microbes isolated from feather waste sites [19]. Enzymes that can break down keratin, the main protein in feathers, are known as keratinases. A basic foundation of our understanding of keratinases has been developed over the past 25 years [20].

Biotechnological solutions to this industrial process have been limited to the commercialization of only one enzyme to aid in feather rendering. BioResource International's Valkerase is able to reduce feather autoclave temperature by up to 15°C, but requires an additional 45-minute incubation at 50°-60°C [15, 21].
Many groups are beginning to recognize the limitations of using only keratinase to degrade chicken feathers. Reductants, such as sulfite or reducing enzymes (reductase), have been found in microbial feather hydrolysate and are thought to aid in disulfide bond reduction, thus providing keratinase with added accessibility to keratin's peptide backbone [22-24]. Our group suspects feather surface lipids as another barrier for keratinase substrate accessibility.

1.4 Uropygial Gland and Feather Lipid Function

Chickens, like most other birds, have a uropygial (or preen) gland to secrete a viscous oil, which is then spread methodically on the host's plumage (Figure 1.2) [25]. Preening increases feather hydrophobicity and creates a physical barrier that offers protection from elements and microbes [26]. It is plausible that the removal of the surface lipids would allow for water-soluble keratinase enzymes to have direct access

to their substrate. The composition of preen oil and feather lipids was previously reported, where wax esters were a major component in both (Figure 1.3) [27].

Figure 1.2 – Uropygial gland of a chicken. The uropygial (preen) gland of the chicken is dorsal and positioned at the base of the chicken's tail. Photo by M. Barcus (2015).

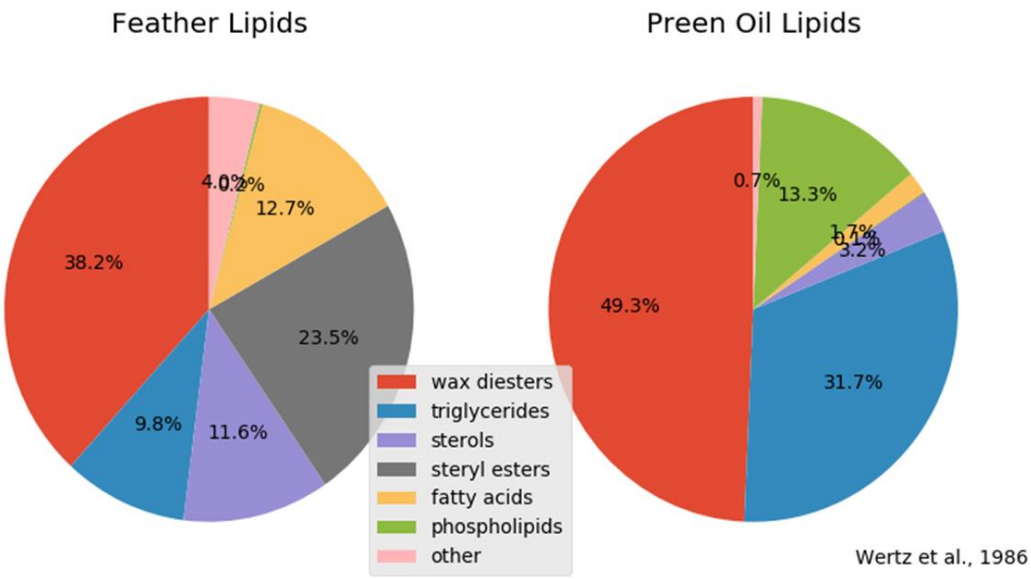

Figure 1.3 - Feather and preen oil lipid composition. Wax (di)esters are the largest lipid class found in both feather lipids and preen oil. Compositions were determined by Wertz et al., 1986 [27].

1.5 Research Aims

Purposely, we selected a feather-degrading soil microorganism and used bioinformatics to screen gene candidates for the hydrolysis of feather lipids. We then devised assays to further evaluate enzyme utility against wax esters. The molecular structure of promising enzymes were modelled and used as a template to engineer mutations for improved affinity towards feather lipids. When the model was not resolute, attempts were made to solve the structure using x-ray crystallography.

CHAPTER TWO

SCREENING OF LIPOLYTIC ENZYMES FROM A FEATHER-DEGRADING STREPTOMYCETE AND RELATED STRAINS

2.1 Summary

Streptomycetes are microbial factories that have led to the discovery of many industrially relevant biomolecules. Most noted for antibiotics, *Streptomycetes* also produce valuable enzymes. Feather-degrading *S. fradiae* var. k11 was investigated for production of lipolytic enzymes which may be beneficial for the hydrolysis of chicken feathers, a major byproduct from the poultry industry. With a draft genome of *S. fradiae* var. k11, gene candidates were screened for lipoytic activity against synthetic substrates p-nitrophenyl palmitate (pNPP) and p-nitrophenyl acetate (pNPA). Other *Streptomycetes, S.avermitilis* and *S. coelicolor* were also screened to expand the pool of enzymes tested. In all, 46 gene candidates were screened. Ten enzymes were active against pNPA and labeled as esterases, while six of the enzymes exhibited activity towards pNPP and were classified as lipase. One enzyme from *S. fradiae* var. k11, SFK3309, was also tested against purified chicken feather lipids and reaction products were analyzed using thin layer chromatography. The formation of products suggested the enzyme was active against feather-lipids, though further work is necessary to determine if the enzyme is able to hydrolyze wax-esters, the largest lipid class found in feather lipids.

2.2 Introduction

The *Actinobacter* phylum comprise Gram-positive bacteria with a characteristic high occurrence of guanine and cystosine nucleotides within their DNA, but are often more noted for their role in medicine, industry, and agriculture [28]. With many *Streptomycetes* regarded as oligotraphs with innate predatory behavior [29], interest in mining the microbe for antibiotics or other important secondary metabolites has also expanded to sourcing industrially important enzymes over the past few decades. Some industrially relevant enzymes studied from *Streptomycetes* include xylanase [30], cellulase [31], lipase [32], esterase [33], mannanase [34], reductase [35], and amylase [36], with the much attention given to proteolytic enzymes.

The ability for some *Streptomycete* proteases to act on keratinous substrates is one of the most promising finds and has been known for nearly half a century [37]. Chicken feathers are a 2 billion kg co-product from the United States poultry industry, but the recalcitrance of the feathers make them difficult to render. Chicken feathers are ~90% protein, most of which is 10 kDa keratin. However, efforts centered on identifying a single keratinolytic protease fall short in keratin hydrolysis and a systematic approach is more likely to achieve desired decomposition, as recently reviewed by Lange et al. [38]. In the review, the authors suggest in some systems endoprotease, exoprotease, and oligopeptidase/metalloprotease synergistically degrade keratinous substrates, while reductase and cysteine dioxygenase improve in substrate access by breaking disulfide bonds.

Our group would like to explore the addition of a lipolysis pretreatment to the model as a means to further improve enzymatic feather degradation. Chickens, like most birds, have a uropygial gland at the base of their tail to secrete oil to be spread on the bird's plummage. This behavior is known as preening and serves as a means to weatherproof and protect the bird. Lipids in chicken feathers are abundant enough that some groups have explored the potential of feathers being used for biodiesel production [39, 40]. A lipolysis step will theoretically aide keratinolytic and reducing enzymes downstream in access to their respective substrates by removing the lipid barrier. To begin evaluating the role of lipid hydrolysis in feather degradation, our group used bioinformatics techniques to screen for lipid hydrolyzing genes from the draft genome of *Streptomyces fradiae* var. k11, a microbe capable of fully degrading feathers. Genes were then expressed in *E. coli* and evaluated for lipolytic activity.

2.3 Materials and Methods

2.3.1 Materials

Chemicals were purchased from Sigma Aldrich unless otherwise noted. The *Streptomyces fradiae* var. k11 strain was gifted to the lab from collaborators [41]. Both *S. avermitilis* (ATCC #31267) and *S. coelicolor* A3(2) were obtained from the American Type Culture Collection [42].

2.3.2 Genomic sequences

A draft genome for *S. fradiae* var. k11 was produced using Illumina paired-end sequencing at the Cornell DNA Sequencing Center using an Illumina/Solexa Genome Analyzer, then assembled with Velvet [43] at the Cornell Computational Biology Service Unit. Genomic information was stored and annotated on the RAST server [44]. A similar draft genome found on the NCBI BLAST database, *Streptomyces sp.* NRRL wc-3719, was aligned to the draft genome of *S. fradiae* var. k11 using the NUCmer script from MUMmer at the Cornell BioHPC Computing Lab [45]. Genomic data for *S. avermitilis* and *S. coelicolor* A3(2) were retrieved from [46] and [47], respectively.

2.3.3 Collection of lipolytic candidates

Genes that were annotated as a lipase or contained a PROSITE pattern characteristic of lipase (PDOC00110, PDOC00111, PDOC00842, and PDOC00903) were used to create the pool of gene candidates. The translated protein sequence was analyzed for presence of a SEC or TAT signal peptide using the PRED-TAT prediction tool [48]. Vector maps were constructed in A Plasmid Editor (ApE)[49]. Complete gene sequences were designed to be in the multiple cloning site (mcs) of the pET28a or pET22b vector behind the pelB signal peptide. The pelB signal sequence on the pET22b vector directs the expressed protein to the periplasm of the Gram-negative expression host and any native signal sequence from the gene was removed during cloning. Native stop codons were also removed from genes to make use of a 6X

histidine tag at the C-terminal end of the vector.

2.3.4 Cloning lipase genes

PCR was used to amplify gene targets from *Streptomyces* genomic DNA. The PCR products were then digested and cloned into either the pET22b or pET28a *E. coli* expression vectors. Template DNA was prepared from the three *Streptomyces* strains using the technique described by Nikodinovic, et al [50]. Primers for target gene amplification were purchased from IDT (www.idtdna.com). Plasmid constructs were cloned into chemi-competent *E. coli* BL21 cells using a heat-shock treatment, then selected on LB agar plates with the appropriate antibiotic. Colonies were selected from the plate and the plasmid DNA was isolated for DNA sequencing at the Cornell Biotechnology Resource Center. Integrity of the DNA sequences were verified in ApE.

2.3.5 Expression and harvesting of lipase

Seed cultures of sequence confirmed constructs in *E. coli* BL21(DE3) cells were used to inoculate 50 mL of Luria broth (LB) with continued selection pressure in a 37°C shaking incubator. After the culture reached an optical density (600 nm) of 0.5, isopropyl β-D-1-thiogalactopyranoside (IPTG) was added to the culture to a final concentration of 0.1 μM. Cultures were then placed in a refrigerated shaking incubator

set to 18℃ for 16 hours. At time of harvesting, cultures were transferred to 50 mL conical tubes and centrifuged at 6000 × *g* for 8 minutes.

Supernatant from the culture was collected and the culture pellet was resuspended in 1X PBS buffer (pH 7.4). The resuspended pellet was then subject to two-minute sonication on ice, then centrifuged at 8000 × *g* for 15 minutes. The collected supernatant from the lysed cells was called the total soluble protein (TSP).

Co-expression of chaperones was also performed in an attempt to improve solubility and recombinant expression for some of the enzymes. The pJKE plasmid contained the DnaK-Dna-J-GrpE chaperone team under the control of the araB promotor. The pG-Tf2 plasmid contained groES-groEL chaperone team and the chaperone tig under the control of the araB Pzt- promoter. Maintenance of pJKE and pG-Tf2 required chloramphenicol pressure, and were induced with L-arabinose and tetracycline, respectively.

2.3.6 Partial protein purification

Active enzyme in either the TSP or supernatant was concentrated by ammonium sulfate precipitation (80%), where the precipitated protein was collected through centrifugation at 15,000 × *g* for 20 minutes. The pellet was then resuspended in a phosphate buffer and dialyzed overnight. Qiagen Ni-NTA agarose was then used according to protocol under non-denaturing conditions to partially purify the enzymes with a 6X histidine tag using gravity-fed chromatography. Samples were taken

throughout the purification process and analyzed by SDS-Page and Coomassie brilliant blue staining.

2.3.7 Enzyme assays

Lipase activity was determined by using the assay previously described by [51]. Briefly, 0.037 grams p-nitropheynyl palmitate (pNPP) was dissolved in 10 mL of 2-propanol. One mL of the dissolved substrate was then added to 9 mL of sodium phosphate buffer (0.05M, pH 8) with a final concentration of 0.1% gum arabic (w/v) and 0.2% sodium deoxycholate (w/v)). After the addition of 10 µL of sample to a 96-well microplate, 240 µL substrate/buffer solution was quickly added to the well and rapidly loaded into a Molecular Devices SpectraMax M2e spectrophotometer. Absorbance was read at 410 nm with a reading once every 15 seconds for a two-minute period. One unit was defined as the hydrolysis of 1 mM pNPP in a minute. The molar extinction coefficient of the p-nitrophenol product used for calculations was 18,300 M^{-1}•cm^{-1}. An assay for esterase activity was carried out much the same way using p-nitrophenyl acetate (pNPA) as substrate, but without a need for gum arabic or sodium deoxycholate. Protein concentration of the samples was determined using the method described by Lowry et al [52].

Activity against feather lipids was evaluated using thin-layer chromatography (TLC). Feathers were collected at the Cornell Poultry Farm (Ithaca, NY) and rinsed with water, then dried. The feathers were then packed into the extraction chamber of a Soxhlet apparatus and lipids were extracted with petroleum ether as solvent for ~16

hours. The lipids were collected in a glass tube and the petroleum ether was evaporated off under nitrogen. Free fatty acids were separated from the feather lipids as described by [53]. Briefly, five grams of silicic acid were weighted and placed in a beaker. Ten mL of 2-propanol-KOH and 30 mL of ethyl ether was added to the silicic acid and let stand for 5 minutes. The silicic acid was then transferred to a gravity column. Feather lipids were dissolved in ethyl-ether, then passed through the column. The free fatty acids were bound to the column and the flow through was collected. Additional ethyl-ether (~25 bed volumes) was passed through the column and the flow-through was merged with the earlier collection. Ethyl ether was then evaporated off from the purified lipids under the flow of nitrogen. An enzyme assay was set up in a similar manner to the pNPP assay, except feather lipids were dissolved in 2-propanol and the reaction was performed in 1.7 mL Eppendorf tubes at 37°C, shaking for one hour. Lipids were recovered from the reaction with a 2:1 chloroform:methanol mixture and 10 µL of the recovered lipids in the mixture was loaded on a silica gel 60 TLC plate and run as described [54]. Briefly, the plate was double-developed with hexane:ethyl ether:acetic acid in a 50:50:1 ratio. The plate was then dried and sprayed with coloring agent (27.4 mM 12-molybdo(VI) phosphoric acid n-hydrate and 50 mM sodium perchlorate in ethanol). The plate was then heated in an oven until the bands were revealed (approximately 2 minutes).

2.4 Results and Discussion

2.4.1 Lipase cloning

While investigating *S. fradiae* var. k11 and its feather-hydrolyzing ability, it was evident lipolytic enzymes were being secreted, as apparent by the enzyme activity detected in the culture supernatant. A draft genome was constructed for *S. fradiae* var. k11 and annotations were performed by the RASTClassic annotation scheme. Only seven genes were identified as lipase, and some of which were incomplete sequences.

In order to start with a larger pool of gene candidates, we explored additional *Streptomycete* strains and used other bioinformatics techniques for gene identification. The lab was able to acquire the strains *S. avermitilis* and *S. coelicolor,* both of their genomes also already having been made publicly available [46, 47]. A publicly available draft genome of *S. sp.* NRRL WC-3719 from a large sequencing project [55] was also identified, and had high resemblance to *S. fradiae* var. k11. The two draft genomes were aligned using the NUCmer script from the MUMmer suite and a dot plot of the alignment was created (Figure 2.1). The slope of the alignment dot plot was close to 1, which represents a high sequence conservation between the two draft genomes [56]. The alignment results suggested we could use the draft genome sequence of *S. sp.* NRRL WC-3719 to complete some of the partial gene sequences identified in *S. fradiae* var. k11. Then, in addition to sequence annotations, PROSITE patterns for lipases were also used to identify gene candidates [57].

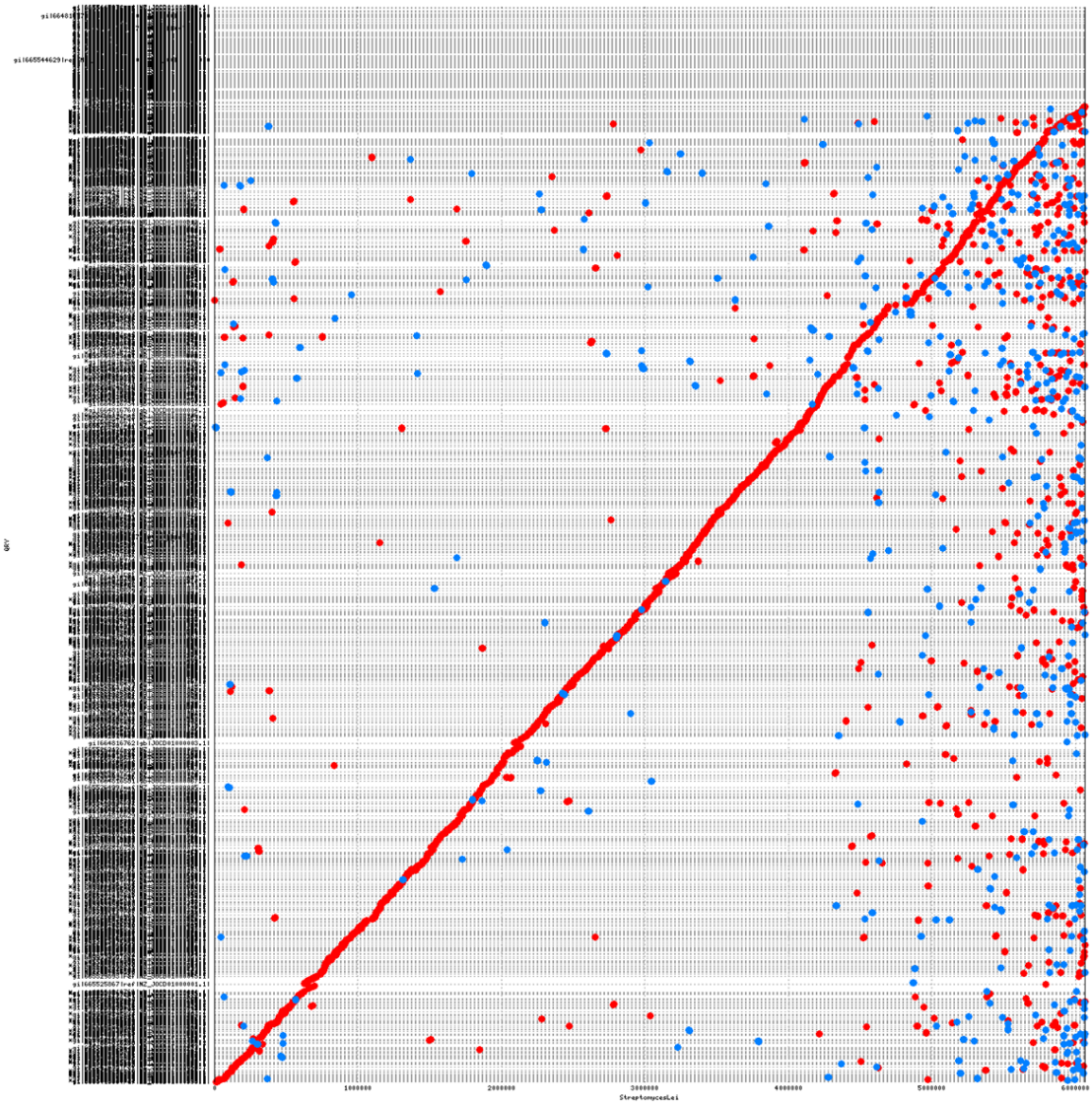

Figure 2.1 – Draft genome alignment dot plot. The draft genomes of *Streptomyces fradiae* var. k11 was aligned against *Streptomyces sp.* NRRL WC-3719 using NUCmer from the MUMmer sequence alignment package. The dot plot has red dots to represent a forward alignment and have positive slope and blue dots, which have negative slope and represent an inverse sequence alignment. A slope equal to 1 would represent conservation between the two sequences. The dots from this alignment have a slope near 1, suggesting high conservation between the two draft genomes.

2.4.2 Lipase expression

In total, 46 lipase gene candidates from the genomes of *S. fradiae* var. k11, *S. avermitilis,* and *S. coelicolor* were identified. Constructs were cloned and expressed and the supernatant and the total soluble protein (TSP) from the lysate was evaluated for enzyme activity. The sole use of pNPP as substrate for the enzyme assays at first yielded just 6 active enzymes from the 46 constructs. When handling a large number of samples, pNPP is an ideal substrate of choice to evaluate lipase activity [58]. However, many other enzymes may be active, but unable to hydrolyze the water insoluble pNPP substrate, a specific characteristic for lipases. Instead, the short-chain, water-soluble substrate, p-nitrophenyl acetate (pNPP), was also used and enzymes were distinguished as a lipase for having activity against pNPP, or as an esterase for having activity only against pNPA [59].

Between the two substrates, pNPA and pNPP, a total of 13 enzymes had detectable activity. The co-expression of chaperones brought the number of active enzymes to 16 of the 46 constructs (Table 2.1-2.3).The DnaJ-DnaK-GrpE chaperone team has been demonstrated to stabilize protein expression by reducing aggregation [60] and was effective for the expression of SCO3644, SCO7131, and SFK2174. Co-expressing groES-groEL and tig chaperones was successful at recovering activity for SCO7131 and SFK2174, just not to the same extent as co-expression with the DnaJ-DnaK-GrpE chaperones. The groES-groEL chaperones are able to create an Anfinsen cage that assists with protein folding before it is released [61]. In all, *S. coelicolor* had the most active enzymes and lipases identified among the three strains.

Table 2.1 - Lipolytic activity screen for genes from *Streptomyces avermitilis*.

ID	Annotation	Species	Vector	Activity
SAV0299	putative secreted esterase/lipase	*S. avermitilis*	pET22b	-
SAV0469	putative secreted lipase	*S. avermitilis*	pET22b	-
SAV0819	putative hydrolase	*S. avermitilis*	pET28a	-
SAV1432	hypothetical protein	*S. avermitilis*	pET28a	-
SAV1549	putative esterase/lipase	*S. avermitilis*	pET22b	Esterase
SAV3099	putative hydrolase	*S. avermitilis*	pET28a	Esterase
SAV3461	putative lipase	*S. avermitilis*	pET22b	-
SAV4531	putative lipase/esterase	*S. avermitilis*	pET22b	Esterase
SAV4968	putative hydrolase	*S. avermitilis*	pET28a	Esterase
SAV5844	hypothetical protein	*S. avermitilis*	pET22b	-
SAV6079	putative esterase/lipase	*S. avermitilis*	pET22b	-
SAV6559	putative secreted lipase	*S. avermitilis*	pET22b	Lipase
SAV6609	hypothetical protein	*S. avermitilis*	pET28a	-
SAV7089	putative secreted lipase	*S. avermitilis*	pET22b	-

Genes were cloned into the pET22b or pET28a expression vectors and expressed in *E. coli* BL21 (DE3) cells. The supernatant and the cell lysate from expressed constructs were tested for activity using substrates p-nitrophenyl palmitate (pNPP) and p-nitrophenyl acetate (pNPA). Lipases were represented by the hydrolysis of pNPP. Esterases were represented by the hydrolysis of pNPA and an inability to hydrolyze pNPP. A lack of activity against pNPP and pNPA was represented by a minus sign. Five active enzymes from *S. avermitilis* were identified (1 lipase and 4 esterases).

Table 2.2 – Lipolytic activity screen for genes from *Streptomyces coelicolor* A3(2).

ID	Annotation	Species	Vector	Activity
SCO0145	putative secreted protein	*S. coelicolor*	pET28a	-
SCO0713	lipase	*S. coelicolor*	pET28a	Lipase
SCO1265	lipase	*S. coelicolor*	pET28a	-
SCO1725	hydrolase	*S. coelicolor*	pET22b	-
SCO1735	lipase	*S. coelicolor*	pET22b	Lipase
SCO2123	esterase/lipase	*S. coelicolor*	pET28a	-
SCO3219	lipase	*S. coelicolor*	pET22b	-
SCO3644	lipase/esterase	*S. coelicolor*	pET22b	Esterase
SCO4368	lipase	*S. coelicolor*	pET28a	-
SCO4746	lipase	*S. coelicolor*	pET28a	Esterase
SCO4799	putative secreted lipase	*S. coelicolor*	pET22b	-
SCO5165	hydrolase	*S. coelicolor*	pET28a	Esterase
SCO6175	hypothetical protein	*S. coelicolor*	pET28a	-
SCO6432	peptide synthase	*S. coelicolor*	pET28a	-
SCO6966	lipase	*S. coelicolor*	pET28a	-
SCO7131	lipase	*S. coelicolor*	pET28a	Esterase
SCO7396	hypothetical protein	*S. coelicolor*	pET22b	-
SCO7513	hydrolase	*S. coelicolor*	pET22b	Lipase

From the description in Table 2.1, seven enzymes were identified to be active against either pNPP or pNPA from *S. coelicolor* (3 lipases and 4 esterases).

Table 2.3 – Lipolytic activity screen for genes from *Streptomyces fradiae* var. k11.

ID	Annotation	Species	Vector	Activity
SFK0710	esterease/lipase/thioesterase	*S. fradiae* var. k11	pET22b	-
SFK0767	ATP-dependent RNA helicase	*S. fradiae* var. k11	pET28a	-
SFK1518	putative lipase/esterase	*S. fradiae* var. k11	pET28a	Esterase
SFK2174	lipase/acylhydrolase	*S. fradiae* var. k11	pET22b	Esterase
SFK2553	thioesterase	*S. fradiae* var. k11	pET28a	-
SFK3087	triacylglycerol lipase precursor	*S. fradiae* var. k11	pET22b	Lipase
SFK3128	hypothetical protein	*S. fradiae* var. k11	pET28a	-
SFK3309	putative secreted lipase	*S. fradiae* var. k11	pET22b	Lipase
SFK3682	lysophospholipase L1	*S. fradiae* var. k11	pET22b	-
SFK4182	Endo-1,4-beta-xylanase A	*S. fradiae* var. k11	pET22b	-
SFK4461	putative hydrolase	*S. fradiae* var. k11	pET28a	-
SFK4667	hypothetical protein	*S. fradiae* var. k11	pET28a	-
SFK5000	cholesterol esterase	*S. fradiae* var. k11	pET22b	-
SFK5309	lysophospholipase L1	*S. fradiae* var. k11	pET22b	-

From the description in Table 2.1, four enzymes were identified to be active against either pNPP or pNPA from *S. fradiae* var. k11. Two of the active enzymes were identified as esterases and two behaved as lipases.

2.4.3 Feather lipid hydrolysis

Despite identifying six active lipases against pNPP, it was important to establish activity against true feather lipids. To this end, lipids were extracted from chicken feathers collected at the Cornell Poultry Farm (Ithaca, NY) using the Soxhlet extraction method. Recovery of feather lipids was ~2% of the feather weight. It has been reported that wax-esters are the predominant lipid class from feather lipids (38.2%), but there is also a large percentage of free fatty acids (12.7%) [27]. As free-fatty acids are a reaction product of lipid hydrolysis, it was important to remove the free fatty acids to minimize the background activity.

Passing the feather lipids through a silicic acid column as described by [53] proved effective at minimizing the free fatty acids. The purified lipids were then eligible for hydrolysis assays. SFK3309 proved to be the most active lipase against pNPP and also had good expression levels. Hydrolysis products of SFK3309 against feather lipids were evaluated using TLC (Figure 2.2). Compared with the heat-deactivated enzyme, which served as negative control, it was clear that much more hydrolysis products were formed with the active enzyme. Although, feather lipids are not homogenous and it is difficult to discern between what lipid class(es) the enzyme was successful at hydrolyzing. Many lipases have already been characterized against triacyclglycerols, but it is worth further investigation into whether the wax-esters are also vulnerable to hydrolysis by lipases from a feather-degrading bacterium.

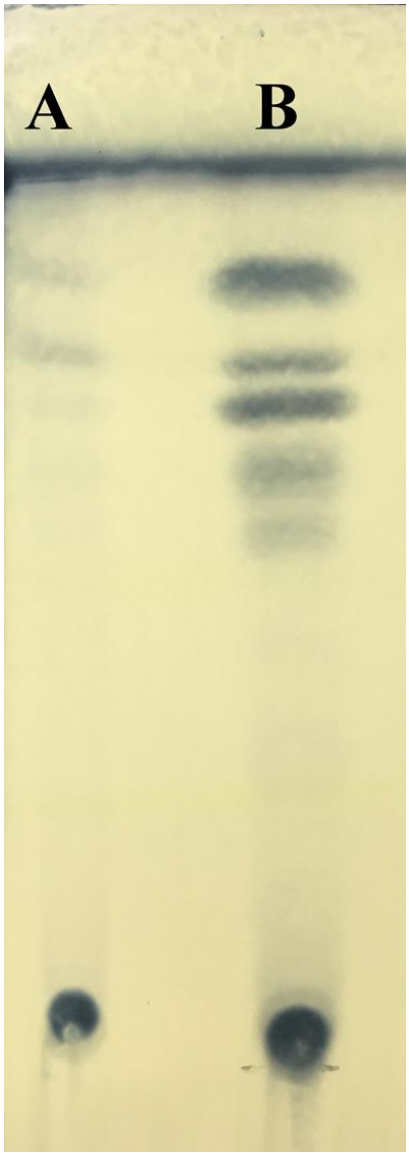

Figure 2.2 – Separation by TLC of feather lipid hydrolysis products. In lane A, the hydrolysis products were run from heat-deactivated lipase SFK3309 that was incubated with purified feather lipids at 37℃. Lane B contained reaction products from the active SFK3309 incubated with feather lipids. The abundance of hydrolysis products in lane B suggests SFK3309 is able to hydrolyze chicken feather lipids.

2.5 Conclusion

In total, 16 lipolytic enzymes were identified as functional from the genome of *S. fradiae* var. k11, *S. coelicolor,* and *S. avermitilis*. Co-expression of chaperones was an effective measure to rescue activity for some of the enzymes that might otherwise have been classified as inactive. The use of pNPP and pNPA allowed for the rapid screening and distinguished active enzymes as either an esterase or lipase. Early TLC experiments suggest *S. fradiae* var. k11 is capable of hydrolyzing feather lipids. Further investigation on enzyme activity towards wax-esters, the major lipid class in feather lipids should be warranted and would provide greater insight on the role lipases have on feather hydrolysis.

ACKNOWLEDGEMENTS

Much appreciation goes to Dr. Jeremy Weaver, who assembled the draft genome of *Streptomyces fradiae* var. k11 and did much of the initial work starting the feather-degradation project in the lab. Dr. YiXuan Zhu was a big help in optimizing heterologous protein expression in *E. coli* and sourcing expression plasmids. Dr. Qi Sun assisted with the genome comparison at the Cornell BioHPC computing lab.

CHAPTER THREE

IDENTIFICATION AND KINETICS CHARACTERIZATION OF A WAX ESTER HYDROLASE FROM A FEATHER-DEGRADING ACTINOMYCETE

3.1 Summary

Streptomyces fradiae var. k11 is a Gram-positive soil microorganism capable of degrading chicken feathers. Apart from being mostly protein, chicken feathers have a considerable level of lipids, with wax esters being the largest lipid class. The waxes may pose a challenge while rendering the feathers into coproducts, such as feather meal, and so the identification of a wax-ester hydrolase is warranted. A draft genome sequence of *S. fradiae* var. k11 was used to identify 11 gene sequences of potential lipid-degrading enzymes. The genes were expressed in *E. coli* BL21(DE3) cells on a pET vector and screened for activity. Four of the 11 enzymes had detectable activity, with two of the enzymes, SFK3309 and SFK3087, active against p-nitrophenyl palmitate, a representative water-insoluble substrate. A modified enzymatic assay was designed to measure activity against three model wax substrates: jojoba oil, beeswax, and cetyl-palmitate. SFK3309 was characterized to hydrolyze all three wax substrates. Kinetic experiments for SFK3309 were performed with cetyl-palmitate at 37^{o}C, pH 8.0. The K_m was determined to be 850 µM and the K_{cat} was 11.63 s^{-1}. Through the characterization of SFK3309 as a wax-ester hydrolase, biotechnological implications

of wax ester hydrolases in the rendering of many industrial wastes can be substantiated for further studies.

3.2 Introduction

Chicken feathers are well known for being predominately protein (90%), mostly comprised of recalcitrant ß-keratin [62]. However fat content has been known to vary inversely with protein content in feather meal, anywhere from 2-12% [63]. Some groups have estimated chicken feather fat to be near 11% [64]. Chickens secrete lipids from the uropygial gland onto their plumage for protection from the elements in an act known as preening. Wax (di)esters account for 49.3% of total preen oil composition and 38.2% of total feather lipids [27].

Feathers represent approximately 3-6% of a chicken's whole body weight [65] and with the annual slaughter of 8.9 billion chickens in the USA [4], effective rendering of chicken feathers is necessary to combat pollution. The protein from chicken feathers has considerable economic value, but the significant presence of fat in chicken feathers may pose a challenge for adequate degradation of the ß-keratin, and thus lower the economic potential.

Over half a century ago, *Streptomyces fradiae* was identified for the biodegradation of wool and feather keratin at enriched waste sites [66] and our lab has recently been investigating enzymes from *S. fradiae* var. k11 for industrial relevance. Already the research community has identified many keratinases and reductases in *S. fradiae* [20], but we wanted to determine if lipolytic enzymes capable of hydrolyzing

the waxy feather lipids were also present. Multiple strains of *Streptomyces* have been previously characterized to utilize beeswax found on ancient artwork as a sole carbon source [67]. Given that *S. fradiae* var. k11 is of the same genus, it may be reasonable to suspect *S. fradiae* var. k11 also produces enzymes capable of catalyzing the hydrolysis of wax esters found on chicken feathers.

A wax ester is a fatty acid esterified to a fatty alcohol and is critical for multiple physiological events. Wax esters are used by some plants and marine organisms as an energy storage [68]. Often on the epicuticular or epidermal layers of plants and animals, wax esters provide defense against pathogens and desiccation [68]. Wax esters are also a buoyancy regulator in fish [69]. The unique properties of wax esters have significant industrial potential for use in cosmetics [70], pharmaceuticals [71, 72], art, food products [73], fuel [74], and as a lubricants [75, 76]. There have been multiple groups that have focused on the biosynthesis of wax esters [77-81], but studies focused on the hydrolysis of wax esters have been few. The literature contains a few examples of wax ester hydrolases (EC 3.1.1.50) from plant [82-84], fungal [85], marine [86-89], and bacterial [75] origins have previously been reported, however kinetic information is scant [82, 84].

The identification and characterization of wax ester hydrolases has utility in the development of biotechnology to process agricultural byproducts with waxy surface lipids, such as wool [90] and feathers. Moreover, the similar physical characteristics of waxes and plastics (solid, insoluble) has facilitated in the discovery of a wax worm digesting plastic bags [91] or cutinase enzymes (EC: 3.1.1.74) hydrolyzing polyethylene terephthalate (PET) [92]. Our report identified, and

characterized, one wax ester hydrolase from a feather-degrading actinomycete with wax ester hydrolase activity.

3.3 Materials and Methods

3.3.1 Materials

Chemicals were purchased from Sigma Aldrich (St. Louis, Missouri, USA) unless otherwise noted. Bacteria strain *Streptomyces fradia* var. k11 was gifted to the lab from collaborators [93].

3.3.2 Cloning of wax esterase genes

S. fradiae var. k11 was cultured in brain heart infusion broth and genomic DNA was isolated as described previously by Nicodinovic, et al [50]. Previous work in the lab has yielded a draft genome for *S. fradiae* var. k11. The genome was annotated on the Rapid Annotation using Subsystem Technology (RAST) server using the RASTClassic annotation scheme to identify potential lipolytic enzymes [94]. Additional enzymes were identified with patterns PDOC00110, PDOC00842, and PDOC00903 from the PROSITE database [57]. Some of the partial sequences were completed using sequence information from Ju et al. [95] and the previously reported *lips221* sequence [51] was downloaded from GenBank (ID: EF429087.1) [96]. Genomic DNA served as template for a polymerase chain reaction (PCR) to amplify

out the genes. Pred-TAT [48], an online signal peptide recognition tool, was used to predict the presence of any signal sequence. Oligonucleotides were designed to pull out the different genes without any native signal peptide or stop codon, while incorporating NcoI and XhoI restriction sites at the 5' and 3' ends, respectively.

The PCR reaction was performed using Platinum pfx polymerase purchased from Thermo Fisher Scientific (Waltham, Massachusetts, USA). The placement of restriction sites allowed for simplified cloning of PCR products into the pET22b(+) vector via double digestion, and made use of the pelB signal peptide and 6X histidine tag at the C—terminal end. Ligated constructs were cloned into *E. coli* BL21(DE3) cells and selected over LB amp^+ plates. Plasmid DNA was isolated using a QIAGEN (Venlo, Netherlands) Qiaprep Spin miniprep kit and the construct was verified at the Cornell Biotechnology Resource Center DNA Sequencing facility using T7 oligonucleotides. Sequencing results were analyzed against a vector map using ApE - A Plasmid Editor (Wayne Davis, Salt Lake City, Utah, USA; version 2.0.49.10) [49].

3.3.3 Expression and Purification

Starter cultures in Luria broth (LB) were grown overnight and used to inoculate expression cultures. Expression cultures used either LB, terrific broth (TB), or autoinduction media (Teknova, Hollister, California, USA) and were grown at 37°C to OD_{600} of 0.6-0.8, then placed into a 16°C, shaking incubator for 22 hours. Cultures in LB or TB were induced with 0.1 mM Isopropyl β-D-1-thiogalactopyranoside (IPTG).

Protein was harvested by first collecting the cells via centrifugation (5000 × *g*

for 5 minutes). Cells were resuspended in lysis buffer (20 mM HEPES, 500 mM NaCl, 10 mM imidazole, pH 7.6). Cells were then sonicated for 8 minutes using 4 second pulses at 45% amplitude on a Sonics (Newtown, Connecticut, USA) Vibracell sonicator (model: VC 130). The disrupted cells were then centrifuged at 15,000 × g for 20 minutes and the total soluble protein was mixed with Ni-NTA agarose (McLab, South San Francisco, California, USA) for 1 hour on a rolling shaker at 4°C. The slurry was then loaded into a gravity flow column and allowed for the agarose to settle. Upon the agarose settling, the column was uncapped and the flow-through was collected. The Ni-NTA agarose was then washed and collected three times with wash buffer (20 mM HEPES, 500 mM NaCl, and 20 mM imidazole, pH 7.6). Protein bound to the Ni-NTA agarose was then eluted with elution buffer (20 mM HEPES, 500 mM NaCl, and 250 mM imidazole, pH 7.6).

The eluted protein was then concentrated in an Amicon ultra-15 centrifuge tube with a molecular weight cut-off of 10 kDa. Concentrated protein then further purified using an ÄKTA Explorer FPLC system (GE Healthcare, USA). Size exclusion chromatography (SEC) was performed on all NiNTA purified proteins. The column employed for purification was Superdex 200 10/300 GL. Standards used to calibrate the SEC column were a lyophilized mix of thyroglobulin, bovine γ-globulin, chicken ovalbumin, equine myoglobin, and vitamin B12 (Molecular weight range: 1,3500-670,000 Da, pI range: 4.5-6.9) (Bio-Rad, Hercules, California, USA). Proteins were stored at 4°C in SEC buffer (20 mM HEPES, 500 mM NaCl, 5 mM $CaCl_2$, pH 7.6) until further analyzed for activity and purity. Protein purity was determined by

sodium dodecyl sulfate - polyacrylamide gel electrophoresis (SDS-PAGE) using Coomassie blue staining [97].

3.3.4 Activity assays

Protein concentration was determined as previously described [98], with the exception of the incubation taking place at 37°C instead of 60°C. Lipase assays were conducted using p-nitrophenyl palmitate as substrate. Assay conditions have been previously described [51]. Briefly, p-nitrophenyl palmitate (pNPP) was dissolved in 2-propanol to make a 10 mM solution. A reaction buffer was prepared (50 mM sodium phosphate, pH 8.0, 0.1% gum arabic, 0.2% sodium deoxycholate) and mixed with the pNPP solution in a 9 to 1 ratio. Enzyme sample (10 µL) was loaded into a 96-well microtiter plate and 240 µL of the substrate solution was added immediately before taking a kinetic read for 2 minutes with 15 second intervals using a wavelength of 410 nm on a SpectraMax M2e spectrophotometer (Molecular Devices, Sunnyvale, California, USA). One enzyme unit was defined as the hydrolysis of 1.0 µmole of p-nitrophenyl palmitate per minute at pH 8.0 at room temperature. Other p-nitrophenyl ester substrates (butyrate, decanoate, and stearate) were used interchangeable with pNPP for the assay.

Wax ester hydrolase activity was determined using three different wax substrates: beeswax, cetyl palmitate, and jojoba oil. Wax substrate was solubilized in 2-propanol, using a heat block when necessary and mixed with the same reaction buffer from the pNPP assay and at the same ratio. The substrate solution was then added to a

microcentrifuge tube that contained the enzyme sample and was incubated in a 37°C, shaking incubator for up to 1 hour. Released fatty acid products from wax ester hydrolysis were then detected using reagents from the NEFA-HR(2) kit from Wako Chemicals (Richmond, Virginia, USA). Briefly, in a 96-well microtiter plate an 8 µL sample from the enzyme reaction was mixed with 144 µL color reagent A, which contained coenzyme A (CoA), acyl-CoA synthetase, and adenosine triphosphate and resulted in the formation of acyl-CoA. After a 5-minute incubation at 37°C, the microtiter plate was read at A_{550}. Color reagent B (acyl-CoA oxidase, peroxidase, 3-methyl-ethyl-N-(ß-hydroxyethyl)-aniline(MEHA), and 4-aminoantipyrine) was then added (48 µL), which oxidized the acyl-CoA into hydrogen peroxide, thus allowing MEHA to undergoing oxidative condensation with 4-aminoantipyrine and create a purple colored product. After a 5-minute incubation at 37°C, a second A_{550} reading was made. A standard curve was created using varying concentrations of oleate and an enzyme unit was defined as the release of 1 millimole-equivalent free fatty acid per minute per milligram of enzyme.

Thin layer chromatography (TLC) was performed as described previously [54]. Briefly, an enzyme reaction with a wax substrate was set up as described earlier. The reactions were then incubated in a 37°C shaking incubator for 1 hour. Methanol (100 µL) was added to the sample and vortexed. Chloroform (200 µL) was then added and the sample was again vortexed. A sample collected from the chloroform layer was used to spot a HPTLC silica gel 60 TLC plate and double-developed with eluent hexane: diisopropyl ether: acetic acid (50:50:1). The plate was dried and then sprayed with coloring agent (27.4 mM 12-molybdo(VI) phosphoric acid n-hydrate and 50 mM

sodium perchlorate dissolved in ethanol). The plate was then heated in an oven for 2 minutes until the bands were revealed. A separate reaction was set up with a heat-deactivated enzyme and was performed concurrently with the reaction containing the active enzyme. The enzyme was heated to 65°C for 10 minutes to fully deactivate it.

Data analysis was carried out using the Pandas module in python [99]. Plots were generated using Matplotlib [100].

3.4 Results

3.4.1 Identification of lipolytic enzymes from Streptomycete genome

From a draft genome sequence of feather-degrading actinomycete *S. fradiae* var. k11, fifteen genes were identified as potential lipases from annotations and ProSite patterns. Four genes, out of the pool of 15, had detectable enzymatic activity against p-nitrophenyl acetate or pNPP (Table 3.1). Lipase activity was observed only in two of the four identified enzymes (SFK3087 and SFK3309), as demonstrated by their ability to hydrolyze pNPP. Both SFK3309 and SFK3087 were tested against the wax ester substrate jojoba oil, but only SFK3309 retained activity and further characterization of SFK3309 was warranted.

Table 3.1 – Lipolytic enzyme screen of *Streptomyces fradiae* var. k11.

ID	Annotation	Activity
SFK0710	esterase/lipase/thioesterase	-
SFK0767	putative ATP-dependent RNA helicase	-
SFK1328	hydrolase	-
SFK1518	putative lipase/esterase	Esterase
SFK2174	lipase/acylhydrolase	Esterase
SFK2553	thioesterase	-
SFK3087	triacylglycerol lipase precursor	Lipase
SFK3128	hypothetical protein	-
SFK3309	putative secreted lipase	Lipase
SFK3682	lysophospholipase L1	-
SFK4182	Endo-1,4-beta-xylanase A precursor	-
SFK4461	putative hydrolase	-
SFK4667	hypothetical protein	-
SFK5000	cholesterol esterase	-
SFK5309	lysophospholipase L1	-

Genes were amplified from genomic DNA in a PCR reaction with gene-specific primers, then cloned into pET22b vector and expressed in *E. coli* BL21(DE3) cells. Activity in the supernatant and cell lysate was tested for hydrolysis of p-nitrophenyl palmitate to represent lipase activity and p-nitrophenyl acetate hydrolysis to represent esterase activity. Four of the fifteen constructs had detectable activity. If no activity was detected then samples were marked with a minus sign.

3.4.2 Sequence characterization of SFK3309

The cloned construct of SFK3309 in the pET22b(+) was verified via Sanger sequencing. Gene sequences of SFK3309 and lips221 which served as the gene template for cloning were aligned (Figure 3.1). The translated sequence codes for four alternative residues from lips221: P86L, L88P, N223S, and L237P.

3.4.3 Expression optimization and purification

Initially, culturing pET22b SFK3309 in *E. coli* BL21(DE3) cells appeared to have some toxicity as indicated by a reduced OD_{600} at harvest time compared to that of the time of IPTG induction. Cultures expressing SFK3309 were tested using different growth media for optimization: Luria broth (LB), terrific broth (TB), and Studier's ZYM-5052 autoinduction media (AT). Not only did the cell density of cultures grown in AT increase compared to LB and TB (OD_{600} ~6.0), the enzyme activity in the lysate was ~3X higher, as seen in Figure 3.2.

The C-terminal His tag on the pET vector was used for the first purification step of SFK3309. After eluting SFK3309 from the Ni-NTA agarose column, the protein was run on an SDS-PAGE gel and stained using Coomassie blue (Figure 3.3). A subsequent gel filtration step was used and separated the multimeric protein forms.

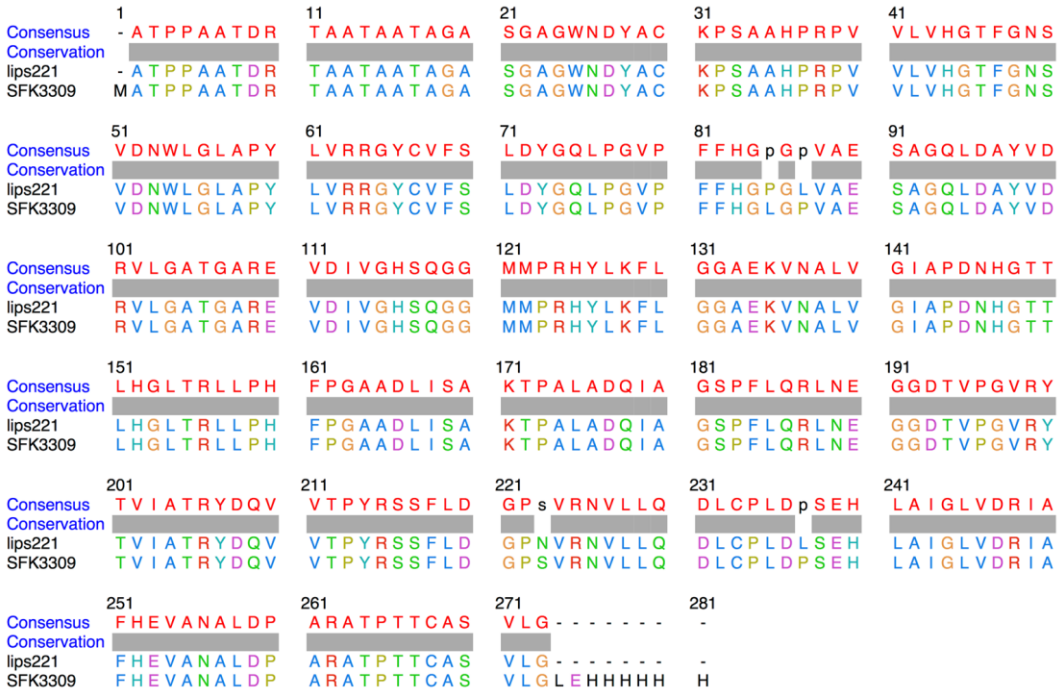

Figure 3.1 - SFK3309 alignment with lips221. Using MAFFT [101] the top performing lipase from this study (SFK3309) was aligned to lips221 (GenBank ID: EF429087.1), a highly similar sequence initially reported by Zhang, et al [51]. Four missense mutations were present between the two sequences: P86L, L88P, N223S, and L237P. Alignment was visualized in Chimera [102].

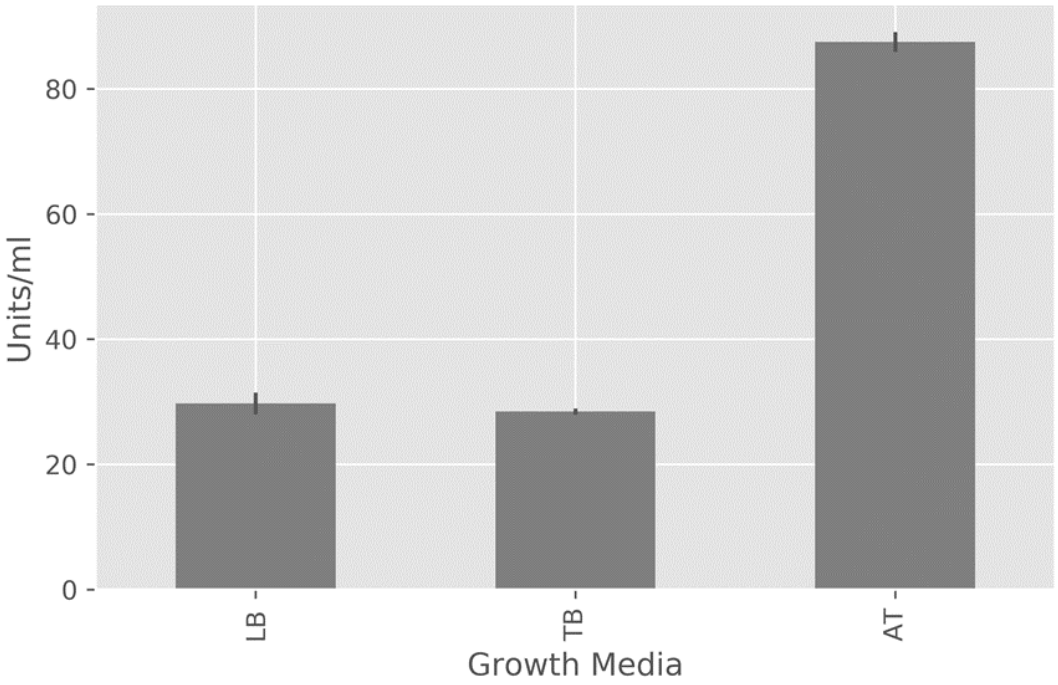

Figure 3.2 - Optimal growth media for SFK3309. Luria broth (LB), Terrific broth (TB), and Studier's ZYM-5052 autoinduction media (AT) were tested for impact on protein expression. Cultures were grown as described in *Materials in Methods*. Assays were performed in duplicate and the standard deviation is represented by the error bars. Both LB and TB had comparable activity in the lysate ~22 hours post IPTG induction while AT had 2.9X the activity in the lysate at the same time period.

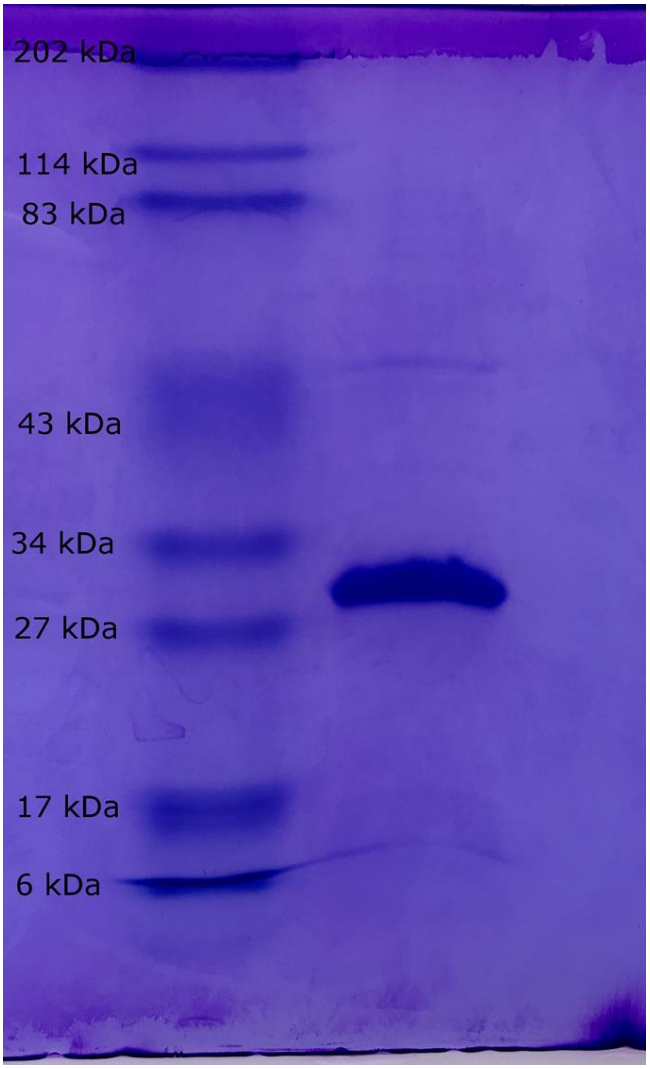

Figure 3.3 - Coomassie blue stained SDS-PAGE gel of his-tag purified SFK3309. The left lane is the Bio-Rad broad range protein marker and its bands are labelled with their respective molecular weights. The right lane is the purified SFK3309 (29.6 kDa) eluted from the Ni-NTA agarose (see Materials and Methods).

3.4.4 Enzyme activity analysis

Substrate chain-length preference of SFK3309 was determined by the release of nitrophenol from synthetic substrates with varying length carbon-chains esterified to nitrophenyl. Substrates included: para nitrophenyl-butyrate (C4), para nitrophenyl-decanoate (C10), para nitrophenyl-palmitate (C16), and para nitrophenyl-stearate (C18). Preference of SFK3309 for the shorter carbon chain of para nitrophenyl-butyrate was evident (Figure 3.4).

Kinetic studies of SFK3309 with cetyl-palmitate as substrate were performed. A Lineweaver-Burk plot was used for the determination of the K_m and V_{max} values (Figure 3.5). The K_m was worked out to be 8.5×10^{-3} M and the K_{cat} was 11.55 s^{-1}, yielding a K_{cat}/K_m value of 1.35 • mMs^{-1} (Table 3.2). Visual hydrolysis of cetyl-palmitate, alongside two more substrates, jojoba oil and beeswax, was carried out using thin layer chromatography (Figure 3.6).

Table 3.2 – Comparison of reported wax-ester hydrolysis kinetics values.

K_m (M)	K_{cat} (1/s)	K_{cat}/K_m (1/mMs^{-1})	Organism	Reference
$2.8 \times 10^{-5\dagger}$	--	--	*Sinapis alba L.*	[84]
$9.3 \times 10^{-5*}$	--	--	*Simmondsia chinensis*	[82]
$8.5 \times 10^{-4\#}$	11.63	13.7	*S. fradiae* var. k11	Current study

†Radiolabeled cetyl-palmitate was used as substrate in this study.

*N-methylindoxyl myristate was used as substrate.

$^{\#}$Unlabeled cetyl-palmitate was used as substrate.

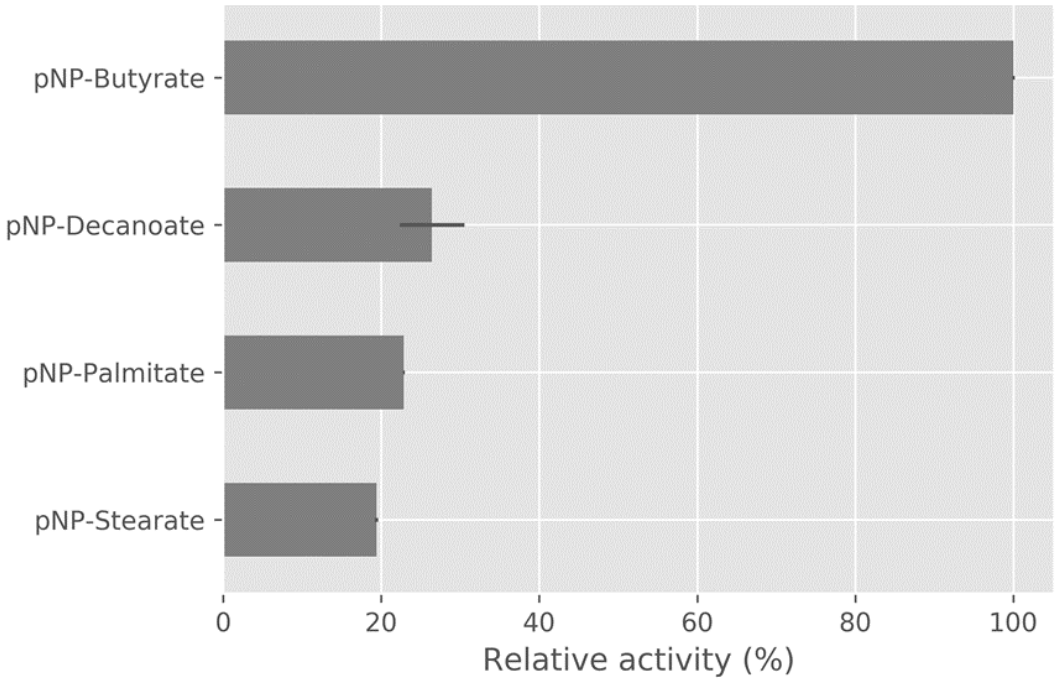

Figure 3.4 - Substrate chain-length preference of SFK3309. Purified SFK3309 was evaluated for enzyme hydrolysis activity against the chromophore p-nitrophenol (pNP) esterified to different carbon-chain length carboxylates: butyrate (C4), decanoate (C10), palmitate (C16), and stearate (C18). Reaction conditions were carried out at room temperature buffered with 0.05 M sodium phosphate, pH 8.0 and performed in duplicate. The average activity of SFK3309 against pNP-Butyrate was considered absolute (100%) and the standard deviation was represented by the error bars. The data suggests SFK3309 has preference for the shorter-chained substrate, yet retains broad specificity, allowing the enzyme to retain activity against all the substrates tested.

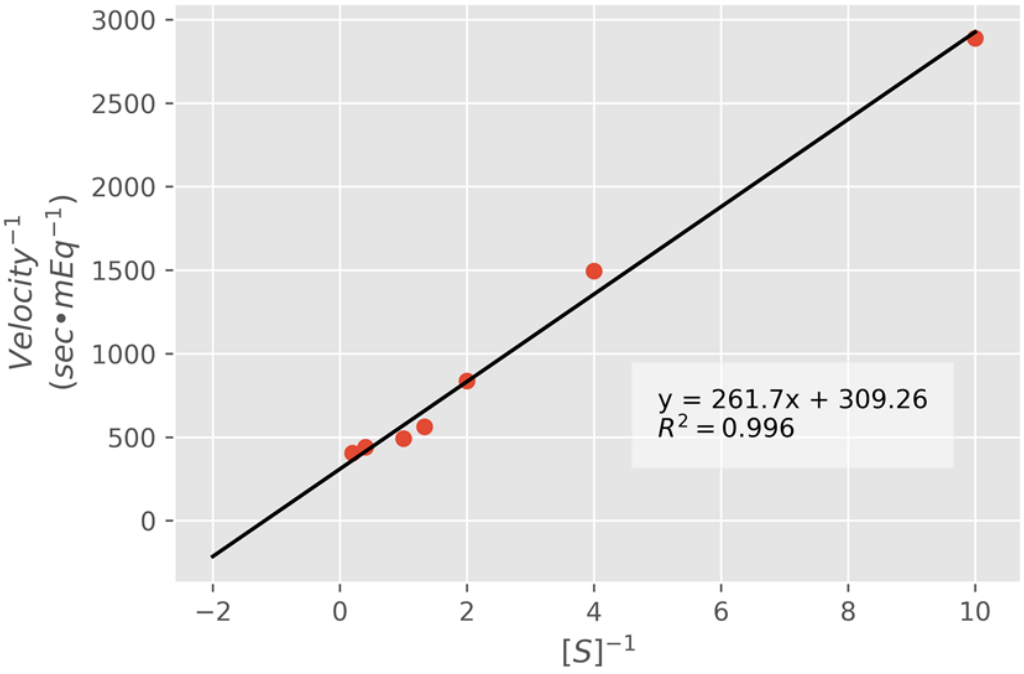

Figure 3.5 - Lineweaver-Burk plot for kinetics calculations of cetyl-palmitate hydrolysis by SFK3309. Cetly-palmitate concentrations ranged from 0.1 to 5 mM. Reactions were carried out at 37°C for 5 minutes. The concentration of SFK3309 was 0.206 mg/mL. All reactions were performed in triplicate and the average values were plotted. The K_{cat} was determined to be 11.63 s^{-1} and the k_{cat}/k_m was 13.74/mM•s^{-1}. The plot was made in python using Matplotlib [100].

Figure 3.6 - Thin layer chromatography of SFK3309 wax hydrolysis products. Wax-ester hydrolase assays were set up with substrates jojoba oil, cetyl-palmitate, and beeswax and treated with active SFK3309 (A) or SFK3309 that had been heat-deactivated (B). Reactions were incubated at 37C for 1 hour and lipids were recovered in a 2:1 chloroform:methanol solution. A 20 µL sample from each of the recovered lipid products was spotted on an HPTLC silica gel 60 TLC plate and double-developed with eluent hexane: diisopropyl ether: acetic acid (50:50:1). The plate was dried and then sprayed with coloring agent (27.4 mM 12-molybdo(VI) phosphoric acid n-hydrate and 50 mM sodium perchlorate dissolved in ethanol). The plate was then heated in an oven for 2 minutes until the bands appeared. The samples with active SFK3309 (A) appeared to create more products than the inactive SFK3309 (B) against each of the substrates.

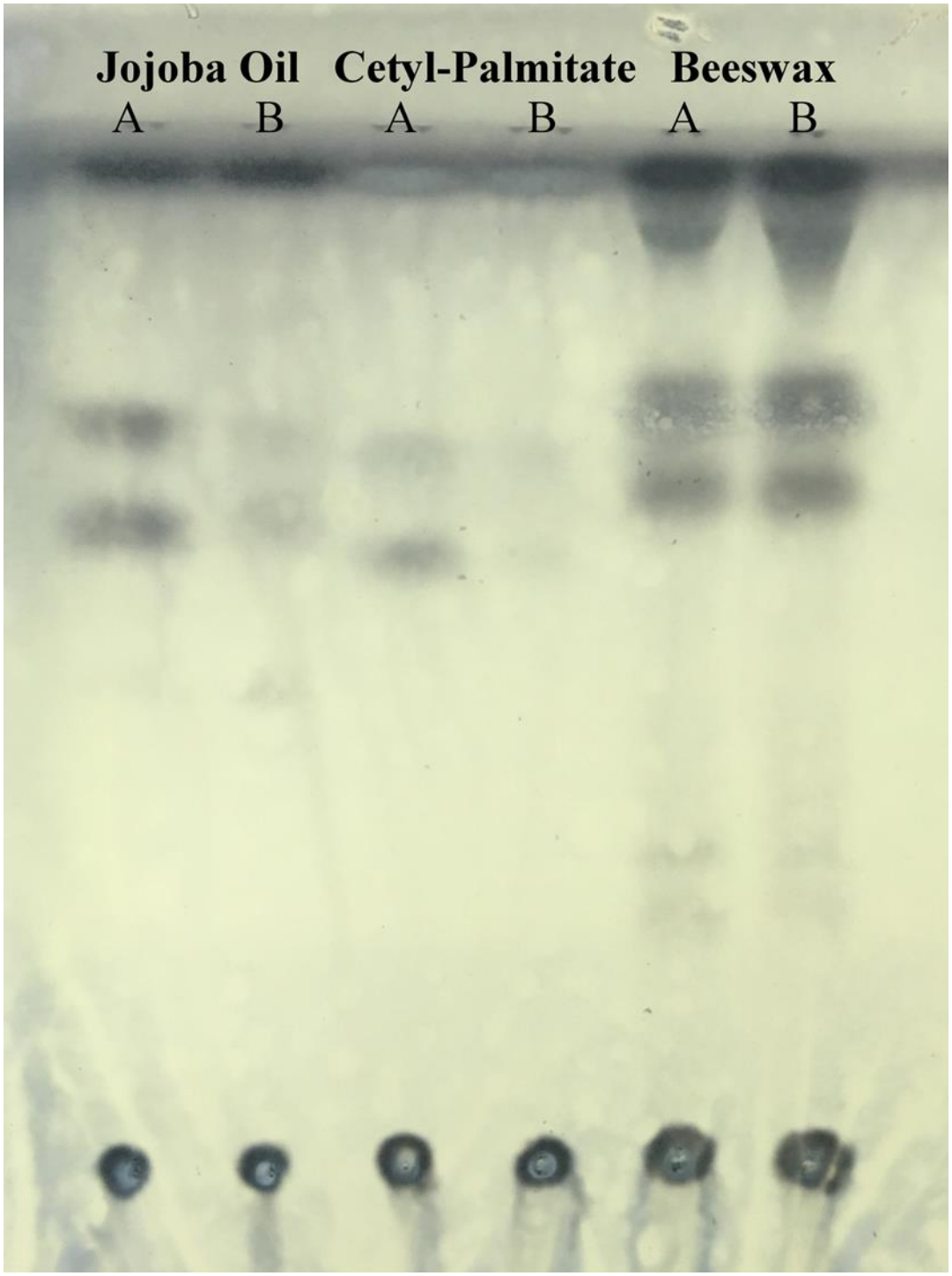
Jojoba Oil
Cetyl-Palmitate
Beeswax
A
B
A
B
A
B

3.5 Discussion

An initial set of 15 gene candidates were identified in feather-degrading bacterial strain *S. fradiae* var. k11 to encode for lipolytic activity. From this set, four enzymes expressed successfully in *E. coli* BL21 (DE3) and had detectable activity towards pNPA or pNPP (Table 3.1). The simplicity of the pNPP and pNPA assays allowed for a rapid identification of active enzymes and permitted the differentiation of enzymes capable of hydrolyzing long-chain, water-insoluble substrates (pNPP) or only active towards short-chained water-soluble substrates (pNPA). As the physical properties of wax suggest, it was necessary to identify the enzymes capable of acting on the water-insoluble substrate. Two enzymes were capable of hydrolyzing pNPP: SFK3087 and SFK3309.

The Lipase Engineering Database (LED) [103] classified SFK3087 as part of the alpha-beta hydrolase superfamily 25, while the ESTHER database [104] classified the enzyme as a member of the lipase class 1 and polyesterase-lipase-cutinase family. SFK3309 was classified by LED to the alpha-beta hydrolase 16 superfamily and the ESTHER database suggested the enzyme belongs to the lipase class 2 family. Given SFK3087 was classified as a member of the polyesterase-lipase-cutinase family, it seemed likely the enzyme would perform well against longer-chained substrates, such as plant cutin. However, only SFK3309 was active against wax substrates, and not SFK3087. Therefore, SFK3309 was selected as the central enzyme of the study.

DNA sequence analysis of SFK3309 cloned in the pET vector indicated four missense mutations (P85L, L87P, N223S, and L237P) from the lips221 sequence, as

shown in the MAFFT [101] alignment (Figure 3.1). Secondary structure prediction of lips221 by JPRED4 [105] suggested all SFK3309 mutations fell in loop regions and are less probable to severely disrupt overall protein structure.

The pelB signal sequence directed SFK3309 to the periplasm to provide an environment for proper protein folding. Expression of SFK3309 was carried out in *E. coli* BL21 (DE3) cells. Lipolytic activity in the supernatant as well as a decrease in final OD_{600} suggested some level of toxicity from expressing SFK3309 in the cells, a familiar issue in heterologous lipase expression [106]. Three different growth media were evaluated for improved SFK3309 expression: LB, TB, and Studier's ZYM-5052 media. LB is standard media found in labs, while TB provides added glycerol and uses a phosphate buffer [107], an understandable advantage considering free fatty acid products from lipolysis can affect pH. Studier's ZYM-5052 media is also buffered, but was able to further improve protein titers through using a blend of carbon sources and bypassing the need for IPTG induction for stable expression [108]. Expression experiments demonstrated LB and TB activity in the cell lysate was comparable, while Studier's ZYM-5052 medium improved expression levels about 3-fold (Figure 3.2).

By using the C-terminal 6X-histidine tag in the pET22b vector SFK3309 was purified from the cell lysate and able to reach approximately 90% purity from one round of Ni-NTA purification as demonstrated from SDS-Page (Figure 3.3). Yields of purified protein for 250 mL cultures were about 2 mg. A subsequent size-exclusion chromatography step was used to further separated SFK3309 from different oligomeric states. While Zhang et al. struggled with *E. coli* BL21 (DE3) as a heterologous host for extracellular expression of lipS221 [51], our experience suggests

reasonable protein expression levels can be achieved in *E. coli* BL21 (DE3) for SFK3309 by coupling periplasmic expression with autoinduction media. The reported K_m of 0.139 mM of lips221 expressed in *Pichia pastoris* [51] was comparable to the K_m of 0.078 mM that our group produced with SFK3309 against pNPP. The K_{cat} of SFK3309 was determined to be 1668 s^{-1}, which was within reason of values reported by similar enzymes [109].

SFK3309 was evaluated for wax ester hydrolase activity using three different substrates: jojoba oil, beeswax, and cetyl palmitate. Jojoba oil is derived from the seeds of *Simmondsia chinensis,* a plant native to the southwestern United States. The major lipid form in jojoba oil are wax esters, with the dominant carbon chain length being C_{40} and C_{42} [110]. Jojoba oil was an ideal substrate to work with initially due to the low melting point (10°C) allowing for easy handling and the negligent levels of free fatty acids made the detection of reaction products unambiguous. Beeswax is produced by honey bees and is 35% composed of wax monoesters with mostly C_{40} – C_{48} chain lengths [111] and myricyl-palmitate as the main component [112]. The higher melting temperature (63°C) of beeswax required heating in order to dissolve into 2-propanol, and the raw substrate further tested enzyme utility. Cetyl-palmitate was the third wax substrate used for analysis of wax-ester hydrolase activity. Cetyl-palmitate, like beeswax is a solid at room temperature (melting point = 54°C) and thus required similar handling. However, given cetyl-palmitate is easily obtained as a pure substrate, wax-ester hydrolase kinetic experiments were possible.

Previous groups have reported wax ester hydrolase assays that rely on radioactively labelled substrates [79, 85, 113], which require resources not accessible

to many labs. Others have also reported colorimetrically detecting free fatty acid products by first converting the fatty acids to copper salts and measured with sodium dithiocarbamate [82, 114] but these assays are time consuming and often rely on using strong organic solvents such as chloroform, thus limiting the use of plastic ware. The wax ester hydrolase assay used for this study first incubates an enzyme with a standard wax substrate, then utilizes the Wako NEFA HR(2) commercial kit to detect released free fatty acids. The entire assay can be performed in a basic lab equipped with a spectrophotometer using standard microtiter plates and microcentrifuge tubes and does not require an extraction step. The linear detection range of free fatty acids using the Wako NEFA HR(2) kit is 0.01-4.0 mEq/L. Since the standard curve is constructed using oleic acid, the millimole-equivalent unit is used to denote any free fatty acid released. Jojoba oil was used initially as a substrate to confirm the reliability of the assay.

SFK3309 exhibited enzyme activity against all three of the wax ester substrates using the described colorimetric assay. TLC was used to confirm the observed enzyme activity. From Figure 3.6, the active enzymes are able to produce more bands, corresponding to the hydrolysis of the substrate, though beeswax was an anomaly, which may be due to a high level of background. Enzyme kinetics were determined using cetyl-palmitate as substrate. Two groups have previously reported on the kinetics of wax-ester hydrolases and their results are available for comparison in Table 3.2. In Huang et al.'s study the synthetic substrate N-methylindoxyl myristate was used for kinetic experiments of an enzyme from jojoba cotyledons [82]. Their work found the enzyme's K_m value to be 9.3×10^{-5} M, within close proximity to the work of

Kalinowska and Wojciechowski, who used cetyl [1-^{14}C]palmitate as substrate and reported a K_m of 2.8×10^{-5} M for an enzyme from the roots of white mustard [84]. The constructed Lineweaver-Burk plot from our study suggests a good linear fit for our data (Figure 3.5). The K_m of SFK3309 was determined to be 8.5×10^{-4}, which is close to the other groups' values. We also found the K_{cat} of SFK3309 to be 11.63 s^{-1}

3.6 Conclusion

From the current study, we were able to identify two lipases from the feather-degrading bacteria *S. fradiae* var. k11 and characterize one of the enzymes as a wax-ester hydrolase. The described wax-ester hydrolase assay from our study allowed for the evaluation of enzyme activity against various wax substrates and permitted a kinetics experiment against cetyl-palmitate. Given the presence of waxy lipids on the surface of chicken feathers, the existence of wax-ester hydrolase activity from SFK3309 in *S. fradiae* var. k11 suggests a potential application in industrial feather hydrolysis.

Current literature on the enzymatic hydrolysis of wax esters is limited, with kinetic studies even more scarce. The adaptation of the wax ester hydrolase assay as reported here allows for a more accessible approach to evaluate wax ester hydrolase activity and yield results comparable with traditional techniques. Waxes are an important lipid class and have a presence across multiple industries. A more comprehensive investigation of enzymes capable of hydrolyzing wax esters may contribute to the development of existing and novel industrial processes.

Acknowledgements

Dr. Dario Mizrachi assisted with protein purification. Dr. Shinya Fushinobu provided suggestions for the substrate specificity assay and TLC, as well as lab space. Dr. Jeremy Baskin and Dr. Robert Moreau provided input in design of the wax ester hydrolase assay. Vectors for heterologous expression in *E. coli* were provided by Dr. Matthew DeLisa.

Notes

This chapter was submitted for publication and is under review.

CHAPTER FOUR

PROTEIN CRYSTALLOGRAPHY AND ATTEMPTS TO SOLVE THE STRUCTURE OF A WAX ESTER HYDROLASE

4.1 Summary

Wax esters are abundant in nature, but can sometimes pose health threats to humans or added laboriousness in processing materials. Our group has characterized SFK3309, a wax-ester hydrolase from feather-degrading microbe *Streptomyces fradiae* var. k11, and aimed to gain structural insight on the molecular mechanism of the enzyme. Homology modeling of SFK3309 proved difficult due to the lack of a suitable template. Attempts were made at crystallography, though diffracting protein crystals have so far been unobtainable. Small angle x-ray scattering experiments suggested SFK3309 was unstable in solution and formed multimeric aggregates. Thermal-shift assay based buffer screens revealed SFK3309 has large, exposed hydrophobic patches on the protein surface, evoking the possibility of hydrophobic interactions at play in the formation of aggregates. An additive screen gives promise of potential means at stabilizing SFK3309 in solution.

4.2 Introduction

Wax is both a synthetic and naturally occurring compound. Natural waxes are esters of monobasic carboxylic acids linked to monohydric or dihydric alcohols, while synthetic waxes are often non-ester, long alkane chains [112]. Natural waxes in plants and animals provide their hosts with a form of energy storage or waterproof protection from elements. Often in agricultural settings wax can become a hindrance in processing biomass [115] or pose a health risk in human nutrition (keriorrhea, steatorrhea, and seborrhea) [116]. Wax ester hydrolases [EC 3.1.1.50] are a potential catalyst to assist in these processes and others in an environmentally sound way.

To date, study on wax hydrolyzing enzymes has been limited. Most of the studies look at either wax digestion in fish [86, 117] or catabolism in wax-rich jojoba seedlings [82, 83], and only a few have looked at the actual characterization of enzyme activities [79, 85]. Our group has reported on the kinetic characterization of SFK3309, a wax-ester hydrolase identified from the feather-degrading bacteria *Streptomyces fradiae* var. k11 (Chapter 3). Chickens have an uropygial gland that excretes a waxy compound to protect their feathers [25]. However, the feather lipids create a barrier in the poultry industry to enzymatically process chicken feathers into animal feed and fertilizer co-products [118]. Structural information would provide fundamental insight on how the enzyme is able to accommodate the large, hydrophobic wax substrate in the enzyme's active site. However, as of yet there have not been any wax ester hydrolase structural studies.

The purpose of this study is to develop an understanding of the molecular structure of SFK3309 through molecular modeling, crystallography, and other experimental methods. Structural information on the enzyme will broaden the scientific cognizance of the enzyme class, and also hold commercial potential, as structural insight could facilitate the design of improved and industry-specific enzyme properties.

4.3 Materials and Methods

4.3.1 Model building

Initial sequence alignment was performed using the SALIGN web server [119], then manually adjusted to maintain the enzyme active site triad as annotated on the Lipase Engineering Database (LED) [120]. Multiple homology models were then built locally with MODELLER [121] using the UCSF Chimera package [102] as an interface. Visualization and molecular graphics were produced using PyMOL [122].

4.3.2 Protein Expression and Purification

SFK3309 was cloned into the pET22b vector, with the native stop codon removed in order to utilize the C' 6X-His tag. A heterologous expression host, E. coli BL21 (DE3), was used. An overnight seed culture was used to inoculate Studier's ZYM-5052 autoinduction media [108], and grown at 37 C, shaking, to an OD_{600} of 0.6-0.8, then transferred to a 16 C shaking incubator.

After 20 hours, the cells were harvested by centrifugation at 3000 × *g* for 10 minutes. The cells were resuspended in lysis buffer (20 mM HEPES, 500 mM NaCl, 10 mM imidazole, pH 7.6), then sonicated on ice for a total of 8 minutes at 50% amplitude with 4 second pulses on a Sonics (Newton, Connecticut, USA) Vibracell sonicator model VC130. After a centrifugation step at 15000 × *g* for 20 minutes at 4°C, the supernatant was collected and mixed with NiNTA agarose (McLab, South San Francisco, California, USA) for one hour. The slurry was then loaded on a gravity flow column (Bio-Rad, Hercules, California, USA) and the flow-through was collected. The column was then washed 3 times with wash buffer (20 mM HEPES, 500 mM NaCl, and 20 mM imidazole, pH 7.6). Elution buffer (20 mM HEPES, 500 mM NaCl, and 250 mM imidazole, pH 7.6) was then used to elute the bound protein from the NiNTA agarose.

The eluted protein was then concentrated in an Amicon ultra-15 centrifuge tube with a molecular weight cut-off of 10 kDa. Concentrated protein then further purified using an ÅKTA Explorer FPLC system (GE Healthcare, USA). Size exclusion chromatography (SEC) was performed on all NiNTA purified proteins. The column employed for purification was Superdex 200 10/300 GL or HiLoad Superdex

75 (GE Healthcare Life Sciences). Standards used to calibrate the Superdex 200 10/300 column were a lyophilized mix of thyroglobulin, bovine γ-globulin, chicken ovalbumin, equine myoglobin, and vitamin B12 (Molecular weight range: 1,3500-670,000 Da, pI range: 4.5-6.9) (Bio-Rad). Proteins were stored at 4℃ in SEC buffer (20 mM HEPES, 500 mM NaCl, 5 mM CaCl2, pH 7.6) until further analyzed for activity and purity. Protein purity was determined by sodium dodecyl sulfate - polyacrylamide gel electrophoresis (SDS-Page) using Coomassie blue staining.

4.3.3 Crystallization screens, optimization, and data collection

The crystallization screen experiments were based upon standard laboratory protocol [123]. Purified and monodispersed proteins were concentrated with an Amicon ultra-15 centrifuge tube to ≥8 mg/mL and measured using BCA. Protein samples were centrifuged at 10,000 × *g* for 3 minutes to remove formed aggregates or amorphous material. Screens were performed in 96-well sitting drop crystallization plates (Intelli-Plate 96, Hampton Research, Aliso Viejo, California, USA). A crystallization screen kit would be set up by first dispensing 40 µL crystallization solution into the plate reservoir. Protein solution (0.2 µL) was then placed in the plate well drop. An equal volume of the crystallization solution was then pipetted into the protein solution and the plate was sealed with film. Crystallization screen plates were incubated at either 4℃, 18℃, or 25℃. Crystallization screening kits included the JCSG kits: +Suite, Core Suite I, Core Suite II, and Core Suite IV (Qiagen, Venlo, Netherlands), and the

Hampton Research crystal screen HT kit (HR2-130). The screens were monitored regularly for signs of crystal growth.

Identified crystalline forms from the screen were further optimized by testing many of the different variables (temperature, pH, salt concentrations, protein concentration, etc.). Optimizations were carried out in 96-well sitting drop crystallization plates and 24-well hanging drop plates (HR3-172, VDX plate with sealant, Hampton Research). Hanging drop experiments were set up with 1 mL of crystallization solution in the reservoir and mixing 1-2 µL protein solution with equal volume crystallization solution for the hanging drop.

Initial crystal diffraction quality was tested using an in-house x-ray source. Diffraction data was collected at synchrotron radiation source at Spring-8 in Harima, Japan on pfBL1A and Cornell High Energy Synchrotron Source in Ithaca, NY on beamline F1.

4.3.4 Thermal-shift assay

A buffer screen was conducted as previously reported by Boivin, Kozak and Meijers (2013) [124] using the RUBIC Buffer Screen kit MD1-96 (Molecular Dimensions, Altamonte Springs, Florida, USA). Briefly, the RUBIC kit was centrifuged for 30 seconds at 500 rpm. From each condition, 21 µL was transferred to a PCR plate on ice. Protein at 1-2 mg/mL concentration was added to each well (2 µL). SYPRO

Orange (5000X) was diluted to 62X, then 2 µL of the diluted SYPRO Orange was added to each well without mixing. The PCR plate was then sealed with film. A melt curve was then run on a Roche LightCycler 480 (Basel, Switzerland).

A thermal shift assay was also performed coupled with an additive screen, similar to what was described before by Santos, et al (2012) [125]. In this case, the Protein Thermal Shift Dye kit by Applied Biosystems (Waltham, Massachusetts, USA) was used to test SFK3309 with different additives using the Additive Screen HR2-428 by Hampton Research (Aliso Viejo, California, USA). Briefly, 5 µL of Protein Thermal Shift buffer was loaded into each well of a PCR plate. A 10 µL protein solution was then added to the wells. Additive (2.5 µL) was then added to each well, followed by 2.5 µL of diluted Protein Thermal Shift dye (8X). The reactions were pipetted up and down 10 times to mix thoroughly. The plate was sealed with adhesive film and briefly centrifugated. The plate was then loaded into a ViiA 7 Real-time PCR system (Applied Biosystems) and the instrument was programmed as described by the reference manual. Melt curves were visualized in python using Matplotlib [100].

4.3.5 Small-angle X-ray scattering

Small angle X-ray scattering (SAXS) data was collected at the Cornell high Energy Synchrotron Source (CHESS) at the G1 station using 9.968 keV X-rays. The beam

diameter was 250 µm × 250 µm with a flux of 1.6×10^{11} photons/second. The detector was a dual Pilatus 100K-S SAXS/WAXS which had a q-space range of 0.006-0.8 $Å^{-1}$.

Protein was prepared and purified as described in 4.3.3 up until the SEC step. Size-exclusion chromatography was performed inline with SAXS (SEC-SAXS) in a similar matter to other groups [126]. Using a GE Åkta Pure FPLC operated at 4°C, a Superdex 200 Increase 10/300 column was pre-equilibrated with sample buffer (10 mM HEPES, 250 mM NaCl, pH 8.0) and used to continuously pass sample through the X-ray sample cell. About 1200 two-second exposures were taken per sample. Analysis of the SEC-SAXS data was performed in BioXTAS RAW [127] following online tutorials at https://sourceforge.net/projects/bioxtasraw/. The 3D reconstruction by a bead model was performed using DAMMIF, a part of the ATSAS package [128], with RAW used as the interface. DAMMIF uses tools DAMAVER to align and average constructed envelopes and DAMMIN to then refine the structure. Chimera was used for the visualization and smoothing of the envelope structure [102].

4.4 Results and Discussion

4.4.1 Sequence analysis, alignment, and model.

The ability to hydrolyze hydrophobic wax-esters and remain relatively stable in solution make the structural study of SFK3309 worthwhile. Structural information

would provide insight to understanding the biochemical function of the enzyme and how the enzyme's active site is able to accommodate such a large, hydrophobic substrate. This information can even be used for protein engineering studies and the development of an enzyme more relevant for industry purposes.

Often, the quickest approach to understand structure while starting with only the protein sequence is to build a homology model. Homology modelling is often based on the use of evolutionary relationships of known structures (template) with the protein of interest (target). Currently, homology modeling and threading are the only techniques available to generate reliable, high-resolution models of protein tertiary structure [129]. The SWISS-MODEL workspace is a quick and simple-to-use web tool to quickly build homology models [130]. However, the resulting templates from SWISS-MODEL for SFK3309 had sequence identity below the 'twilight zone' cutoff of 30%, which is thought to yield models of unreliable quality.

Instead, a comparative model template was identified by the National Center for Biotechnology Information (NCBI) Basic Local Alignment Search Tool (BLAST) [131] with the SFK3309 protein query sequence used against the protein data bank database [132]. A *Bacillus subtilis* lipase (PDB: 1I6W) that was first reported by van Pouderoyen, et al [133] had a sequence identity of 34%, and was determined to be the homology model template. A protein sequence alignment between SFK3309 and target 1I6W was then performed using Salign. The alignment was then manually edited for the conservation of the catalytic triad in 1I6w (S77, D133, and H156) as

annotated by the Lipase Engineering Database. The alignment can be seen in Figure 4.1.

With the generated sequence alignment, MODELLER was then used to construct five homology models. As can be seen in Figure 4.2a, the active triad was well conserved in the model, where residues S83, D174, and H206 correspond to S77, D133, and H156 from the template. An overlay of all five models can be seen in Figure 4.2b. Perhaps most noticeable is the mid region from residues 130-156, which are unmapped to a template and appear scattered as a result. The uncertainty surrounding such a large unmapped loop adds to the complexity in understanding how the enzyme may interact with the wax substrate. Not shown is a hydrophobicity color map of the protein surface, which suggested the exposure of multiple hydrophobic patches on the protein surface. The overabundance of hydrophobic residues on the surface of the protein would negatively affect SFK3309's solubility in water, incongruent with what was seen in the practical handling of the enzyme. Despite maintaining the active site in the model, the ambiguity of multiple residues and the overabundance of hydrophobic residues on the surface suggest the homology model as unreliable, and warranted the need for crystallography studies.

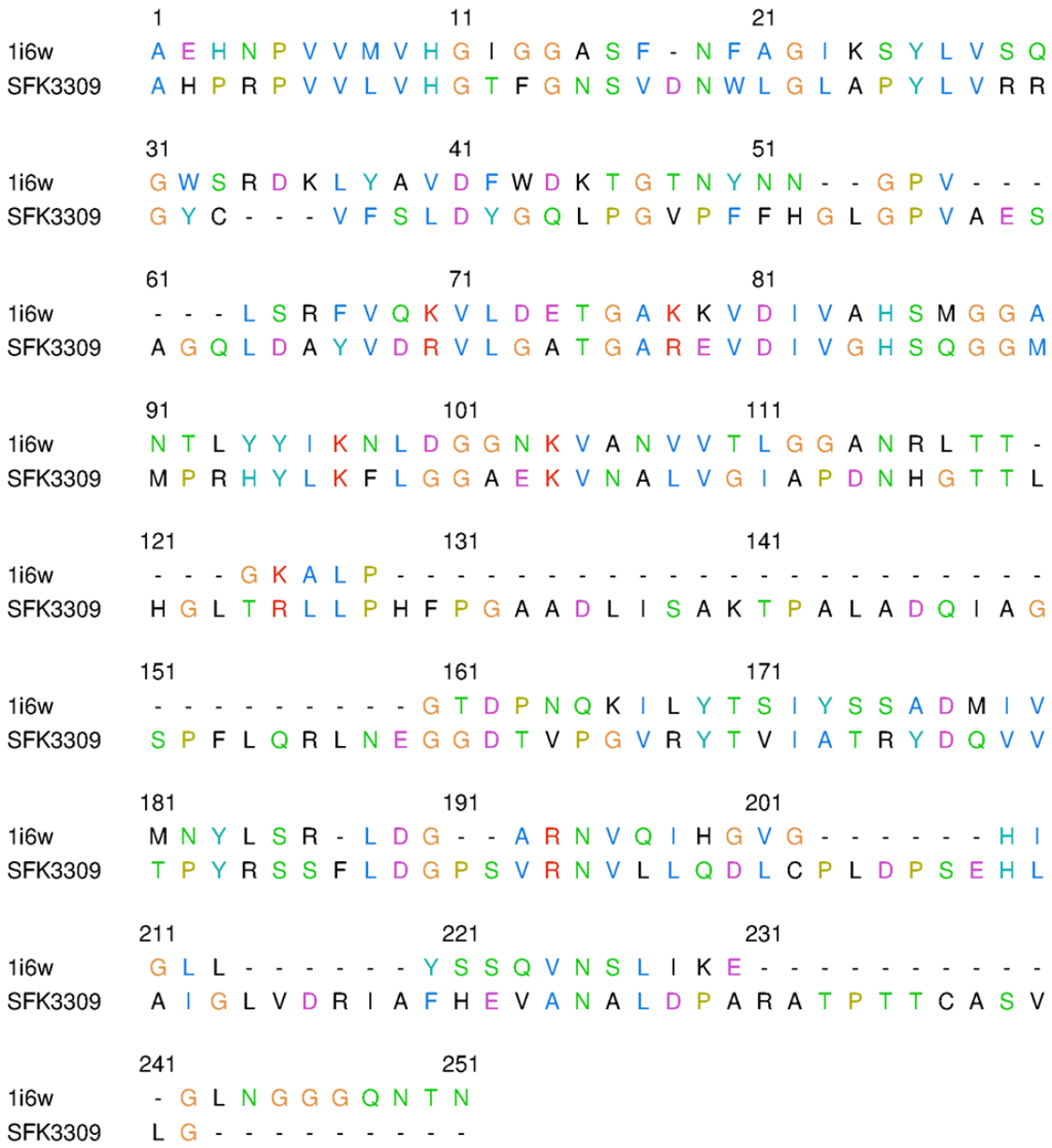

Figure 4.1 – Protein sequence alignment of SFK3309 with 1I6W. Chain A from PDB 1I6W was used as template and SFK3309 as target in the alignment. The alignment was generated using Salign, then manually edited to confirm the preservation of the catalytic triad (S77, D133, and H156), as annotated by the Lipase Engineering Database.

Figure 4.2 – SFK3309 homology models. On top (A) is model 1 of 5 generated using MODELLER with PDB 1I6W as template and SFK3309 as target. The active site was well conserved in the model with residues S83, D174, and H206 corresponding to the catalytic triad in 1I6W ((S77, D133, and H156). On bottom (B) is an overlay of all five models created by MODELLER. The white region corresponds to residues 130-156 and were largely unmapped to the template, which resulted in a loose loop. MODELLER was run using Chimera as an interface. Anaglyph image was rendered in PyMol.


A
S83
H206
D174
B

4.4.2 Crystallography screen

Protein X-ray crystallography is considered the gold-standard in terms of solving structures of biomolecules at atomic resolution. However, the technique is dependent on the ability to grow diffracting crystals of the biomolecule. Growing protein crystals is largely influenced by protein purity and the identification of suitable conditions (pH, temperature, buffer, protein concentration, etc.). Highly purified SFK3309 in the dimeric form was obtained after two rounds of chromatography (Ni-affinity, SEC). The protein was concentrated to 15 mg/mL and first tested with the JCSG core suite crystallization screening kits.

Two crystalline forms for SFK3309 were identified. Yielded crystals from the first crystalline form are seen in Figure 4.3. The reservoir solution consisted of 0.1 M sodium formate and 20% PEG 3350. Resulting crystals took on a tetragonal shape of about 0.05 mm in diameter after one week of growth at 18℃. Yet, efforts to recreate and optimize the crystal growth conditions were unsuccessful. Additionally, the crystals that grew from the screen were not large enough to test for diffraction. The second crystalline form identified from the screen had a reservoir solution of 0.2 M lithium sulfate, 50% PEG400, and 0.1 M sodium acetate (pH 4.5), which gave rise to rectangular crystals. The crystals were tested using an in-house x-ray and yielded a weak diffraction pattern and so efforts to optimize the crystal growth conditions were sought. Figure 4.4 shows one of the many crystals that grew from the optimization. However, diffraction patterns of the crystals collected on the 1A beamline at Spring-8 suggested a diffraction pattern other than a protein.

Additional screens were set up using the Hampton Research crystal screen HT kit (HR2-130) at room temperature. The crystalline form with a reservoir solution of 0.4 M ammonium phosphate monobasic was identified. Crystals took on a thin needle-like shape after two weeks of incubation (Figure 4.5). However, the crystals were either too thin, or did not diffract when tested at the F1 beamline at CHESS. The crystal growth conditions were reproducible using the hanging drop technique and conditions were further optimized and incubated at 18°C. After four weeks, the thin needle crystals began to form larger bundles. Diffraction quality of the crystals has yet to be determined.

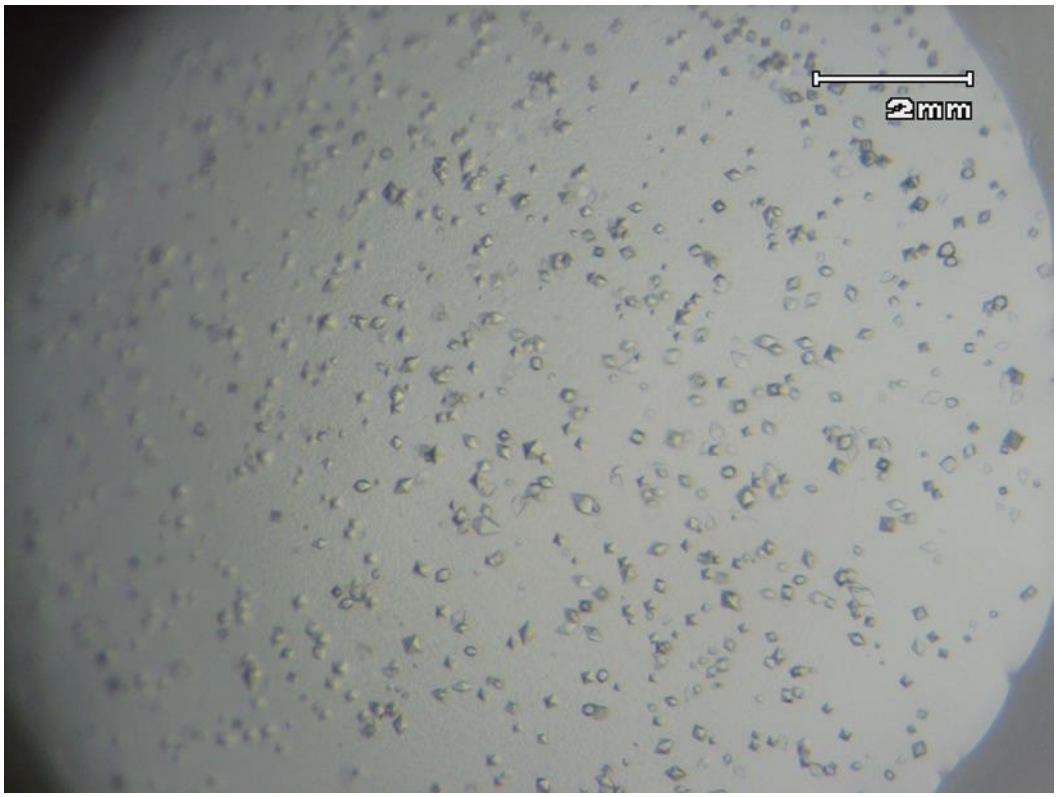

Figure 4.3 – Crystalline form for SFK3309 crystals identified using JCSG Core + kit. Protein was in 20 mM HEPES, 500 mM, and 5 mM $CaCl_2$ with pH 7.6 and protein concentration was 15 mg/mL. The reservoir solution was 0.1 M sodium formate and 20% PEG 3350. Crystal growth occurred after approximately 1 week while being incubated at 18℃. Yielded crystals formed a tetragonal shape, approximately 0.05 mm in diameter.

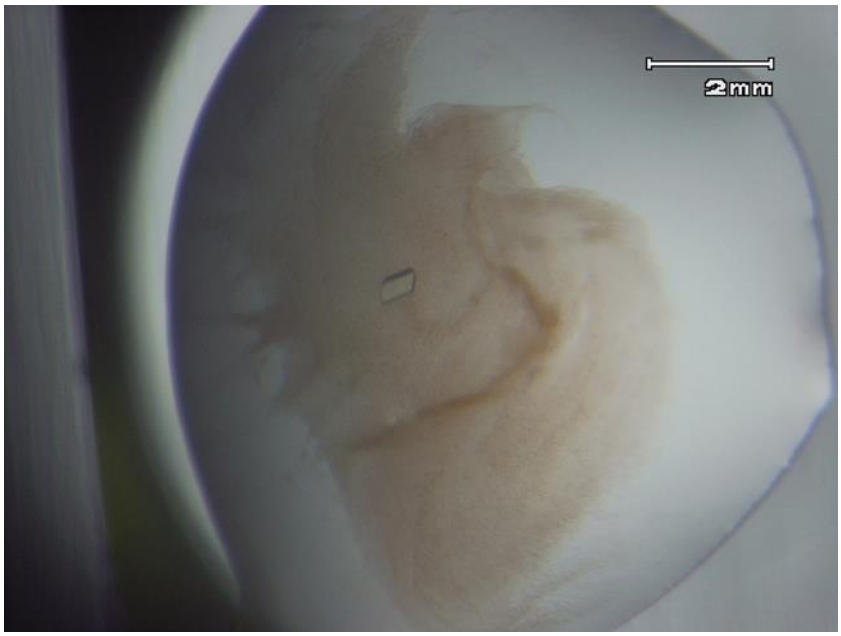

Figure 4.4 – SFK3309 optimization of crystalline form. Multiple concentrations of lithium sulfate and PEG400 were tested, along with varying pH of sodium acetate. The conditions for the image contained 0.18 M lithium sulfate, 42% PEG 400, and 0.1 M Sodium acetate, at pH 4.1.

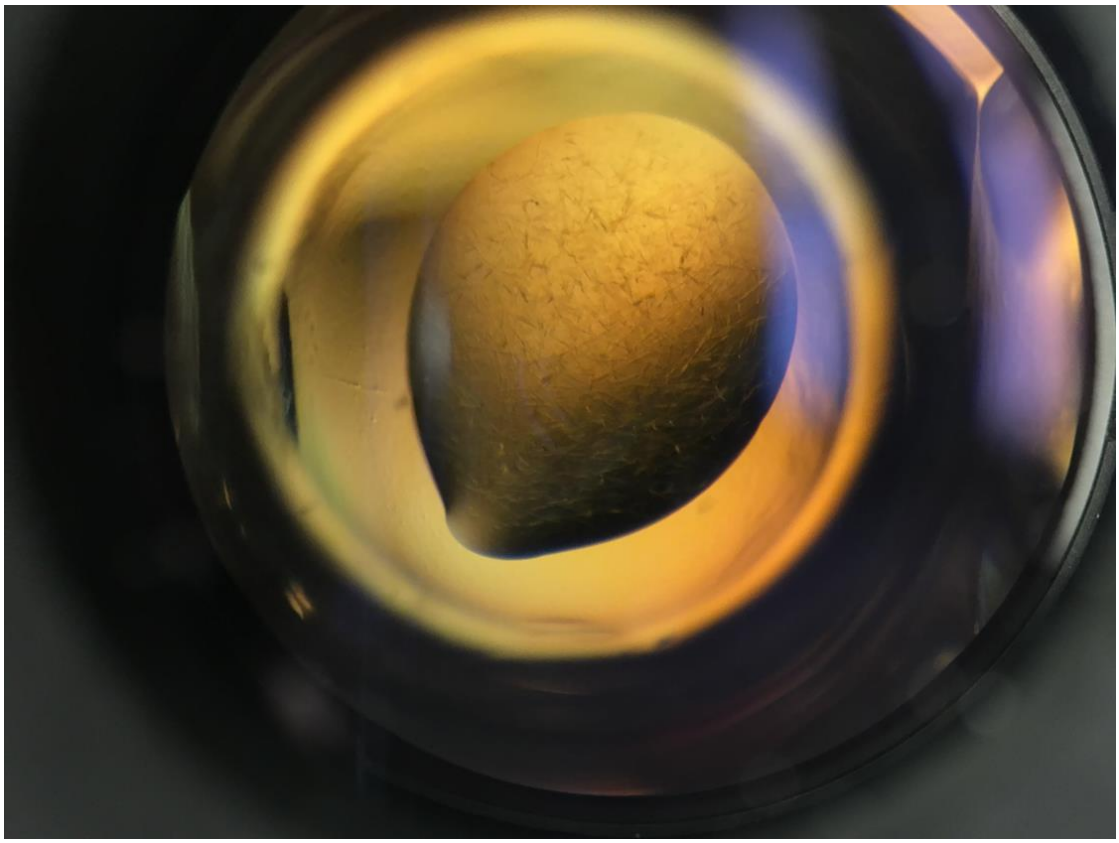

Figure 4.5 – Crystalline form identified for SFK3309 from Hamilton screen. Concentration was at 15 mg/mL in 10 mM HEPES, 250 mM NaCl, pH 8.0 buffer. The reservoir solution was 0.4 M ammonium phosphate monobasic. Growth conditions were carried out at a controlled room temperature.

4.4.3 Small angle x-ray scattering

Often when one is unable to grow diffracting protein crystals, SAXS is considered a viable alternative to gain structural insight on a protein. Like protein crystallography, SAXS requires the protein of interest to be highly purified, monodisperse, and free from aggregation. However, SAXS experiments can be performed with much less protein, usually on the order of 1-10 mg/mL and progressively less for larger molecules [134]. SAXS also has the advantage of speed compared to crystallography and NMR, as well as limited buffer restrictions, where physiological buffers are often okay. These advantages come at the cost of resolution, where SAXS envelope structures are limited to about 10 Å. Additionally, SAXS can provide information on the molecular weight, oligomeric state of the protein in solution, and flexibility or unfoldedness often undetected in x-ray crystallography experiments.

The G-line at CHESS allows for SEC to be run inline with SAXS, allowing for immediate diffraction data to be collected as the protein is eluted from the column. For this reason, SEC-SAXS works well for some aggregating proteins, but requires a more concentrated protein to accommodate for the dilution on the column. SFK3309 was concentrated to 13.7 mg/mL and separated on a Superdex 200 Increase 10/300 column set up on G1 at CHESS. Unfortunately, SFK3309 did not separate well and appeared to have heavy aggregation. Nonetheless, RAW was used in an attempt to construct a Guinier plot with one of the multimeric forms of the protein. The Guinier is a straightforward way to assess sample quality and can be used to derive R_g and mass

information [135, 136]. The q range for the Guinier plot was between 0.011 and 0.021, yielding a good linear fit (R^2=0.966). The R_g was determined to be 60.62 Å and an I(0) score of 0.0012. The molecular weight was estimated to be between 200 and 250 kDa, suggesting 7-8 chains in complex. A bead model was then constructed with DAMMIF from the ATSAS package where 15 reconstructions were created. The envelopes were aligned and averaged with DAMAVER, then averaged and refined with DAMMIN. The mean normalized spatial discrepancy (NSD) was 0.567, where an NSD below 0.7 is considered good. The ensemble resolution was estimated to be 43±3 Å as calculated by SASRES [137]. The envelope structure of the SFK3309 multimer was rendered in Chimera and can be seen in Figure 4.6, resembling a drumstick.

The propensity for lipases to aggregate into complex multimers is not uncommon. From the PDB structure 3D2C of a *Bacillus subtilis* lipase reported by Ahmad, et al [138], the assembly of a dodecamer can be seen (Figure 4.7A). By applying a hydrophobicity filter on the surface display of the structure, it is obvious that the protein chains are susceptible to hydrophobic interactions (Figure 4.7B). A deeper look at the complex reveals three chains grouped together around their hydrophobic active sites (Figure 4.8). The ability of SFK3309 to hydrolyze large wax substrates suggests the enzyme has a large hydrophobic active site, which may be a liability for aggregating in solution. The data obtained from the SEC-SAXS experiments implies the need to identify better buffer conditions for SFK3309 in order to preserve protein monodispersity and for structural studies to continue.

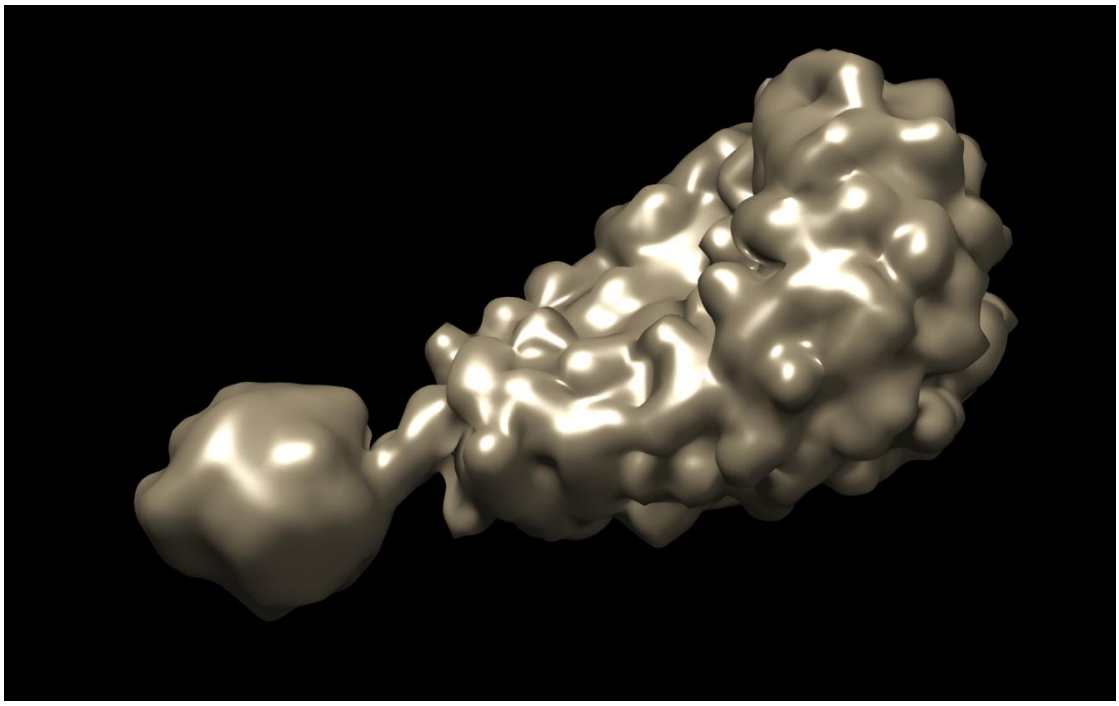

Figure 4.6 – Envelope structure of SFK3309. A 3D reconstruction by bead models was first performed with DAMMIF/N in RAW and the consensus shape of 15 generated models was prepared in DAMAVER, a part of the ATSAS package. The surface was then constructed with FOXS with Chimera from the SAXS data. The resulting structure is large enough for the formation of an octamer of SFK3309.

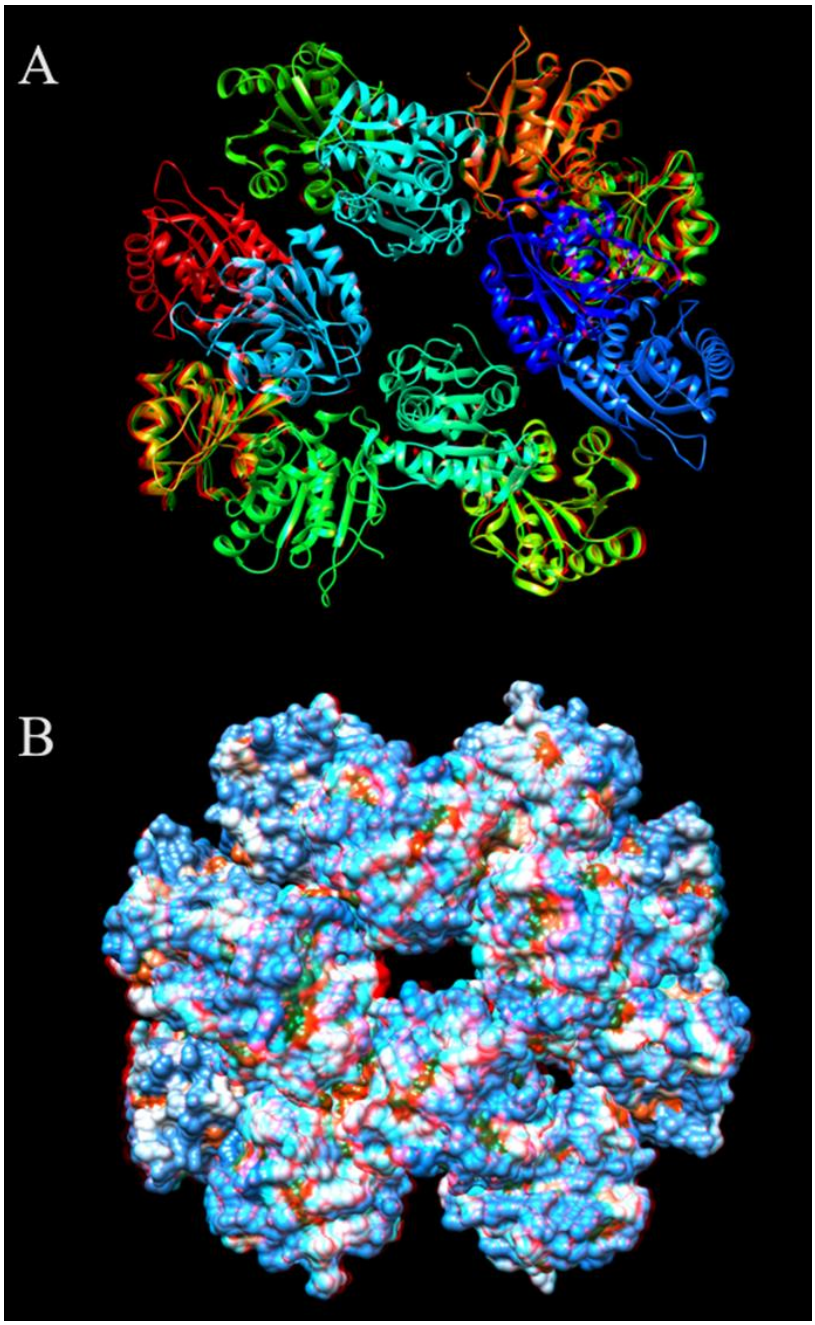

Figure 4.7 – A ribbon and surface representation of PDB 3D2C. The protein assembled into a dodecamer (12-mer) as can be seen in the ribbon representation (A). A hydrophobicity scale was applied (B), where blue represents hydrophilic residues and orange for hydrophobics. The hydrophobic interactions of the protein appear responsible for the multimeric state of the enzyme. Image produced with Chimera.

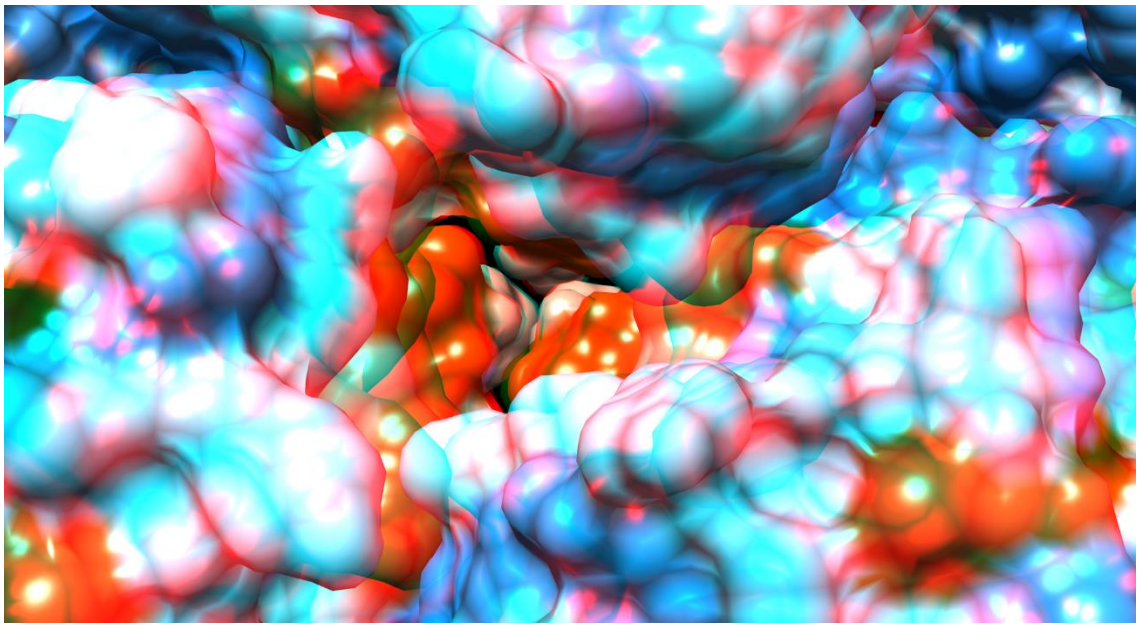

Figure 4.8 – Hydrophobic clustering in PDB 3D2C. A close-up anaglyph image reveals the hydrophobic clustering present in the 3D2C lattice. The surface structure is displayed with a hydrophobicity coloring scale used. Blue represents hydrophilic residues, white is for neutral residues, and orange represents hydrophobic residues. The hydrophobic active site from the individual protein chains group together to limit the hydrophobicity of the surface. The image was rendered with Chimera.

4.4.4 Protein optimization

The stability of a protein in solution has tremendous effect on the success of crystallization experiments [139]. High throughput screening of suitable buffers and even additives to improve protein monodispersity has been reported with some success [140]. Thermofluor or thermal-shift assays to determine protein stability in solution are a fast and inexpensive approach [141] and can be carried out for high throughput screens of buffers and additives [142]. The principle for thermal-shift assays is simple: a protein is heated in the presence of a hydrophobic dye, such as SYPRO Orange, which as the protein begins to unfold at an elevated temperature, the dye will bind to the exposed hydrophobic protein core and a fluorescent signal can be detected in a qPCR thermal cycler. Stable proteins will unfold at higher temperatures than their less stable counterparts. Results from the thermal-shift experiments would provide insight on suitable buffers and additives to stabilize SFK3309.

The RUBIC buffer screen (Molecular Dimensions) consists of 96 conditions to test global parameters that effect protein stability: salt concentration, buffer type, buffer concentration, and pH. Results from the RUBIC buffer screen for SFK3309 can be seen in Figure 4.9. A general trend in all the melt curves from the buffer screen has a high fluorescent signal at the start, which then tapers out by 85°C. This suggests SFK3309 has a large enough hydrophobic patch on the surface, most likely at the enzyme active site, that the SYRPO Orange is binding before the protein even needs to unfold. This would support our earlier claim that SFK3309 is likely aggregating due to

hydrophobic interactions. Since a single buffer was not identified from the buffer screen to establish a proper melt curve for SFK3309, the use of additives to provide protein stability was evaluated.

An additive screen from Hampton Research (HR2-428) was used to evaluate the effects on SFK3309 in attempts to reduce the premature hydrophobic interaction with the thermofluor dye and provide a homogenous, monodisperse environment of the protein. The additive screen kit covered 18 different reagent classes and contained 96 distinct reagents and excipients. Results from coupling the additive screen with a thermal-shift assay are represented in Figures 4.10-12. Although a traditional melt-curve was not observed in any of the samples, many additives had a profound impact on starting fluorescent levels. Notably, additives classified as non-detergents, volatile organics, amphiphiles, and chaotropes appeared to have the best results at reducing initial binding with the dye. Interestingly, the volatile organic, 2-propanol, is also present in the enzyme activity assays used to characterize SFK3309. Still, the initial fluorescent levels are not at baseline, the slopes are not as steep as a typical melt curve, and the presence of a second peak suggests complex binding with the dye. The use of additives does seem promising for structural studies of SFK3309, and may be necessary in order to achieve stable and monodisperse SFK3309 in solution.

Figure 4.9 – SFK3309 Buffer Screen. The RUBIC buffer screen from Molecular Dimensions was used to test SFK3309 96 conditions with a range of ionic strengths, pH values, and salt concentrations. The thermofluor, SYPRO Orange, would activate when bound to unfolded protein. A melt curve was then run on a Roche LightCycler 480 up to 95°C. Neither condition produced a standard melt curve to indicate favorable buffer conditions for SFK3309. The plots were made with Matplotlib.

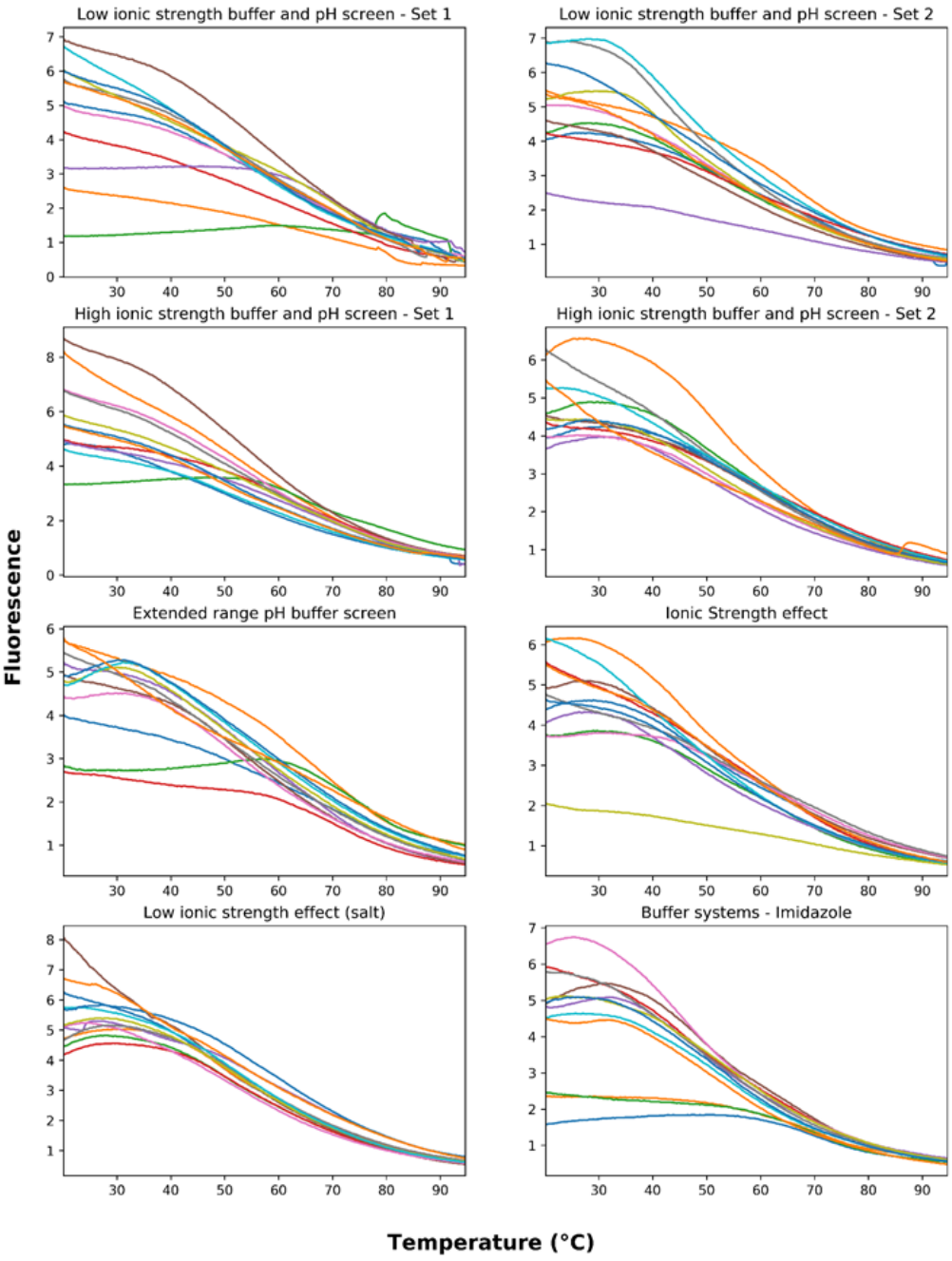
Low ionic strength buffer and pH screen - Set 1
Low ionic strength buffer and pH screen - Set 2
High ionic strength buffer and pH screen - Set 1
High ionic strength buffer and pH screen - Set 2
Extended range pH buffer screen
Ionic Strength effect
Low ionic strength effect (salt)
Buffer systems - Imidazole
Fluorescence
Temperature (°C)

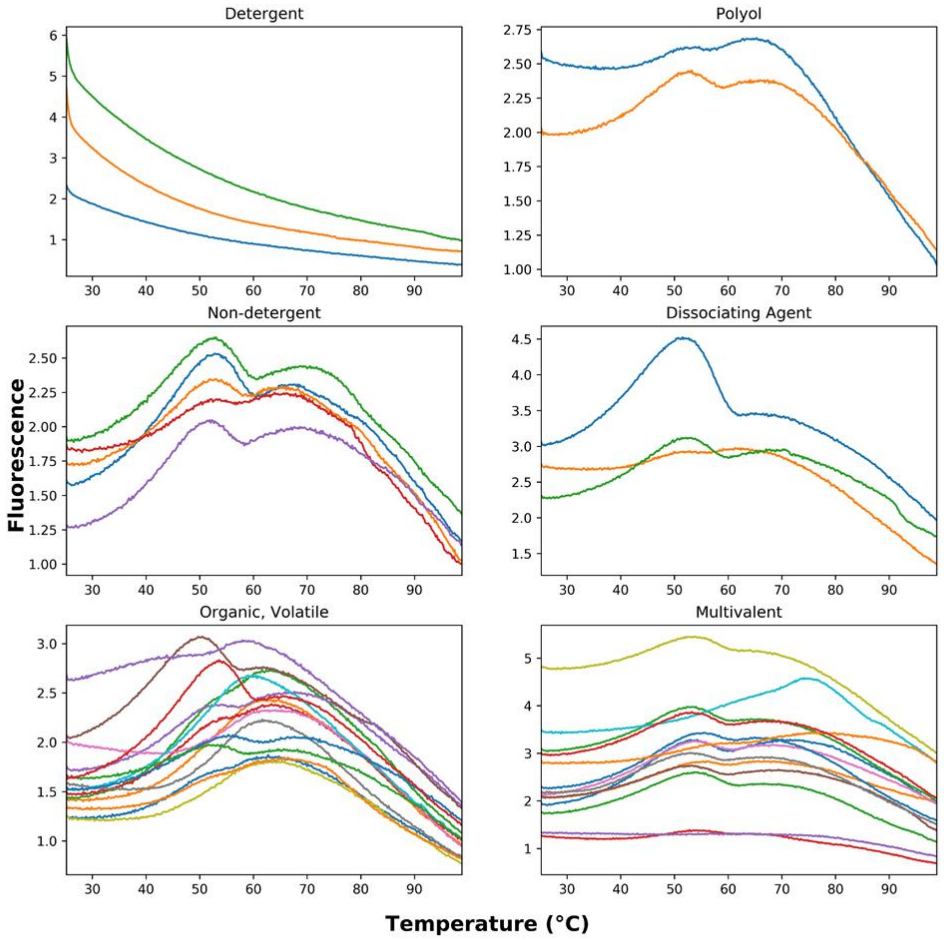

Figure 4.10 – SFK3309 additive screen 1 of 3. The protein thermal shift dye kit from Applied Biosystems was used in conjunction with Hampton Research's additive screen kit HR2-428 to test SFK3309 for favorable additives. The melt curve was obtained on a ViiA 7 Real-time PCR system (Applied Biosystems) for a temperature range of 25 to 95°C. Displayed additive classifications include: detergent; polyol; non-detergent; dissociating agent; organic, volatile; and multivalent.

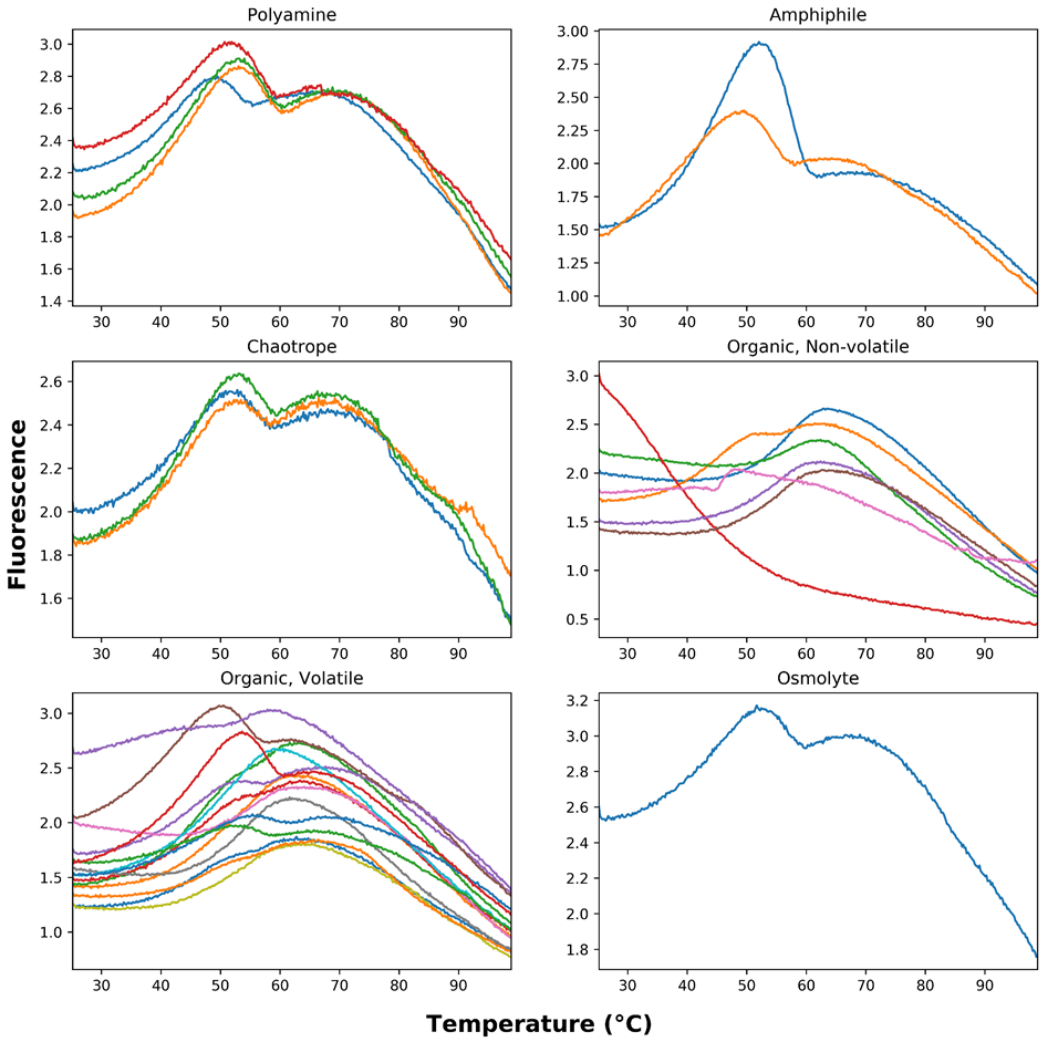

Figure 4.11 – SFK3309 additive screen 2 of 3. In continuation to Figure 4.10, additive classifications include: polyamine; amphiphile; chaotrope; organic, non-volatile; organic, volatile; and osmolyte.

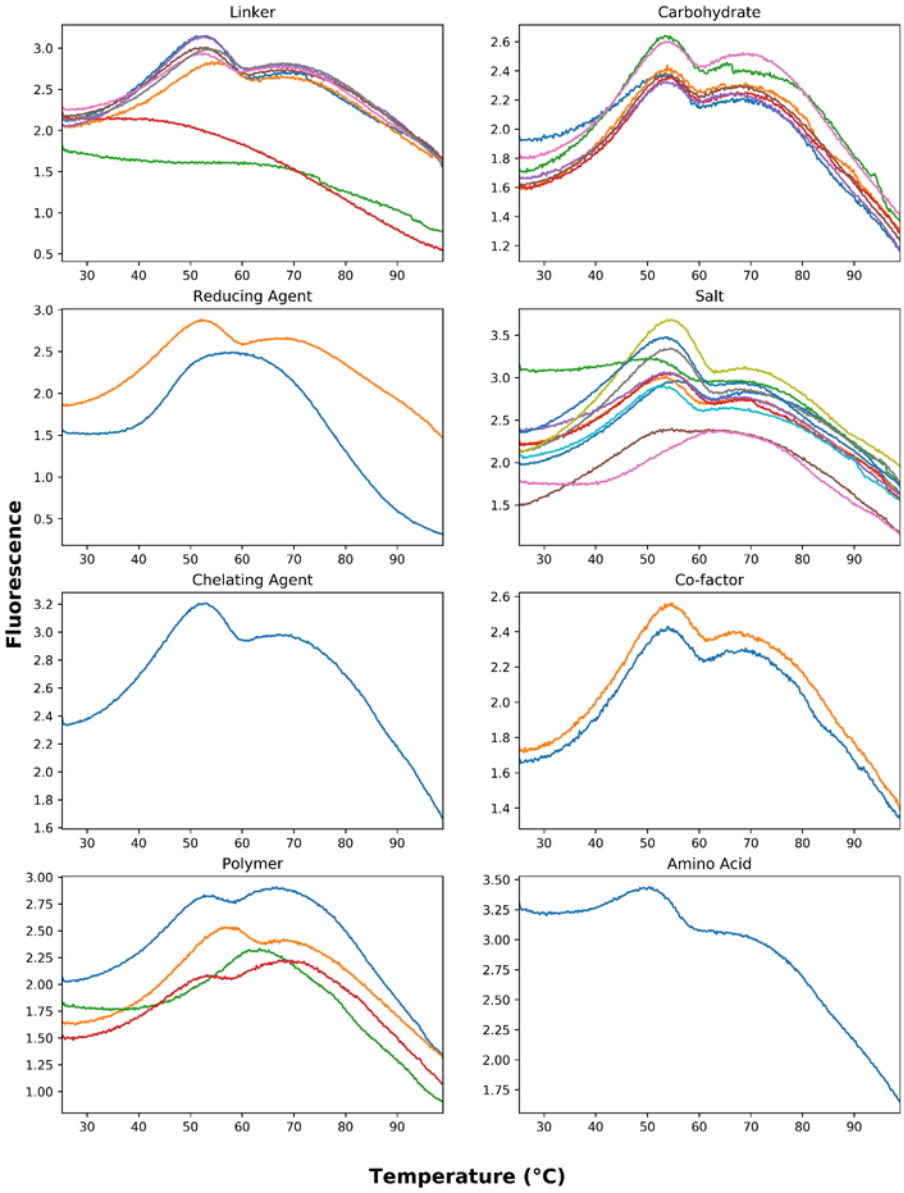

Figure 4.12 – SFK3309 additive screen 3 of 3. In continuation with Figures 4.10 and 4.11, additive classifications include: linker; carbohydrate; reducing agent; salt; chelating agent; co-factor; polymer; and amino acid.

4.5 Conclusion

The absence of a suitable template has made homology modeling unreliable for SFK3309. The large gaps and limited sequence identity (<35%) provides limited confidence in the generated models. Attempts at crystallizing SFK3309 have so far, fallen short, and given the data generated from the SAXS experiments and buffer screens, the stability of SFK3309 in solution is in question. A plausible explanation is SFK3309 is susceptible to hydrophobic interactions at the enzyme active site, forming aggregates in solution and preventing any chances at monodispersity. Additives appear promising for improving SFK3309, particularly non-detergents, volatile organics, amphiphiles, and chaotropes, though further investigation is necessary.

ACKNOWLEDGEMENTS

Prof. Shinya Fushinobu provided lab space and screening kits and helped with initial experiments to get started with crystallography and modelling. Prof. Tohru Terada assisted with selection of the molecular model template and alignment. Dr. Takatoshi Arakawa was able to analyze some of the crystals at Spring-8. Dr. Irina Kriksunov assisted with analyzing crystals at CHESS. Dr. Dario Mizrachi and Dr. Qingqiu Huang helped with protein purification. Steve Halaby and Prof. Chris Fromme helped with crystallization screens and the buffer screen.

CHAPTER FIVE

MOLECULAR MODELING AND ENGINEERING OF A LIPASE

5.1 Summary

Attempts were made to engineer a lipase from the feather-degrading microorganism, *Streptomyces fradiae* var. k11, for improved catalytic activity and thermal stability. A structure-guided consensus approach was used for identification of amino acid residue targets to modify and bring about desired protein characteristics. By coupling bioinformatics analysis of the protein sequence and a homology model built using SWISS-MODEL using PDB 1JFR as template, five surface mutants were designed and tested for impacts on protein stability. The Y83A mutation on the surface of the lipase increased protein stability by over 3.76℃ ($P<0.01$), however the mutation had a profound negative impact on enzyme activity. Other mutations had negligible effects on thermal stability. A residue near the active site of the lipase (S119) was also investigated for its suspect position and potential impact on catalytic activity. Saturation mutagenesis was used to test ten different amino acids at residue 119. Most mutations generated at residue 119 negatively affected enzyme activity. An exception was found in S119F, which saw a slight increase in thermal stability (+0.31℃) (not significant) and an overall improvement in enzyme performance, as demonstrated by a 47% better K_{cat}/K_m score ($P<0.01$). The structure-guided consensus approach lead to minor improvements of SFK3087, but a more aggressive strategy is necessary to bring

about dramatic changes and the accommodation of wax esters at the enzyme active site.

5.2 Introduction

Lipases are a popular enzyme class and have a large presence in industry [143]. Applications of lipases has been considered 'boundless' and have already been employed in the manufacture of pharmaceuticals, food, biofuels, leather, cosmetics, medical diagnostics, and detergents, just to name a few [144]. Our group's interest in lipase stems from an overall goal of enzymatically hydrolyzing chicken feathers, a 5 million ton waste product generated annually from the poultry industry [145]. Feathers have been estimated to contain approximately 11% fat content [64] and we suspect removing the lipids with a lipase will allow for a more synergistic hydrolysis of the dominant ß-keratin found in the feathers by other enzymes.

Lipase hydrolysis of lipid substrates is able to occur due to the enzyme's catalytic triad, which contains aspartate, histidine, and serine, and the presence of an oxyanion hole which provides intermediary stability during hydrolysis. Lipase catalysis is described by Casas-Godoy et al. [146], which is initiated by an acylation step, where a proton is transferred from the aspartate, to the histidine, and then on to the catalytic serine residue's hydroxyl group. The serine becomes activated and performs a nucleophilic attack on the substrate's carbonyl group, resulting in a tetrahedral intermediate with a negative charge on the oxygen group of the carbonyl group. Hydrogen bonding between the oxyanion hole of the enzyme and the substrate

provide necessary stabilization to the charge distribution. Water is then able to carry out a nucleophilic attack on the enzyme, resulting in the release of the product and regeneration of the enzyme in the deacylation step.

Our lab has identified two lipolytic enzymes from the feather-degrading microorganism *Streptomyces fradiae* var. k11, though only one of the enzymes is capable of hydrolyzing the major lipid class on feathers, wax-esters [27]. The enzyme without activity against wax-esters, SFK3087, was used in this study for structural characterization using homology modelling and site-directed mutagenesis. The study was designed to probe residues for improved catalytic activity and thermal stability and lay the foundation for future work in extending SFK3087 specificity to wax esters.

5.3 Materials and Methods

5.3.1 Materials

Chemicals were purchased from Sigma Aldrich (St. Louis, Missouri, USA) unless otherwise noted.

5.3.2 Sequence analysis and homology modelling

The SFK3087 sequence was annotated by the RAST server using the RASTClassic annotation scheme [94]. SFK3087 was further classified by the Lipase Engineering Database (LED) [103] and the ESTHER database [104]. Pred-TAT was used for the

determination of any signal peptide [48]. Evolutionary conservation of the SWISS-MODEL workspace was used to quickly build homology models for SFK3087 [130].

5.3.3 Docking

The structure of cetyl-palmitate was constructed in the Maestro software package (Schrödinger, LLC, Tokyo, Japan) [147]. AutoDock Tools was used to add polar hydrogens to the protein model and set up a grid box for the search space for ligand confirmations in the enzyme active site [148, 149]. The box origin (x, y, z) coordinates were set to (50, 30, 39) and dimensions were sized to 24$Å^3$. AutoDock Vina was then run with an exhaustiveness score of eight to dock cetyl palmitate into the active site of SFK3087 [150]. Results were visualized in PyMOL [151].

5.3.4 Cloning, expression, and purification

The gene sequence for SFK3087 was amplified from prepared genomic DNA of *Streptomyce fradiae* var. k11 using Platinum Pfx polymerase purchased from Thermo Fisher Scientific (Waltham, Massachusetts, USA). Genomic DNA from *S. fradiae* var. k11 was purified as described elsewhere [50]. PCR products were ligated into the pET22b(+) vector and made use of the vector's pelB signal peptide and C-terminal 6X histidine tag. The completed construct was cloned into *E. coli* BL21(DE3) cells and selected over LB ampicillin plates. Plasmid DNA was isolated using a QIAGEN (Venlo, Netherlands) Qiaprep Spin miniprep kit and the DNA sequence was verified

using A Plasmid Editor (ApE)[49] with the sequencing results from the Cornell Biotechnology Resource Center DNA Sequencing facility (Ithaca, NY, USA).

Proteins were expressed by first growing an overnight seed culture. The seed culture was then used to inoculate fresh Luria broth (LB) or Studier's ZYM-5052 autoinduction media [108], and grown at 37℃, shaking, to an OD_{600} of 0.6-0.8. LB cultures were then inoculated with isopropyl-ß-1-thiogalactopyranosid (IPTG) to a final concentration of 0.01 μM. Cultures were then transferred to a 16℃, shaking incubator for ~20 hours.

Cells were harvested by centrifugation at 3,000 × *g* for 10 minutes and resuspended in 1/10 of the culture volume with lysis buffer (20 mM HEPES, 500 mM NaCl, 10 mM imidazole, pH 7.6). The cells were then placed on ice and sonicated in two 4-minute intervals at 50% amplitude with 4-second pulses on a Sonics (Newton, Connecticut, USA) Vibracell sonicator model VC130. The lysed cells were centrifuged at 15,000 × *g* for 20 minutes at 4℃ and the supernatant was saved. The soluble proteins were then mixed with Ni-NTA agarose (McLab, South San Francisco, California, USA) for one hour at 4℃. The slurry was then loaded onto a gravity column. After the agarose settled the flow-through was collected. Fifteen bed volumes of Wash buffer (20 mM HEPES, 500 mM NaCl, and 20 mM imidazole, pH 7.6) was used to wash the column. Ni-NTA bound protein was eluted with five bed volumes of elution buffer (20 mM HEPES, 500 mM NaCl, and 250 mM imidazole, pH 7.6).

5.3.5 Enzyme assays

Protein concentration was determined using the Bicinchoninic Acid (BCA) assay as described [98] with the incubation step taking place at 37°C. Lipolytic enzyme activity was determined by the hydrolysis of p-nitrophenyl palmitate (pNPP). Lipase assays were set up as described [51]. Briefly, a 10 mM substrate solution of pNPP was constructed in 2-propanol. Reaction buffer was prepared separately (50 mM sodium phosphate, pH 8.0, 0.1% gum arabic, 0.2% sodium deoxycholate) and mixed 9 to 1 with substrate solution. Enzyme (10 µL) was loaded into wells of a 96-well microtiter plate and the buffered substrate solution (240 µL) was rapidly added to each well. A kinetic read was taken for 2 minutes with 15 second intervals taking readings at 410 nm on a SpectraMax M2e spectrophotometer (Molecular Devices, Sunnyvale, California, USA). One enzyme unit was defined as the hydrolysis of 1.0 µmole of pNPP per minute at pH 8.0 at room temperature and was represented by the release of p-nitrophenol. The p-nitrophenol millimolar extinction coefficient of 18.3 was used.

5.3.6 Mutagenesis

The Q5 site-directed mutagenesis kit (New England Biolabs, Ipswich, Massachusetts, USA) was used to introduce mutations into the SFK3087 gene on the pET22b expression vector according to the provided instructions. Oligonucleotides used during the PCR reaction to incorporate the intended mutations were designed using the NEBaseChanger web tool (http://nebasechanger.neb.com/) and then ordered from Integrated DNA Technologies (Coralville, Iowa, USA). In designing oligonucleotides for the generation of the saturated mutagenesis experiments, mixed DNA bases with

the degenerate codons NDT and NRT were used. Apart from the standard A, T, G, and C nucleotides, N Is a mix of all four, D encompasses A, G, and T, while R is a mix of only A and G.

5.3.7 Thermal-shift assay

The Protein Thermal Shift Dye kit by Applied Biosystems (Waltham, Massachusetts, USA) was used to determine the thermal stability of SFK3087 and the designed mutants. As described in the provided instructions with the kit, 5 µL of Protein Thermal Shift buffer was loaded into wells of a 96-well PCR plate. A 12.5 µL protein solution was then added to the wells in replicates of four. Then 2.5 µL of the diluted Protein Thermal Shift dye (8X) was added to each well and mixed by pipette. The plate was sealed with adhesive film and briefly centrifugated. The plate was then loaded into a ViiA 7 Real-time PCR system (Applied Biosystems) and the instrument was programmed as described by the reference manual. Melt curves were visualized using Matplotlib [100] and the T_m was calculated in python [148].

5.3.8 Statistical analyses

Analysis of kinetics and thermal shift data was performed in RStudio [152]. One-way ANOVA was used to describe the differences of the group and the Tukey's HSD test

created multiple comparisons of the sample means. A P value below 0.05 was considered significant.

5.4 Results and Discussion

5.4.1 Sequence analysis of SFK3087

The bacteria strain *S. fradiae* var. k11 has been characterized by other groups to hydrolyze chicken feathers. Earlier work by our group suggests *S. fradiae* var. k11 has two active lipase enzymes, yet only one of the lipases is capable of hydrolyzing wax esters, the dominant lipid on the surface of chicken feathers. SFK3087 was the identified lipase that lacked an ability to hydrolyze wax-esters. In agreement with the RASTClassic annotation, SFK3087 behaved as a triacylglycerol lipase, as supported by the enzyme's hydrolysis of the representative synthetic substrate pNPP. Both LED and the ESTHER database classified SFK3087 as a member of the lipase class I family. Interestingly, the ESTHER database annotated SFK3087 as a polyesterase, a lipase, and a cutinase, suggesting the enzyme has the ability to hydrolyze a dynamic range of substrates. Although polyesters were not tested, the lack of hydrolase activity against the wax-esters leaves the annotation as a cutinase for SFK3087 suspect. Some of the lab's effort was focused on the structural characterization of the enzyme capable of hydrolyzing wax-esters, but just as interesting was investigating SFK3087 for its lack of wax-ester hydrolase activity, especially after the suggestion of broad substrate specificity. The objective of this study was to structurally characterize SFK3087 by

homology modelling and rationally design mutations to explore the potential of improving the enzyme for industrial relevance through increases in thermal stability and improved accommodation of large, hydrophobic substrates.

The structure-guided consensus approach to rationally designing proteins has been met with success in studying lipases before, yielding results comparable to random mutagenesis but without the exhaustive screening efforts [153]. Structure-guided consensus is a data-driven technique that relies on information derived from the protein sequence and any structural insight that can be generated [154].

Evolutionary conservation for each amino acid residue of SFK3087 was evaluated using the ConSurf server (http://consurf.tau.ac.il) (Figure 5.1). The importance and functional role is often reflected in the level of preservation the residue has maintained [155]. The 50 variable residues at the N-terminal end of SFK3087 can be accounted for as the TAT signal peptide, as determined by the Pred-TAT server. The catalytic triad of the lipase was identified by LED to contain S181, D227, and H259, and all three residues were highly conserved as the ConSurf results suggested.

5.4.2 Homology modeling of SFK3087

Sequence information for SFK3087 was further supported with structural data, using a homology model generated by the SWISS-MODEL workspace. The model template was from a *Streptomyces exfoliatus* lipase crystal structure (PDB code 1JFR) [156]. The sequence identity was 81.54% and had full coverage once the signal peptide was

removed. The QMEAN, Cß, solvation, and torsion scores were -0.31, -0.16, -0.52, and -0.14, respectively; all reasonable numbers that support the validity of the model. A hydrophobicity coloring scheme was applied to the model (Figure 5.2B) that shows the characteristic hydrophobic loops surrounding the catalytic serine of lipolytic enzymes to aid in the interfacial binding with the substrate [157]. The complementary Figure 5.2C displays an overlay of the ConSurf residue scores on the surface of SFK3087.

AutoDock Vina was used to interpret the accessibility of a substrate into the active site of SFK3087 (Figure 5.2A). Cetyl-palmitate was chosen for use as the substrate in the docking study because it supports our interest in studying the hydrolysis of feather lipids and cetyl-palmitate being a standard wax substrate. The side-chains of the catalytic triad were shown in green and the substrate docked reasonably well in the active site. Although, the catalytic S181 was 4.1Å from the cetyl-palmitate ester bond, not particularly practical for a nucleophilic attack to occur. Furthermore, it is suggested that the S119 residue on the edge of the pocket, also highlighted in green, may be groove digging and preventing the substrate from properly laying across the surface of the enzyme. This information was used collectively with the earlier sequence characterization and ConSurf results to make decisions on potential amino acid substitutions that can impact SFK3087 stability and kinetics.

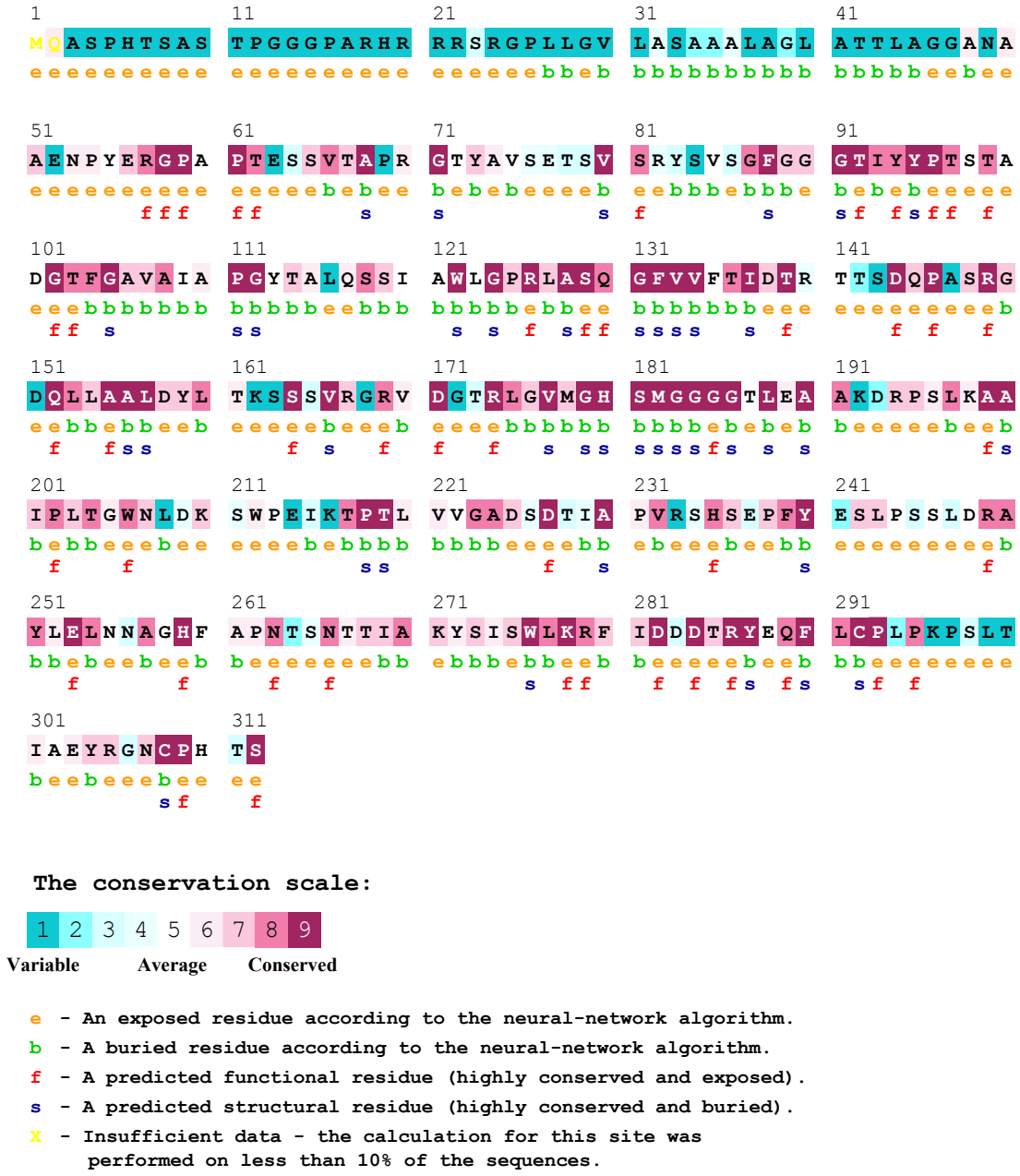

Figure 5.1 – SFK3087 ConSurf server results. The first 50 residues constitute the TAT signal peptide as predicted by Pred-Tat, and was removed during cloning into the pET22b vector. The catalytic triad of the SFK3087 lipase is represented by S181, H259, and D227.

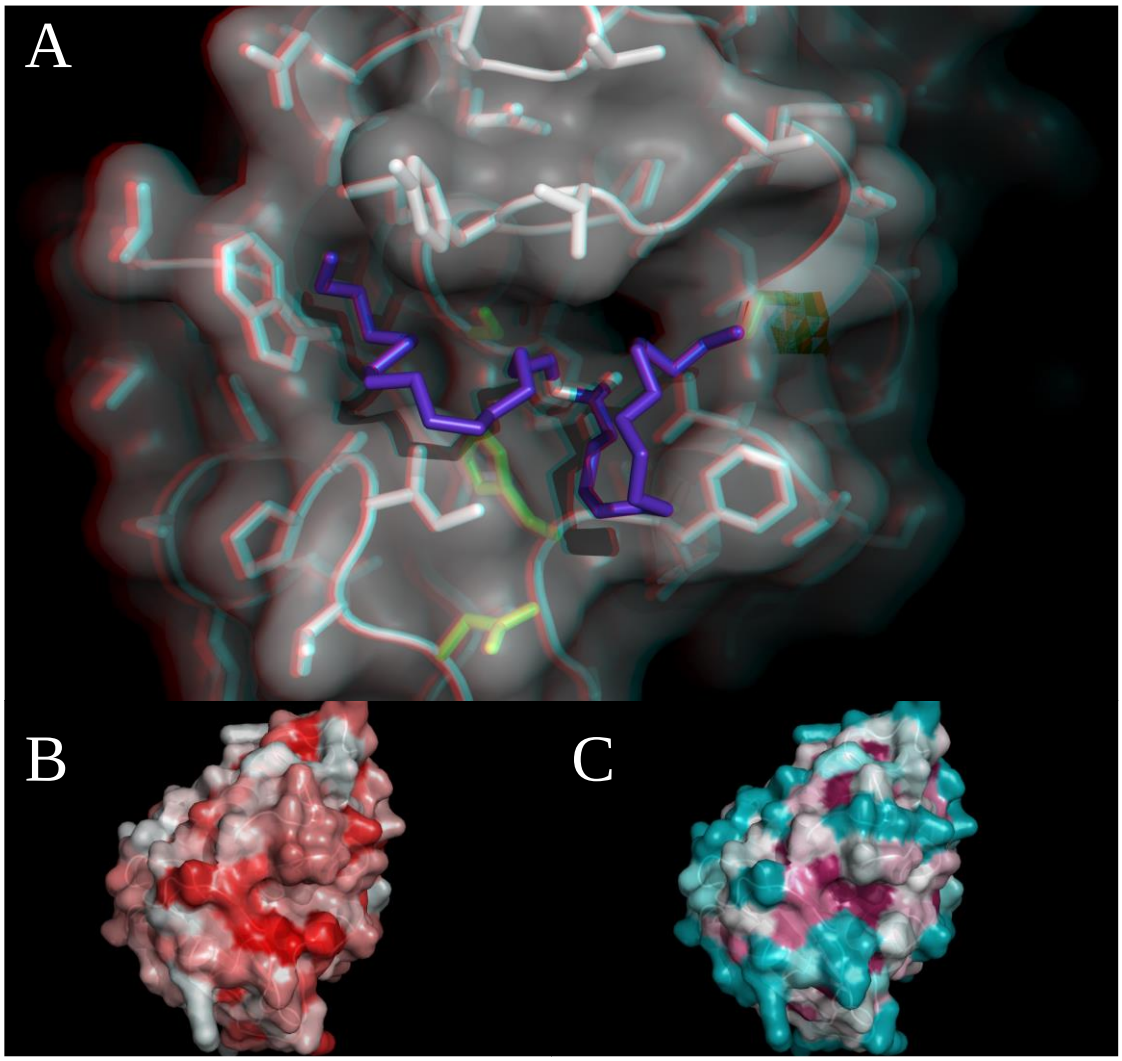

Figure 5.2 – Homology modeling of SFK3087. SWISS-MODEL was used to generate a homology model of SFK3087 with PDB 1JFR chain A as template. The sequence identity was 81.54% with 100% coverage after the removal of the signal peptide. AutoDock Vina was used to dock cetyl-palmitate into the active site of SFK3087 (A). The side-chains of the active triad (S181, H259, D227) is shown in green, as well as residue S119 on the right edge of the pocket. Residues from the SFK3087 model are colored based upon hydrophobicity where white represents hydrophilic residues and red for hydrophobic residues (B). Conservation scores from Figure 5.1 are shown in C.

5.4.3 Surface engineering

Mutating surface residues on a protein can have profound effect on stability in solution and has been an effective strategy in engineering lipases [153]. Replacing hydrophobic residues at the surface has been successful in improving enzyme stability before [158] and this strategy was the basis for the study of SFK3087.

With the hydrophobicity color map on SFK3087 (Figures 5.3 and 5.4), five residues were identified to potentially have profound impact on protein stability: P69, Y83, L116, K216, and L299. Residue K216, though not hydrophobic, protrudes out from the surface of the enzyme as seen in Figure 5.4B and was worth evaluating if the residue played a special role in activity and/or stability. Upon expressing the enzymes in *E. coli* BL21(DE3) cells and purifying the protein, relative activity of the mutations compared to wild-type was minimally impacted for all of the mutants, except for Y83A (Figure 5.5). It is not uncommon for single mutations to be severely disruptive of enzyme activity [159].

A thermal-shift assay was used to evaluate the thermal stability of the enzymes. Thermal-shift assays are principled on a hydrophobic dye, like SYPRO Orange, that binds to inner-core, hydrophobic protein residues that become exposed as the temperature is raised and the protein unfolds [141]. The assay is performed in qPCR machines that are able to control a ramp in the temperature and detect fluorescent signals. Interestingly, Y83A increased the stability of SFK3087 by 3.76℃ ($P<0.01$) in the thermal-shift assay (Figure 5.6). Despite not being near the active site

of SFK3087, Y83A likely induced a considerable structural change that negatively affected the enzyme activity, but lead to a more favorable protein conformation that allowed for a thermal tolerance increase. The other mutations, particularly the hydrophobic residues L299 and L116, had no impact on protein stability. There was a decrease of 0.92℃ ($P<0.01$) in enzyme stability with the K216A mutation, though the change is physiologically irrelevant and minimal change was seen in enzyme activity.

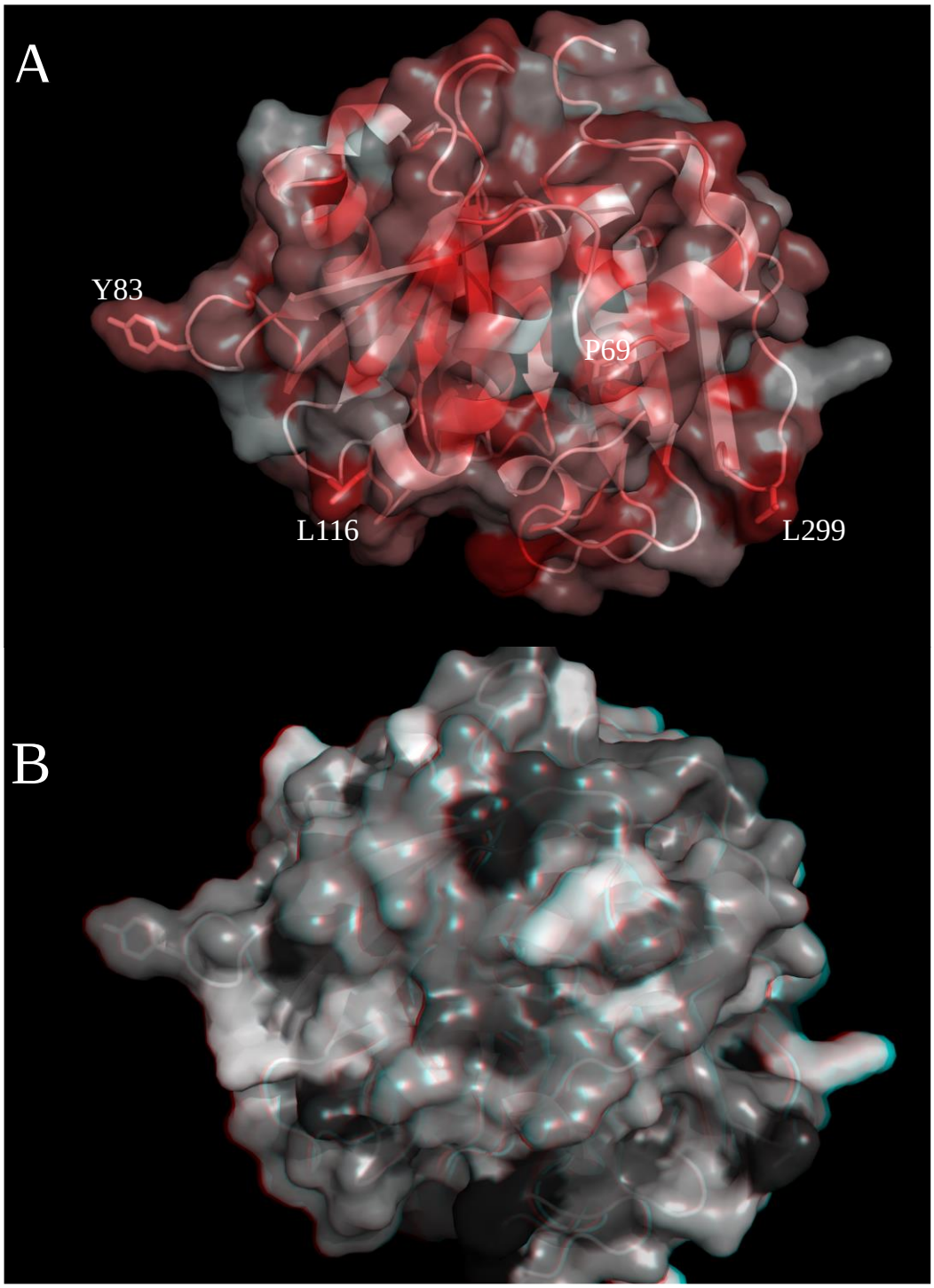

Figure 5.3 – SFK3087 surface mutant targets 1 of 2. Targets are labelled and a hydrophobic coloring scheme is applied and described earlier (A). An anaglyphic image with 20% surface transparency is shown in B. Images rendered in PyMol.

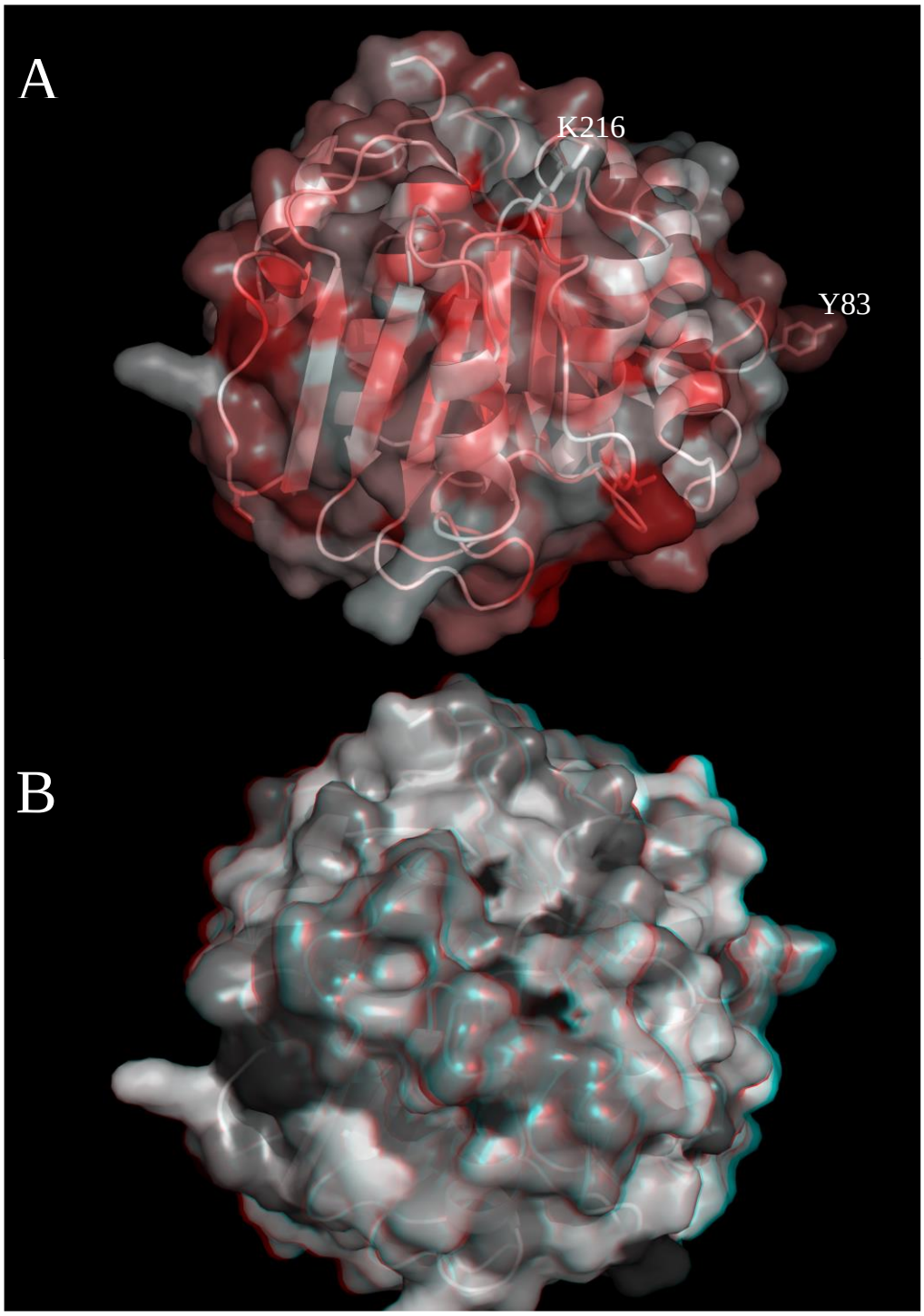

Figure 5.4 – SFK3087 surface mutant targets 2 of 2. A and B are 160 degree transpositions around the Y-axis from Figure 5.3, permitting the visibility of K216, the last of the surface mutant targets. Images were rendered in PyMol.

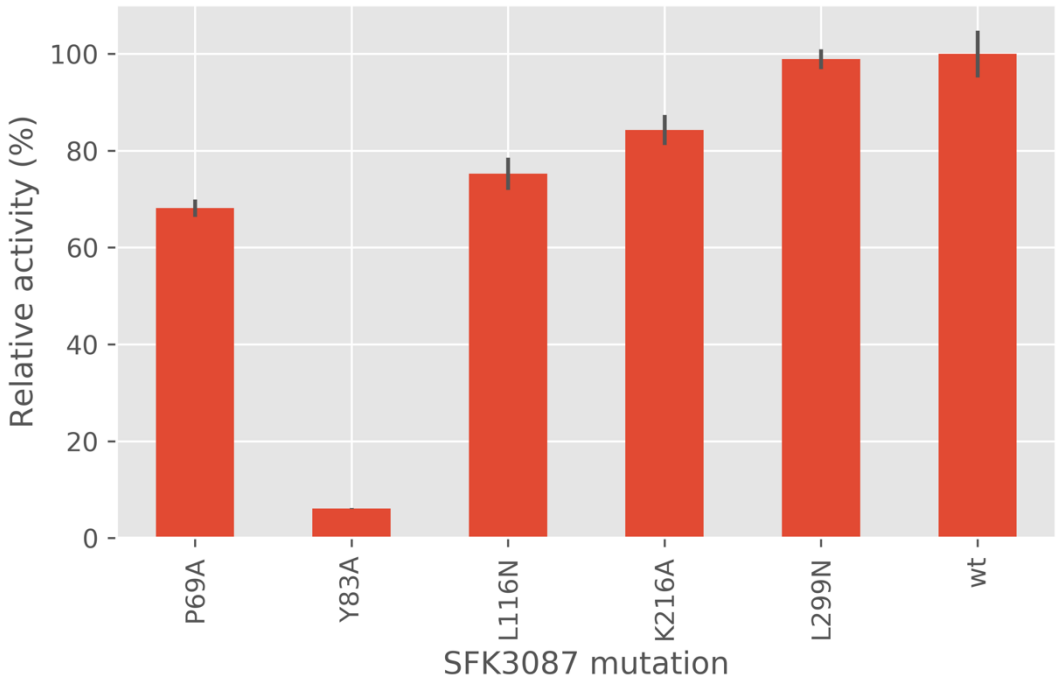

Figure 5.5 – Surface mutant relative activity. Protein was semi-purified making use of the C-terminal 6X-His tag. Activity per milligram of purified protein was determined against p-nitrophenyl palmitate (pNPP) as described in *Materials and Methods*. The wild-type SFK3087 was used as the baseline for activity and mutant activity was reported in regards to wt activity as a percentage. The error bars represent the standard deviation from the sample. Experiments were performed in triplicate.

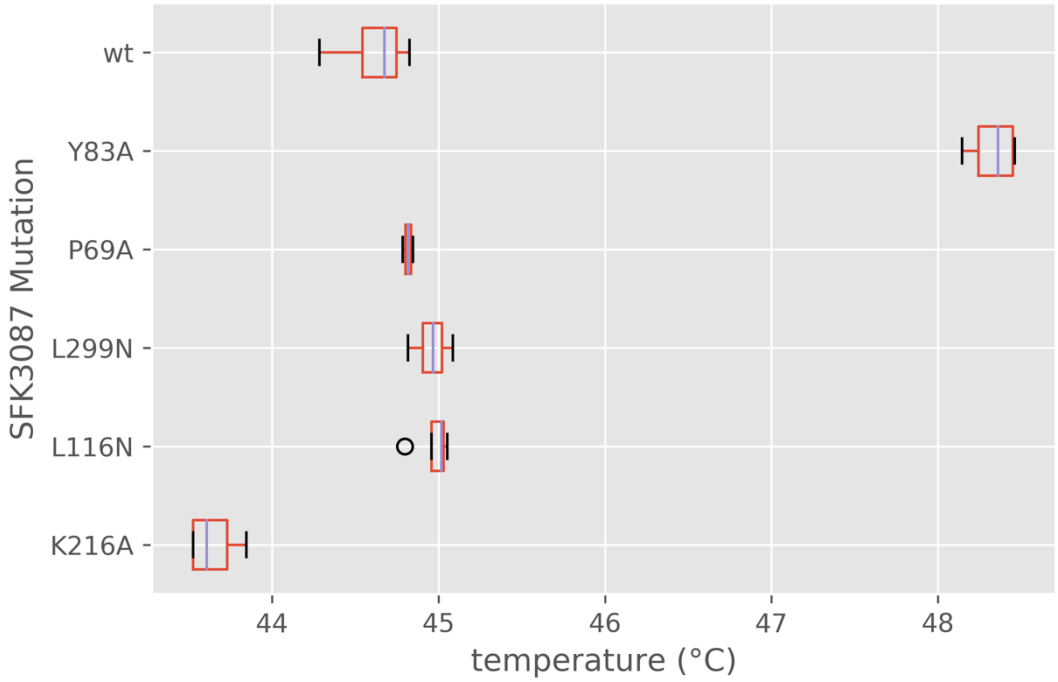

Figure 5.6 – SFK3087 surface mutant thermal shift assay boxplot. The Applied Biosystems thermal shift dye kit was used to determine the melting temperature of the SFK3087 surface mutants using purified protein. The thermal shift assay was run on a ViiA 7 Real-time PCR system (Applied Biosystems). Melt curve data was analyzed with python as described in *Materials and Methods*. The experiment was performed in quadruplicate.

5.4.4 Saturation mutagenesis

Preliminary mutations were constructed for SFK3087 in an attempt to probe relative residues for enzyme activity. The substitution of serine at residue 119 for alanine was identified to significantly diminish activity of the enzyme against pNPP. As S119 can be shown on the edge of the binding pocket of SFK3087 (Figure 5.2A), the residue is oriented in a way as to dig into a groove that may have otherwise lent to the accommodation of large, hydrophobic substrates. S119 was therefore selected as a site for saturation mutagenesis experiments.

Saturation mutagenesis is a powerful tool at improving an enzyme's substrate selectivity and thermal stability [160, 161]. Low mutation rates from directed evolution techniques in modifying proteins rely on single base mutations, which significantly limits the protein sequence space in mutagenesis experiments [162]. Single DNA base changes, on average, will only be able to encode for an average of 5.7 different amino acids, excluding an average of 13.3 other potential amino acids for substitution at that spot [163]. Additionally, single nucleotide substitutions tend to result in conservative mutations, where the new amino acid likely carries similar physiochemical properties [162]. Saturation mutagenesis experiments excel at testing a broad range of amino acids at targeted residues.

During the generation of saturated mutations at residue 119, mixed nucleotide bases were used to significantly reduce screening efforts that would have resulted from codon redundancy, where 64 possible codons are possible from the degenerate DNA code. Codons with mixed nucleotides are able to focus efforts and odds of

generating a mutant encoding an amino acid that encompasses unique physiochemical properties. Different amino acid properties include: size, polarity, charge, hydrophobicity, aromaticity, and others. The mixed codons 'NDT' and 'NRT' were used for our experiments, where the codons had the potential to encode 12 and 8 different amino acids, respectively, creating a 'smarter' library of mutants [164]. Results from screening 80 constructs of generated mutants is shown in Figure 5.7. From 80 screened constructs, in all there were nine different amino acids that were incorporated through saturation mutagenesis. An alanine substitution from earlier experiments was added to the lot for a total of 10 different amino acids to test at residue 119. Only aspartate, histidine, and isoleucine were potential mutations that were not integrated. Disappointingly, almost half of the constructs screened did not take any amino acid change. The reason behind the low efficiency of generating mutations remains ambiguous, though it may be due to incomplete hydrolysis of a template plasmid. Also, some of the constructs had incomplete or rearranged gene sequences and were labelled as 'bad'. The generated pool of saturated mutagens allowed for the testing of aromatic, aliphatic, small, very small, large, charged, polar, and non-polar properties at residue 119.

Expression of the saturated mutants was done using Studier's autoinduction media and resulted in better expression than LB. After a 6X Histidine-tag purification step, the mutants were run on an SDS-PAGE gel and stained with Coomassie Blue (Figure 5.8). Non-polar, aliphatic amino acids (leucine, valine, and alanine) all had a negative impact on the yield of SFK3087 when compared to the native serine. Interestingly, the large aromatic phenylalanine and tyrosine had limited change on

expression. The remaining amino acids (cysteine, asparagine, glycine, and arginine) seemed to have some negative impact on expression. The purification of the enzymes contained multiple variables, though earnest effort was taken for consistency in handling the different samples. Multiple factors could have been at play, where the mutation may have impacted protein stability, his-tag binding, or something else.

Thermal stability of the saturated mutants was evaluated using a thermal-shift assay. A boxplot of the thermal-shift assay results for the saturation mutants is shown in Figure 5.9. The overall impact on protein stability for most of the mutants appeared to be negative by 1-3℃. Substitution of phenylalanine at residue 119 did show a slight increase in stability by 0.31℃, but was statistically insignificant ($P>0.05$). Worth noting is the mutations with valine and leucine were unable to produce a reliable melt curve and were therefore excluded from the boxplot. This is likely due to an overall negative influence on the protein integrity.

Kinetics experiments were performed on the saturated mutants for effect on enzyme activity. The substrate pNPP was used as it is a standard lipase substrate and is relatively simple to handle. Recall in Figure 5.2 the close proximity of residue 119 at the edge of the binding pocket of SFK3087, it was likely the saturated mutants would have a profound impact on the affinity towards the substrate. Figure 5.10 suggests all but asparagine and cysteine were able to reduce the K_m of the enzyme, compared to wild-type, but at the cost of a lower V_{max}. All mutants had a decrease in K_{cat}, but accounting for the decrease in K_m, S119Y was on par with the wild-type enzyme and S119F had slightly better performance, with a K_{cat}/K_m score 47% above wild-type ($P<0.01$). Overall, the replacement of serine at residue 119 of SFK3087 was

disruptive. However, the replacement of S119 with large, aromatic residues was comparable to wild-type for enzyme expression, stability, and activity. And the catalysis of pNPP and enzyme stability was slightly more favorable with nonpolar phenylalanine.

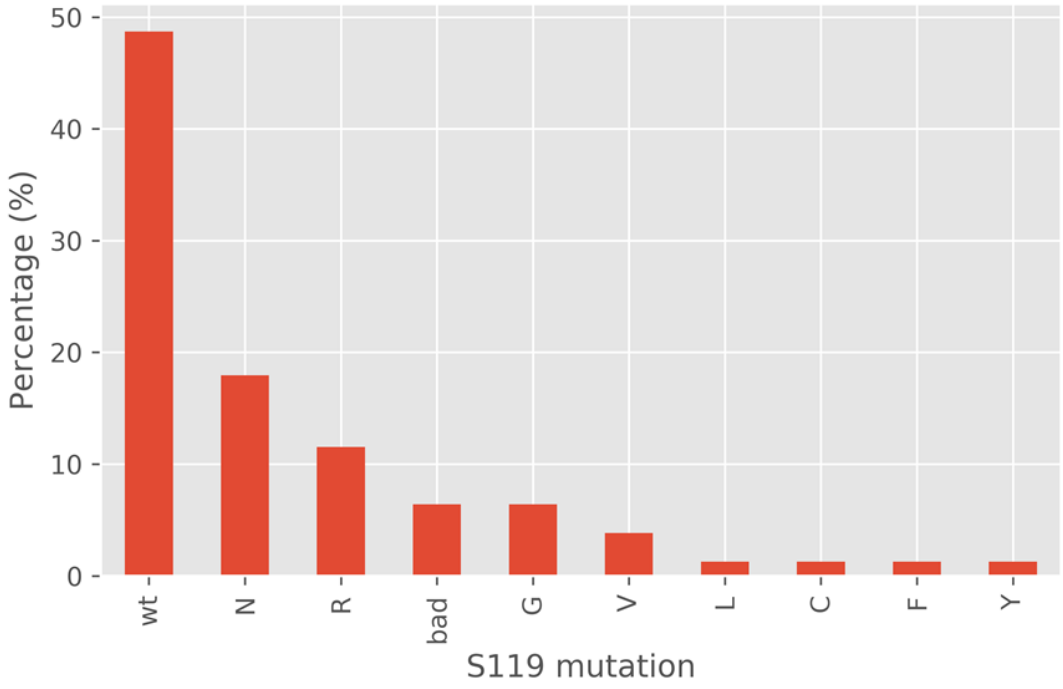

Figure 5.7 – Saturation mutagenesis yielded constructs. A total of 80 constructs were sequenced and analyzed for mutagenesis at residue 119 of SFK3087. Two sets of degenerate primers were used with the potential of incorporating 12 different amino acids. Three amino acids were not identified in any of the constructs: aspartate, histidine, and isoleucine. Constructs with disrupted sequences were labeled as ‘bad’.

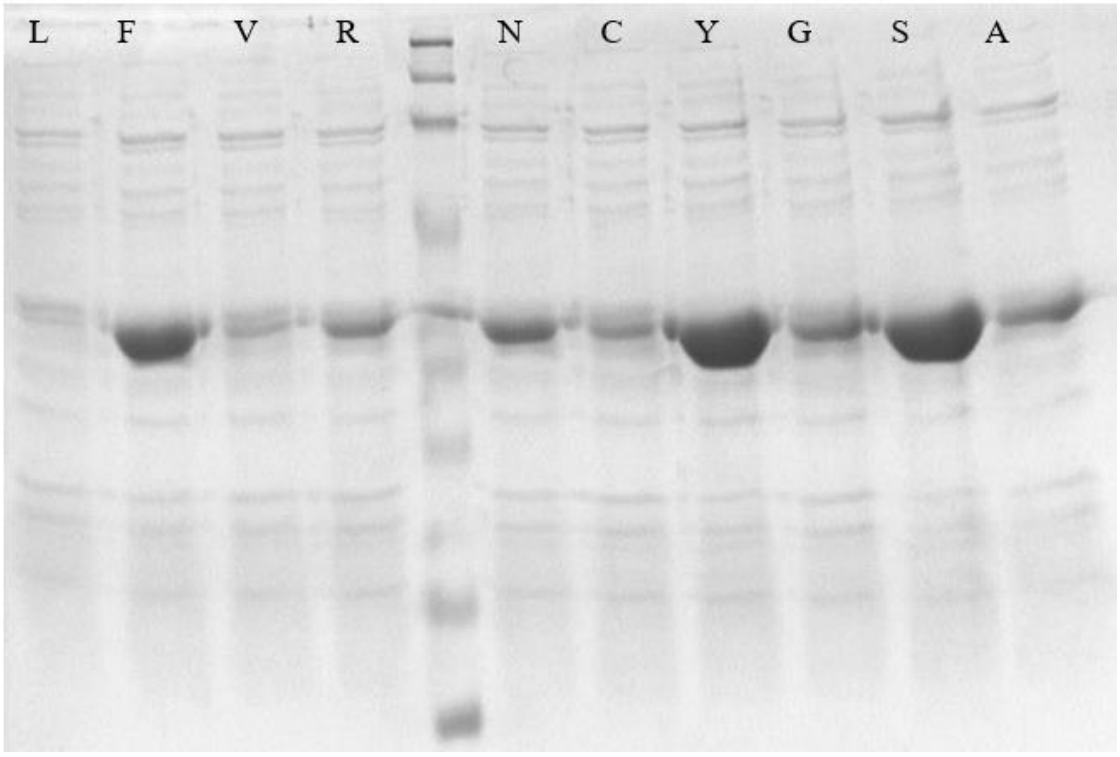

Figure 5.8 – SDS-PAGE gel of purified SFK3087 saturation mutants. Cultures of each construct were grown in Studier's autoinduction media and purified as described in *Materials and Methods*. The one-letter amino acid abbreviations represent the amino acid at residue 119 and corresponds to their respective lane on the SDS-Page gel. The Bio-Rad broad range protein marker was run between S119R and S119N. The large band in the middle of the gel in each of the lanes corresponds to the 29 kDa size protein expected for SFK3087.

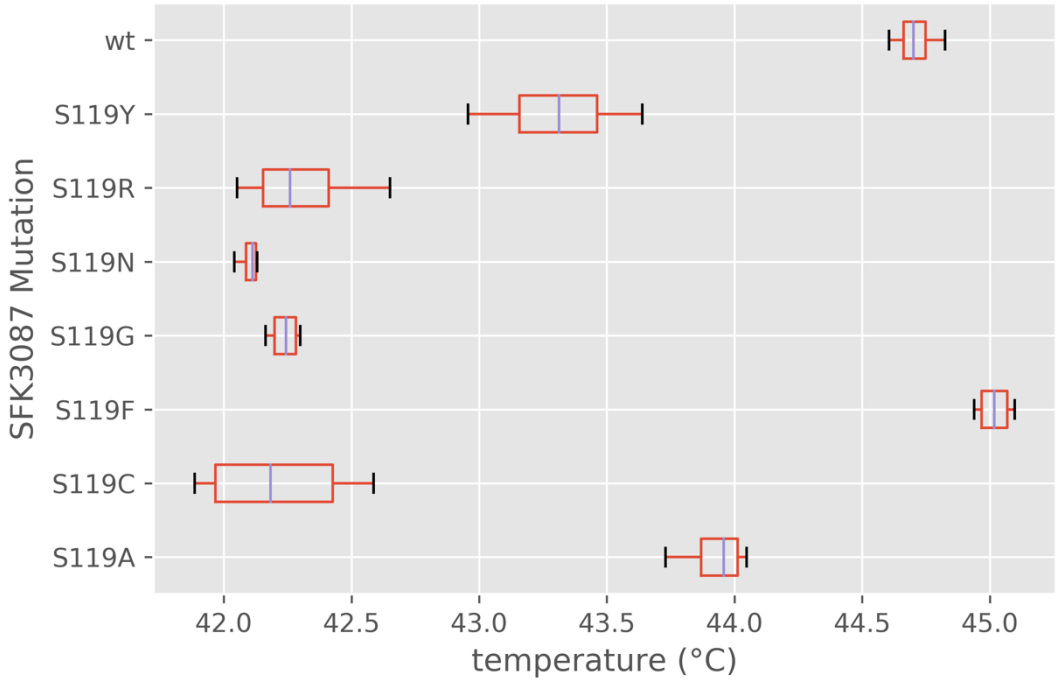

Figure 5.9 – SFK3087 thermal shift assay of saturation mutants. The melting temperature for each of the saturated mutants was determined using the Applied Biosystems thermal shift dye kit and deriving the melting point from the melt curve. Experimental data was collected on a ViiA 7 Real-time PCR system (Applied Biosystems). The SFK3087 mutation is plotted on the Y-axis. Samples were prepared in quadruplicate.

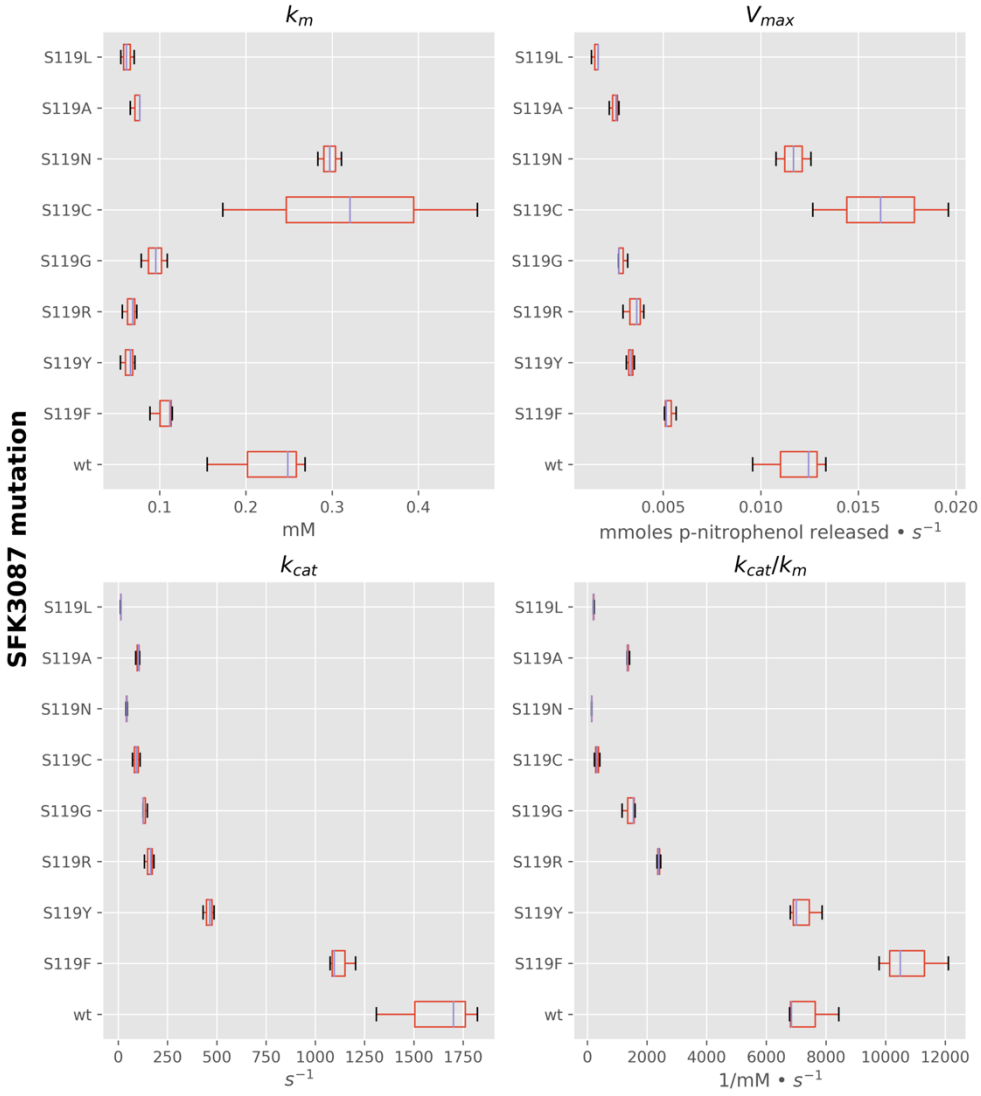

Figure 5.10 – Kinetics boxplots for SFK3087 saturation mutants. Kinetic data for each of the saturated mutants was collected against p-nitrophenyl palmitate as substrate at room temperature. Experiments were run in triplicate, with the exception of S119C and S119N, which were performed in duplicate.

5.5 Conclusion

The lipolytic enzyme SFK3087 was explored for beneficial mutations that would improve the enzyme's stability and catalytic efficiency through standard site-directed mutagenesis and saturation mutagenesis approaches. The data-driven strategy of using sequence information and a homology model was able to focus efforts on five surface residues and one residue on the edge of the enzyme's binding pocket. The substitution Y83A brought about an adequate increase of 3.76℃ to the stability of the enzyme, but arrested much of the enzyme activity. Other surface mutants had negligible effect. The saturation of mutants at S119 yielded a pool of 10 different residues with a wide range of biophysiological properties. Large, aromatic residues phenylalanine and tyrosine were the only substitutions that met the threshold of the wild-type serine residue. And, S119F was able to slightly improve enzyme stability and increase overall enzyme performance, with a higher K_{cat}/K_m score. Future studies may wish to explore a broader range of residues with potential impact on substrate specificity towards wax esters.

ACKNOWLEDGEMENTS

Dr. Ailong Ke and Dr. Shinya Fushinobu aided in the identification of residues to mutate. Dr. John Brady assisted with interpreting the homology model and with docking studies.

CHAPTER 6

CONCLUSION

For the research project, we have sought to characterize lipolytic enzymes associated with feather hydrolysis. Lipids are a major component in feathers and by enzymatically removing the lipids, we hope processing waste feathers from the poultry industry into useable co-products may be more economical. We were successful in identifying multiple lipolytic enzymes and characterizing our best enzyme for hydrolysis of feather lipids and wax esters, the major lipid class in feathers. Our efforts will hopefully contribute to the development of a sustainable and systematic process in managing the feathers from the poultry industry. Structural studies of the wax-degrading enzyme were also performed, which should lay the ground work in understanding the enzyme's molecular mechanism and designing improved enzymes for use in industry.

Our work was centralized around the feather-degrading microorganism *S. fradiae* var. k11 where we used a draft genome to identify candidate genes that encode lipolytic enzymes. Between *S. fradiae* var. k11 and two related actinomycetes, 16 enzymes were identified as being an active esterase or lipase. SFK3309 expressed well in *E. coli* BL21(DE3) cells and had the highest activity against pNPP amongst the enzymes tested. SFK3309 was challenged against feather lipids and was successful at creating hydrolysis products.

Since feather lipids are a mix of many different types of lipids, it was meaningful to determine if SFK3309 was also active against wax esters, the largest lipid class in feather lipids. Optimization of protein expression conditions and a purification scheme was carried out for SFK3309. A colorimetric assay was modified to quantitate released free fatty acids from the different wax ester substrates upon hydrolysis. Jojoba oil, beeswax, and cetyl-palmitate were three wax substrates tested, all of which were susceptible to hydrolysis by SFK3309. Kinetic experiments were performed with SFK3309 against cetyl-palmitate and the K_m was determined to be 850 µM and the K_{cat} was calculated as 11.63 s^{-1}. Previous to our study, only two other groups reported on the kinetics of a wax ester hydrolase. Our reported kinetic values are more complete and will hopefully serve as a threshold for development of wax ester hydrolases for use in industry.

Structural information on SFK3309 would help unravel mechanistic information on how the enzyme is able to accommodate large, hydrophobic wax ester substrates. Interestingly, SFK3309 shares little protein sequence similarity with any protein structure in the Protein Data Bank and so homology modelling proved to be a challenge. Crystallography experiments were initiated but were ultimately unsuccessful at yielding diffracting protein crystals. Small-angle X-ray scattering experiments were also performed in anticipation of gathering a low-resolution envelope structure of the enzyme, but the tendency of SFK3309 to aggregate in solution prevented a reliable envelope structure from being determined. Additional experiments were performed to identify an optimal buffer that would improve the stability of SFK3309, but instead revealed a large hydrophobic patch on the protein as

a likely vulnerability. An additive screen was also carried out for SFK3309, which suggested much promise with volatile organics, amphiphiles, chaotropes, and non-detergents as additives to stabilize the enzyme. The unique enzyme activity of SFK3309 and novel protein sequence should warrant further exploration into the structure of the enzyme, but it will be necessary to first find better conditions that will stabilize SFK3309 in solution. An alternative approach to understanding structurally relevant residues in SFK3309 and developing an improved enzyme would be to employ random mutagenesis experiments. Mutations responsible for changes in enzyme activity and stability could provide key insight into the role of the residue and provide novel functions for commercial applications. Even so, recent developments on the identification of diffracting crystals from a crystallization optimization screen for SFK3309 suggests we may be one step closer to solving the protein structure of this unique enzyme (*see* Appendix).

One more active lipase, SFK3087, was identified from *S. fradiae* var. k11, but lacked wax ester hydrolase activity. We were interested to see if we can engineer the enzyme for improved industrial characteristics, with the long-term goal of broadening the substrate specificity of SFK3087 to accommodate wax esters. SFK3087 had sufficient sequence similarity with known structures to create a reliable homology model. Coupled with information derived from the sequence, a data-driven approach was used to design promising mutations for SFK3087. Five surface mutants were designed and tested for enhanced thermal stability of the enzyme. The mutation Y183A improved the thermal stability of the enzyme over wild-type by 3.76°C, however enzyme activity ultimately suffered. Other surface mutants were unsuccessful

at improving enzyme stability. On the edge of the binding pocket of SFK3087 the S119 residue was targeted for saturation mutagenesis. Ten different amino acids were incorporated at the 119th residue, but only the large, aromatic residues phenylalanine and tyrosine were able to maintain reasonable expression levels and minimal changes to thermal stability. The S119F mutation actually improved thermal stability by 0.31°C as well as overall enzyme efficiency with a K_{cat}/K_m increase of 47% against pNPP. Overall, enzyme improvements from the mutants were modest and a more aggressive approach would be necessary for a more dramatic impact. Future work may wish to screen a larger number of mutation targets and couple mutations in order to engineer SFK3087 with desired characteristics, such as wax ester specificity.

In all, we have been successful at identifying an enzyme capable of hydrolyzing feather lipids, and more importantly, characterized the enzyme as able to hydrolyze wax esters, the largest lipid class from feather lipids. Attempts were made to solve the enzyme structure and insight gained gives promise for future endeavors. Mutagenesis experiments may be a powerful alternative to study SFK3309 and could be performed independently of solving the structure. Protein engineering was employed on a lipase that lacked wax ester hydrolase activity to bring about improved characteristics. However, impact was moderate and a more aggressive approach is necessary to introduce desired changes and specificity towards wax esters. Much hype behind the potential of wax ester hydrolases at improving the enzymatic processing of chicken feathers has been generated from the research presented, but such experiments exceeded the scope of this study and further investigation is needed.

APPENDIX

Figure A.1 - Data collection of SFK3309 crystals. Further optimization of SFK3309 crystalline form conditions using the hanging drop technique yielded rhombohedra crystals (A) grown at 18°C for one month with a protein concentration of 15 mg/mL and 0.3 M ammonium phosphate as reservoir solution. The crystal was looped (C) and a cryo-protectant solution with 30% glycerol was used. Diffraction data (B) was collected at the Cornell High Energy Synchrotron Source (Ithaca, NY) at the F1 station. The diffraction pattern is promising of being a protein and efforts are being made to analyze the collected diffraction data.

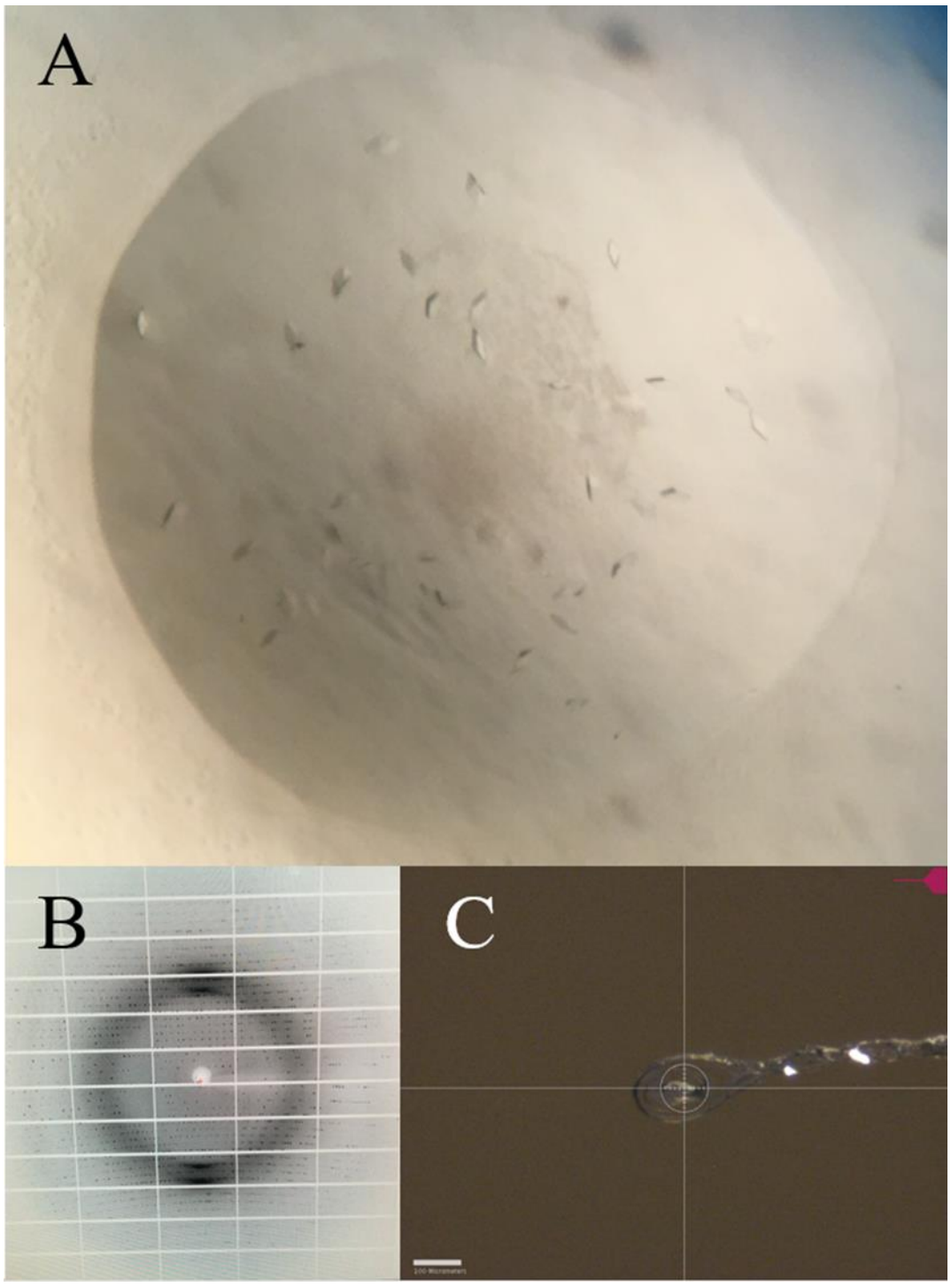
A
B
C

REFERENCES

[1] K. Mathews, USDA Economic Research Service - Livestock & Meat Domestic Data. http://www.ers.usda.gov/data-products/livestock-meat-domestic-data.aspx#26056.

[2] National Chicken Council - US Broiler Performance. http://www.nationalchickencouncil.org/about-the-industry/statistics/u-s-broiler-performance/.

[3] D.W. Shike, Beef cattle feed efficiency, 2013. https://www.beefusa.org/CMDocs/BeefUSA/Resources/cc2012-Beef-Feed-Efficiency--Dan-Shike.pdf.

[4] N.A.S.S. USDA (U.S. Department of Agriculture), Poultry Slaughter - 2016 Summary, in: USDA (Ed.) USDA, 2017, pp. 1-35.

[5] N.A.S.S. USDA (U.S. Department of Agriculture), Poultry - Production and Value 2016 Summary, in: USDA (Ed.) USDA.

[6] A.A. Onifade, N.A. Al-Sane, A.A. Al-Musallam, S. Al-Zarban, A review: Potentials for biotechnological applications of keratin-degrading microorganisms and their enzymes for nutritional improvement of feathers and other keratins as livestock feed resources, Bioresource Technol 66(1) (1998) 1-11.

[7] D.C. Love, R.U. Halden, M.F. Davis, K.E. Nachman, Feather Meal: A Previously Unrecognized Route for Reentry into the Food Supply of Multiple Pharmaceuticals and Personal Care Products (PPCPs), Environ Sci Technol 46(7) (2012) 3795-3802.

[8] H.K. Ahn, M.S. Huda, M.C. Smith, W. Mulbry, W.F. Schmidt, J.B. Reeves, Biodegradability of injection molded bioplastic pots containing polylactic acid and poultry feather fiber, Bioresource Technol 102(7) (2011) 4930-4933.

[9] M.J. Zhan, R.P. Wool, J.Q. Xiao, Electrical properties of chicken feather fiber reinforced epoxy composites, Compos Part a-Appl S 42(3) (2011) 229-233.

[10] A. Hadas, L. Kautsky, Feather Meal, a Semi-Slow-Release Nitrogen-Fertilizer for Organic Farming, Fert Res 38(2) (1994) 165-170.

[11] K. Swisher, Market Report US Rendering: A $10 Billion Industry, Render (April) (2013) 10-17.

[12] P.W. Wertz, P.M. Stover, W. Abraham, D.T. Downing, Lipids of Chicken Epidermis, J Lipid Res 27(4) (1986) 427-435.

[13] R.D.B. Fraser, T.P. Macrae, D.A.D. Parry, E. Suzuki, Structure of Feather Keratin, Polymer 12(1) (1971) 35-&.

[14] K. Chojnacka, H. Gorecka, I. Michalak, H. Gorecki, A Review: Valorization of Keratinous Materials, Waste Biomass Valori 2(3) (2011) 317-321.

[15] K.E. Nachman, G. Raber, K.A. Francesconi, A. Navas-Acien, D.C. Love, Arsenic species in poultry feather meal, Sci Total Environ 417 (2012) 183-188.

[16] C.K. Hong, R.P. Wool, Development of a bio-based composite material from soybean oil and keratin fibers, J Appl Polym Sci 95(6) (2005) 1524-1538.

[17] M.C. Papadopoulos, A.R. Elboushy, A.E. Roodbeen, E.H. Ketelaars, Effects of Processing Time and Moisture-Content on Amino-Acid-Composition and Nitrogen Characteristics of Feather Meal, Anim Feed Sci Tech 14(3-4) (1986) 279-290.

[18] A. Grazziotin, F.A. Pimentel, E.V. de Jong, A. Brandelli, Nutritional improvement of feather protein by treatment with microbial keratinase, Anim Feed Sci Tech 126(1-2) (2006) 135-144.

[19] C.M. Williams, J.C.H. Shih, Enumeration of Some Microbial Groups in Thermophilic Poultry Waste Digesters and Enrichment of a Feather-Degrading Culture, J Appl Bacteriol 67(1) (1989) 25-35.

[20] R. Gupta, P. Ramnani, Microbial keratinases and their prospective applications: an overview, Appl Microbiol Biot 70(1) (2006) 21-33.

[21] Valkerase® Keratinase Processing Enzyme BRI. http://briworldwide.com/products/valkerase/. 08/01/2015).

[22] S. Sangali, A. Brandelli, Feather keratin hydrolysis by a Vibrio sp strain kr2, J Appl Microbiol 89(5) (2000) 735-743.

[23] S. Yamamura, Y. Morita, Q. Hasan, K. Yokoyama, E. Tamiya, Keratin degradation: a cooperative action of two enzymes from Stenotrophomonas sp., Biochem Bioph Res Co 294(5) (2002) 1138-1143.

[24] P. Ramnani, R. Singh, R. Gupta, Keratinolytic potential of Bacillus licheniformis RG1: structural and biochemical mechanism of feather degradation, Can J Microbiol 51(3) (2005) 191-196.

[25] V. Sandilands, K. Powell, L. Keeling, C.J. Savory, Preen gland function in layer fowls: factors affecting preen oil fatty acid composition, Brit Poultry Sci 45(1) (2004) 109-115.

[26] A.R. Gunderson, Feather-Degrading Bacteria: A New Frontier in Avian and Host-Parasite Research?, Auk 125(4) (2008) 972-979.

[27] P.W. Wertz, P.M. Stover, D.T. Downing, A Survey of Polar and Nonpolar Lipids from Epidermis and Epidermal Appendages of the Chicken (Gallus-Domesticus), Comp Biochem Phys B 84(2) (1986) 203-206.

[28] E.A. Barka, P. Vatsa, L. Sanchez, N. Gaveau-vaillant, C. Jacquard, H.-P. Klenk, C. Clément, Y. Ouhdouch, G.P. van Wezel, Taxonomy, Physiology, and Natural Products of Actinobacteria, Microbiology and Molecular Biology Reviews 80 (2016) 1-43.

[29] C. Kumbhar, P. Mudliar, L. Bhatia, A. Kshirsagar, M. Watve, Widespread predatory abilities in the genus Streptomyces, Archives of Microbiology 196 (2014) 235-248.

[30] K. Wang, H.Y. Luo, J. Tian, O. Turunen, H.Q. Huang, P.J. Shi, H.F. Hua, C.H. Wang, S.H. Wang, B. Yao, Thermostability Improvement of a Streptomyces Xylanase by Introducing Proline and Glutamic Acid Residues, Appl Environ Microb 80(7) (2014) 2158-2165.

[31] H.D. Jang, K.S. Chen, Production and characterization of thermostable cellulases from Streptomyces transformant T3-1, World J Microb Biot 19(3) (2003) 263-268.

[32] M. Abramic, I. Lescic, T. Korica, L. Vitale, W. Saenger, J. Pigac, Purification and properties of extracellular lipase from Streptomyces rimosus, Enzyme Microb Tech 25(6) (1999) 522-529.

[33] Y.Y. Wei, J.L. Schottel, U. Derewenda, L. Swenson, S. Patkar, Z.S. Derewenda, A Novel Variant of the Catalytic Triad in the Streptomyces-Scabies Esterase, Nat Struct Biol 2(3) (1995) 218-223.

[34] P.J. Shi, T.Z. Yuan, J.Q. Zhao, H.Q. Huang, H.Y. Luo, K. Meng, Y.R. Wang, B. Yao, Genetic and biochemical characterization of a protease-resistant mesophilic beta-mannanase from Streptomyces sp S27, J Ind Microbiol Biot 38(3) (2011) 451-458.

[35] L.J. Wang, C.X. Li, Y. Ni, J. Zhang, X. Liu, J.H. Xu, Highly efficient synthesis of chiral alcohols with a novel NADH-dependent reductase from Streptomyces coelicolor, Bioresource Technol 102(14) (2011) 7023-7028.

[36] M.J. Virolle, C.M. Long, S. Chang, M.J. Bibb, Cloning, Characterization and Regulation of an Alpha-Amylase Gene from Streptomyces-Venezuelae, Gene 74(2) (1988) 321-334.

[37] K. Morihara, T. Oka, H. Tsuzuki, Multiple proteolytic enzymes of Streptomyces fradiae production, isolation, and preliminary characterization, Biochimica et Biophysica Acta (BBA) - Enzymology 139 (1967) 382-397.

[38] L. Lange, Y. Huang, P.K. Busk, Microbial decomposition of keratin in nature—a new hypothesis of industrial relevance, Appl Microbiol Biot 100 (2016) 2083-2096.

[39] M.A. Abdoli, F. Mohamadi, B. Ghobadian, E. Fayyazi, Effective Parameters on Biodiesel Production from Feather fat oil as a Cost-Effective Feedstock, Int. J. Environ. Res 8 (2014) 139-148.

[40] N. Kondamudi, J. Strull, M. Misra, S.K. Mohapatra, A Green Process for Producing Biodiesel from Feather Meal, J. Agric. Food Chem 57 (2009) 6163-6166.

[41] J. Li, P.-J. Shi, W.-Z. Zhang, X.-Y. Han, L.-L. Xu, H.-T. Zhang, B. Yao, Y.-L. Fan, Gene cloning and expression of serine protease SFP2 from Streptomyces fradiae var. k11, Sheng wu gong cheng xue bao = Chinese journal of biotechnology 21 (2005) 782-8.

[42] R. Gherna, P. Pienta, R. Cote, American type culture collection: catalogue of bacteria and phages, (1992).

[43] D.R. Zerbino, E. Birney, Velvet: Algorithms for de novo short read assembly using de Bruijn graphs, Genome Research 18 (2008) 821-829.

[44] R.K. Aziz, D. Bartels, A.A. Best, M. DeJongh, T. Disz, R.A. Edwards, K. Formsma, S. Gerdes, E.M. Glass, M. Kubal, F. Meyer, G.J. Olsen, R. Olson, A.L. Osterman, R.A. Overbeek, L.K. McNeil, D. Paarmann, T. Paczian, B. Parrello, G.D. Pusch, C. Reich, R. Stevens, O. Vassieva, V. Vonstein, A. Wilke, O. Zagnitko, The RAST Server: Rapid Annotations using Subsystems Technology, BMC Genomics 9 (2008) 75.

[45] S. Kurtz, A. Phillippy, A.L. Delcher, M. Smoot, M. Shumway, C. Antonescu, S.L. Salzberg, Versatile and open software for comparing large genomes, Genome Biol 5(2) (2004).

[46] H. Ikeda, J. Ishikawa, A. Hanamoto, M. Shinose, H. Kikuchi, T. Shiba, Y. Sakaki, M. Hattori, S. Ōmura, Complete genome sequence and comparative analysis of the industrial microorganism Streptomyces avermitilis, Nature Biotechnology 21(5) (2003) 526-531.

[47] S.D. Bentley, K.F. Chater, A.M. Cerdeno-Tarraga, G.L. Challis, N.R. Thomson, K.D. James, D.E. Harris, M.A. Quail, H. Kieser, D. Harper, A. Bateman, S. Brown, G. Chandra, C.W. Chen, M. Collins, A. Cronin, A. Fraser, A. Goble, J. Hidalgo, T. Hornsby, S. Howarth, C.H. Huang, T. Kieser, L. Larke, L. Murphy, K. Oliver, S. O'Neil, E. Rabbinowitsch, M.A. Rajandream, K. Rutherford, S. Rutter, K. Seeger, D. Saunders, S. Sharp, R. Squares, S. Squares, K. Taylor, T. Warren, A. Wietzorrek, J.

Woodward, B.G. Barrell, J. Parkhill, D.A. Hopwood, Complete genome sequence of the model actinomycete Streptomyces coelicolor A3(2), Nature 417(6885) (2002) 141-147.

[48] P.G. Bagos, E.P. Nikolaou, T.D. Liakopoulos, K.D. Tsirigos, Combined prediction of Tat and Sec signal peptides with hidden Markov models, Bioinformatics 26(22) (2010) 2811-2817.

[49] M. Davis, Ape: A plasmid editor, 2008.

[50] J. Nikodinovic, K.D. Barrow, J.-A. Chuck, High yield preparation of genomic DNA from Streptomyces, Biotechniques 35(5) (2003) 932-936.

[51] Y. Zhang, K. Meng, Y. Wang, H. Luo, P. Yang, P. Shi, N. Wu, Y. Fan, J. Li, B. Yao, A novel proteolysis-resistant lipase from keratinolytic Streptomyces fradiae var. k11, Enzyme Microb Tech 42 (2008) 346-352.

[52] O.H. Lowry, N.J. Rosebrough, A.L. Farr, R.J. Randall, Protein measurement with the Folin phenol reagent, J biol Chem 193(1) (1951) 265-275.

[53] R.D. Mccarthy, A.H. Duthie, Rapid Quantitative Method for Separation of Free Fatty Acids from Other Lipids, J Lipid Res 3(1) (1962) 117-&.

[54] C. Yamada, K. Sawano, N. Iwase, M. Matsuoka, T. Arakawa, S. Nishida, S. Fushinobu, Isolation and characterization of a thermostable lipase from Bacillus thermoamylovorans NB501, J Gen Appl Microbiol 62(6) (2016) 313-319.

[55] J.R. Doroghazi, J.C. Albright, A.W. Goering, K.S. Ju, R.R. Haines, K.A. Tchalukov, D.P. Labeda, N.L. Kelleher, W.W. Metcalf, A roadmap for natural product discovery based on large-scale genomics and metabolomics, Nat Chem Biol 10(11) (2014) 963-968.

[56] A.L. Delcher, S.L. Salzberg, A.M. Phillippy, Using MUMmer to identify similar regions in large sequence sets, Current Protocols in Bioinformatics (2003) 10.3. 1-10.3. 18.

[57] N. Hulo, A. Bairoch, V. Bulliard, L. Cerutti, E. De Castro, P.S. Langendijk-Genevaux, M. Pagni, C.J.A. Sigrist, The PROSITE database, Nucleic Acids Res 34 (2006) D227-D230.

[58] R. Gupta, P. Rathi, N. Gupta, S. Bradoo, Lipase assays for conventional and molecular screening: an overview, Biotechnol Appl Bioc 37 (2003) 63-71.

[59] D. Gilham, R. Lehner, Techniques to measure lipase and esterase activity in vitro, Methods 36(2) (2005) 139-147.

[60] K. Nishihara, M. Kanemori, M. Kitagawa, H. Yanagi, T. Yura, Chaperone coexpression plasmids: Differential and synergistic roles of DnaK-DnaJ-GrpE and GroEL-GroES in assisting folding of an allergen of Japanese cedar pollen, Cryj2 in Escherichia coli, Appl Environ Microb 64(5) (1998) 1694-1699.

[61] F.U. Hartl, M. Hayer-Hartl, Protein folding - Molecular chaperones in the cytosol: from nascent chain to folded protein, Science 295(5561) (2002) 1852-1858.

[62] A. Gupta, N.B. Kamarudin, C.Y.G. Kee, R.B.M. Yunus, Extraction of keratin protein from chicken feather, Journal of Chemistry and Chemical Engineering 6(8) (2012) 732.

[63] N. Dale, True metabolizable energy of feather meal, The Journal of Applied Poultry Research 1(3) (1992) 331-334.

[64] N. Kondamudi, J. Strull, M. Misra, S.K. Mohapatra, A Green Process for Producing Biodiesel from Feather Meal, J Agr Food Chem 57(14) (2009) 6163-6166.

[65] S. Leeson, T. Walsh, Feathering in commercial poultry - I. Feather growth and composition, World Poultry Sci J 60(1) (2004) 42-51.

[66] J.J. Noval, W.J. Nickerson, Decomposition of Native Keratin by Streptomyces-Fradiae, J Bacteriol 77(3) (1959) 251-263.

[67] A.A. Sakr, M. Ghaly, M. Ali, M. Abdel-Haliem, Biodeterioration of binding media in tempera paintings by Streptomyces isolated from some ancient Egyptian paintings, African Journal of Biotechnology 12(14) (2013) 1644.

[68] C. Leray, Waxes, Kirk-Othmer Encyclopedia of Chemical Technology (2006).

[69] C.F. Phleger, Buoyancy in marine fishes: Direct and indirect role of lipids, Am Zool 38(2) (1998) 321-330.

[70] D. Schlossman, Y. Shao, Natural ester, wax or oil treated pigment, process for production thereof, and cosmetic made therewith, Google Patents, 2014.

[71] M.J. Coffey, Ophthalmic compositions with wax esters, Google Patents, 2012.

[72] N.S. El Mogy, Medical effect of Jojoba oil in the treatment of anal diseases, Google Patents, 2004.

[73] P. Hepburn, P.T. Quinlan, K.W. Smith, J.V. Watts, R.P.J. van der Wielen, Wax ester compositions, Google Patents, 2000.

[74] M.I. Al-Widyan, M.A. Al-Muhtaseb, Experimental investigation of jojoba as a renewable energy source, Energ Convers Manage 51(8) (2010) 1702-1707.

[75] R. Kalscheuer, A. Steinbuchel, A novel bifunctional wax ester synthase/acyl-CoA : diacylglycerol acyltransferase mediates wax ester and triacylglycerol biosynthesis in Acinetobacter calcoaceticus ADP1, Journal of Biological Chemistry 278(10) (2003) 8075-8082.

[76] V.K. Bhatia, A. Chaudhry, G.A. Sivasankaran, R.P.S. Bisht, M. Kashyap, Modification of Jojoba Oil for Lubricant Formulations, J Am Oil Chem Soc 67(1) (1990) 1-7.

[77] S. Santala, E. Efimova, P. Koskinen, M.T. Karp, V. Santala, Rewiring the Wax Ester Production Pathway of Acinetobacter baylyi ADP1, Acs Synth Biol 3(3) (2014) 145-151.

[78] M. Trani, F. Ergan, G. Andre, Lipase-Catalyzed Production of Wax Esters, J Am Oil Chem Soc 68(1) (1991) 20-22.

[79] T. Tsujita, M. Sumiyoshi, H. Okuda, Wax ester-synthesizing activity of lipases, Lipids 34(11) (1999) 1159-1166.

[80] M. Heilmann, T. Iven, K. Ahmann, E. Hornung, S. Stymne, I. Feussner, Production of wax esters in plant seed oils by oleosomal cotargeting of biosynthetic enzymes, J Lipid Res 53(10) (2012) 2153-2161.

[81] G.M. Rodriguez, Y. Tashiro, S. Atsumi, Expanding ester biosynthesis in Escherichia coli, Nat Chem Biol 10(4) (2014) 259-+.

[82] A.H.C. Huang, R.A. Moreau, K.D.F. Liu, Development and Properties of a Wax Ester Hydrolase in Cotyledons of Jojoba Seedlings, Plant Physiol 61(3) (1978) 339-341.

[83] R.A. Moreau, A.H. Huang, [93] Enzymes of wax ester catabolism in jojoba, Methods in Enzymology 71 (1981) 804-813.

[84] M. Kalinowska, Z.A. Wojciechowski, Characterization of Wax-Ester Hydrolase from Roots of White Mustard (Sinapis-Alba L) Seedlings, Acta Biochim Pol 32(3) (1985) 259-269.

[85] M.C. Brahimihorn, M.L. Guglielmino, L.G. Sparrow, Wax Esterase-Activity in a Commercially Available Source of Lipase from Candida-Cylindracea, J Biotechnol 12(3-4) (1989) 299-306.

[86] J.S. Patton, J.C. Nevenzel, A.A. Benson, Specificity of Digestive Lipases in Hydrolysis of Wax Esters and Triglycerides Studied in Anchovy and Other Selected Fish, Lipids 10(10) (1975) 575-583.

[87] M. Kayama, M. Mankura, Y. Ikeda, Hydrolysis and Synthesis of Wax Esters by Different Systems of Carp Hepatopancreas Preparation, J Biochem-Tokyo 85(1) (1979) 1-6.

[88] A.A. Benson, J.S. Patton, C.E. Field, Wax Digestion in a Crown-of-Thorns Starfish, Comp Biochem Phys B 52(2) (1975) 339-340.

[89] M. Mankura, M. Kayama, S. Saito, Wax Ester Hydrolysis by Lipolytic Enzymes in Pyloric Ceca of Various Fishes, B Jpn Soc Sci Fish 50(12) (1984) 2127-2131.

[90] M.C. Brahimihorn, C.A. Mickelson, M.L. Guglielmino, A.M. Gaal, L.G. Sparrow, Identification of Lipolytic-Activity in a Multitrophic Population Grown in Wool Scour Effluent, J Ind Microbiol 8(1) (1991) 53-58.

[91] P. Bombelli, C.J. Howe, F. Bertocchini, Polyethylene bio-degradation by caterpillars of the wax moth Galleria mellonella, Curr Biol 27(8) (2017) R292-R293.

[92] G.M. Guebitz, A. Cavaco-Paulo, Enzymes go big: surface hydrolysis and functionalisation of synthetic polymers, Trends Biotechnol 26(1) (2008) 32-38.

[93] K. Meng, J. Li, Y.A. Cao, P.J. Shi, B. Wu, X.Y. Han, Y.G. Bai, N.F. Wu, B. Yao, Gene cloning and heterologous expression of a serine protease from Streptomyces fradiae var.k11, Can J Microbiol 53(2) (2007) 186-195.

[94] R.K. Aziz, D. Bartels, A.A. Best, M. DeJongh, T. Disz, R.A. Edwards, K. Formsma, S. Gerdes, E.M. Glass, M. Kubal, F. Meyer, G.J. Olsen, R. Olson, A.L. Osterman, R.A. Overbeek, L.K. McNeil, D. Paarmann, T. Paczian, B. Parrello, G.D. Pusch, C. Reich, R. Stevens, O. Vassieva, V. Vonstein, A. Wilke, O. Zagnitko, The RAST server: Rapid annotations using subsystems technology, Bmc Genomics 9 (2008).

[95] K.S. Ju, J.T. Gao, J.R. Doroghazi, K.K.A. Wang, C.J. Thibodeaux, S. Li, E. Metzger, J. Fudala, J. Su, J.K. Zhang, J. Lee, J.P. Cioni, B.S. Evans, R. Hirota, D.P. Labeda, W.A. van der Donk, W.W. Metcalf, Discovery of phosphonic acid natural products by mining the genomes of 10,000 actinomycetes, P Natl Acad Sci USA 112(39) (2015) 12175-12180.

[96] D.A. Benson, M. Cavanaugh, K. Clark, I. Karsch-Mizrachi, D.J. Lipman, J. Ostell, E.W. Sayers, GenBank, Nucleic Acids Res 41(D1) (2013) D36-D42.

[97] R.J. Simpson, Staining proteins in gels with coomassie blue, CSH protocols 2007 (2007) pdb. prot4719.

[98] J.M. Walker, The Bicinchoninic Acid (BCA) Assay for Protein Quantitation, Springer Protoc Hand (2009) 11-15.

[99] W. McKinney, pandas: a foundational Python library for data analysis and statistics, Python for High Performance and Scientific Computing (2011) 1-9.

[100] J.D. Hunter, Matplotlib: A 2D graphics environment, Comput Sci Eng 9(3) (2007) 90-95.

[101] K. Katoh, D.M. Standley, MAFFT multiple sequence alignment software version 7: improvements in performance and usability, Molecular biology and evolution 30(4) (2013) 772-780.

[102] E.F. Pettersen, T.D. Goddard, C.C. Huang, G.S. Couch, D.M. Greenblatt, E.C. Meng, T.E. Ferrin, UCSF chimera - A visualization system for exploratory research and analysis, J Comput Chem 25(13) (2004) 1605-1612.

[103] M. Fischer, J. Pleiss, The Lipase Engineering Database: a navigation and analysis tool for protein families, Nucleic Acids Res 31(1) (2003) 319-321.

[104] N. Lenfant, T. Hotelier, E. Velluet, Y. Bourne, P. Marchot, A. Chatonnet, ESTHER, the database of the alpha/beta-hydrolase fold superfamily of proteins: tools to explore diversity of functions, Nucleic Acids Res 41(D1) (2013) D423-D429.

[105] A. Drozdetskiy, C. Cole, J. Procter, G.J. Barton, JPred4: a protein secondary structure prediction server, Nucleic Acids Res 43(W1) (2015) W389-W394.

[106] S. Drouault, G. Corthier, S.D. Ehrlich, P. Renault, Expression of the Staphylococcus hyicus lipase in Lactococcus lactis, Appl Environ Microb 66(2) (2000) 588-598.

[107] J.T. Boock, D. Waraho-Zhmayev, D. Mizrachi, M.P. DeLisa, Beyond the cytoplasm of Escherichia coli: localizing recombinant proteins where you want them, Insoluble Proteins: Methods and Protocols (2015) 79-97.

[108] F.W. Studier, Protein production by auto-induction in high-density shaking cultures, Protein Expression and Purification 41(1) (2005) 207-234.

[109] D.S. Dheeman, G.T.M. Henehan, J.M. Frias, Purification and properties of Amycolatopsis mediterranei DSM 43304 lipase and its potential in flavour ester synthesis, Bioresource Technol 102(3) (2011) 3373-3379.

[110] J. Bussonbreysse, M. Farines, J. Soulier, Jojoba Wax - Its Esters and Some of Its Minor Components, J Am Oil Chem Soc 71(9) (1994) 999-1002.

[111] A. Tulloch, Beeswax: structure of the esters and their component hydroxy acids and diols, Chemistry and Physics of Lipids 6(3) (1971) 235-265.

[112] W. Riemenschneider, H. Bolt, Esters, Organic, Ulmann's Encyclopedia of Industrial Chemistry, 2005, pp. 8676-8694.

[113] A.S. Bogevik, D.R. Tocher, R. Waagbo, R.E. Olsen, Triacylglycerol-, wax ester- and sterol ester-hydrolases in midgut of Atlantic salmon (Salmo salar), Aquacult Nutr 14(1) (2008) 93-98.

[114] W. Heinen, H. De Vries, A combined micro-and semi-micro colorimetric determination of long-chain fatty acids from plant cutin, Archiv für Mikrobiologie 54(4) (1966) 339-349.

[115] P. Wang, L. Cui, Q. Wang, X. Fan, X. Zhao, J. Wu, Combined use of mild oxidation and cutinase/lipase pretreatments for enzymatic processing of wool fabrics, Engineering in Life Sciences 10(1) (2010) 19.

[116] A.S. Bogevik, Marine wax ester digestion in salmonid fish: a review, Aquaculture Research 42(11) (2011) 1577-1593.

[117] A.A. Benson, J.S. Patton, C.E. Field, Wax digestion in a Crown-of-Thorns starfish, Comp Biochem Physiol B 52(2) (1975) 339-40.

[118] W. Deshan, Z. Tieying, L. Zhengwen, Z. Linyuan, Effects of lipid in feathers on degrading feathers by B. licheniformis CP-16, Feed Industry 19 (2014) 007.

[119] H. Braberg, B.M. Webb, E. Tjioe, U. Pieper, A. Sali, M.S. Madhusudhan, SALIGN: a web server for alignment of multiple protein sequences and structures, Bioinformatics 28(15) (2012) 2072-2073.

[120] J. Pleiss, M. Fischer, M. Peiker, C. Thiele, R.D. Schmid, Lipase engineering database - Understanding and exploiting sequence-structure-function relationships, J Mol Catal B-Enzym 10(5) (2000) 491-508.

[121] A. Sali, T.L. Blundell, Comparative Protein Modeling by Satisfaction of Spatial Restraints, J Mol Biol 234(3) (1993) 779-815.

[122] W.L. DeLano, The PyMOL molecular graphics system, (2002).

[123] M. Benvenuti, S. Mangani, Crystallization of soluble proteins in vapor diffusion for x-ray crystallography, Nat Protoc 2(7) (2007) 1633-1651.

[124] S. Boivin, S. Kozak, R. Meijers, Optimization of protein purification and characterization using Thermofluor screens, Protein Expression and Purification 91(2) (2013) 192-206.

[125] S.P. Santos, T.M. Bandeiras, A.F. Pinto, M. Teixeira, M.A. Carrondo, C.V. Romao, Thermofluor-based optimization strategy for the stabilization and crystallization of Campylobacter jejuni desulforubrerythrin, Protein Expression and Purification 81(2) (2012) 193-200.

[126] S.P. Meisburger, A.B. Taylor, C.A. Khan, S.N. Zhang, P.F. Fitzpatrick, N. Ando, Domain Movements upon Activation of Phenylalanine Hydroxylase

Characterized by Crystallography and Chromatography-Coupled Small-Angle X-ray Scattering, J Am Chem Soc 138(20) (2016) 6506-6516.

[127] S.S. Nielsen, K.N. Toft, D. Snakenborg, M.G. Jeppesen, J.K. Jacobsen, B. Vestergaard, J.P. Kutter, L. Arleth, BioXTAS RAW, a software program for high-throughput automated small-angle X-ray scattering data reduction and preliminary analysis, J Appl Crystallogr 42 (2009) 959-964.

[128] M.V. Petoukhov, D. Franke, A.V. Shkumatov, G. Tria, A.G. Kikhney, M. Gajda, C. Gorba, H.D.T. Mertens, P.V. Konarev, D.I. Svergun, New developments in the ATSAS program package for small-angle scattering data analysis, J Appl Crystallogr 45 (2012) 342-350.

[129] Y. Zhang, J. Skolnick, The protein structure prediction problem could be solved using the current PDB library, P Natl Acad Sci USA 102(4) (2005) 1029-1034.

[130] L. Bordoli, F. Kiefer, K. Arnold, P. Benkert, J. Battey, T. Schwede, Protein structure homology modeling using SWISS-MODEL workspace, Nat Protoc 4(1) (2009) 1-13.

[131] M. Johnson, I. Zaretskaya, Y. Raytselis, Y. Merezhuk, S. McGinnis, T.L. Madden, NCBI BLAST: a better web interface, Nucleic Acids Res 36 (2008) W5-W9.

[132] H.M. Berman, J. Westbrook, Z. Feng, G. Gilliland, T.N. Bhat, H. Weissig, I.N. Shindyalov, P.E. Bourne, The Protein Data Bank, Nucleic Acids Res 28(1) (2000) 235-242.

[133] G. van Pouderoyen, T. Eggert, K.E. Jaeger, B.W. Dijkstra, The crystal structure of Bacillus subtilis lipase: A minimal alpha/beta hydrolase fold enzyme, J Mol Biol 309(1) (2001) 215-226.

[134] C.M. Jeffries, M.A. Graewert, C.E. Blanchet, D.B. Langley, A.E. Whitten, D.I. Svergun, Preparing monodisperse macromolecular samples for successful biological small-angle X-ray and neutron-scattering experiments, Nat Protoc 11(11) (2016) 2122-2153.

[135] S. Skou, R.E. Gillilan, N. Ando, Synchrotron-based small-angle X-ray scattering of proteins in solution, Nat Protoc 9(7) (2014) 1727-1739.

[136] D.A. Jacques, J. Trewhella, Small-angle scattering for structural biology-Expanding the frontier while avoiding the pitfalls, Protein Sci 19(4) (2010) 642-657.

[137] A.T. Tuukkanen, G.J. Kleywegt, D.I. Svergun, Resolution of ab initio shapes determined from small-angle scattering, Iucrj 3 (2016) 440-447.

[138] S. Ahmad, M.Z. Kamal, R. Sankaranarayanan, N.M. Rao, Thermostable Bacillus subtilis lipases: In vitro evolution and structural insight, J Mol Biol 381(2) (2008) 324-340.

[139] R.A. Gosavi, T.C. Mueser, C.A. Schall, Optimization of buffer solutions for protein crystallization, Acta Crystallogr D 64 (2008) 506-514.

[140] J. Jancarik, R. Pufan, C. Hong, S.H. Kim, R. Kim, Optimum solubility (OS) screening: an efficient method to optimize buffer conditions for homogeneity and crystallization of proteins, Acta Crystallogr D 60 (2004) 1670-1673.

[141] J.J. Lavinder, S.B. Hari, B.J. Sullivan, T.J. Magliery, High-Throughput Thermal Scanning: A General, Rapid Dye-Binding Thermal Shift Screen for Protein Engineering, J Am Chem Soc 131(11) (2009) 3794-+.

[142] L. Reinhard, H. Mayerhofer, A. Geerlof, J. Mueller-Dieckmann, M.S. Weiss, Optimization of protein buffer cocktails using Thermofluor, Acta Crystallogr F 69 (2013) 209-214.

[143] O. Kirk, T.V. Borchert, C.C. Fuglsang, Industrial enzyme applications, Curr Opin Biotech 13(4) (2002) 345-351.

[144] N.N. Gandhi, Applications of lipase, J Am Oil Chem Soc 74(6) (1997) 621-634.

[145] A.J. Poole, J.S. Church, M.G. Huson, Environmentally Sustainable Fibers from Regenerated Protein, Biomacromolecules 10(1) (2009) 1-8.

[146] L. Casas-Godoy, S. Duquesne, F. Bordes, G. Sandoval, A. Marty, Lipases: an overview, Lipases and Phospholipases: Methods and Protocols2012, pp. 3-30.

[147] S. Release, 1: Maestro, version 10.1, Schrödinger, LLC, New York, NY (2015).

[148] M.F. Sanner, Python: A programming language for software integration and development, J Mol Graph Model 17(1) (1999) 57-61.

[149] G.M. Morris, R. Huey, W. Lindstrom, M.F. Sanner, R.K. Belew, D.S. Goodsell, A.J. Olson, AutoDock4 and AutoDockTools4: Automated docking with selective receptor flexibility, J Comput Chem 30(16) (2009) 2785-2791.

[150] O. Trott, A.J. Olson, Software News and Update AutoDock Vina: Improving the Speed and Accuracy of Docking with a New Scoring Function, Efficient Optimization, and Multithreading, J Comput Chem 31(2) (2010) 455-461.

[151] W.L. DeLano, The PyMOL molecular graphics system, http://pymol. org (2002).

[152] R. Team, RStudio: integrated development for R, RStudio, Inc., Boston, MA URL http://www. rstudio. com (2015).

[153] A. Dror, E. Shemesh, N. Dayan, A. Fishman, Protein Engineering by Random Mutagenesis and Structure-Guided Consensus of Geobacillus stearothermophilus Lipase T6 for Enhanced Stability in Methanol, Appl Environ Microb 80(4) (2014) 1515-1527.

[154] E. Vazquez-Figueroa, J. Chaparro-Riggers, A.S. Bommarius, Development of a thermostable glucose dehydrogenase by a structure-guided consensus concept, Chembiochem 8(18) (2007) 2295-2301.

[155] G. Celniker, G. Nimrod, H. Ashkenazy, F. Glaser, E. Martz, I. Mayrose, T. Pupko, N. Ben-Tal, ConSurf: Using Evolutionary Data to Raise Testable Hypotheses about Protein Function, Isr J Chem 53(3-4) (2013) 199-206.

[156] Y.Y. Wei, L. Swenson, C. Castro, U. Derewenda, W. Minor, H. Arai, J. Aoki, K. Inoue, L. Servin-Gonzalez, Z.S. Derewenda, Structure of a microbial homologue of mammalian platelet-activating factor acetylhydrolases: Streptomyces exfoliatus lipase at 1.9 angstrom resolution, Struct Fold Des 6(4) (1998) 511-519.

[157] C. Martinez, P. Degeus, M. Lauwereys, G. Matthyssens, C. Cambillau, Fusarium-Solani Cutinase Is a Lipolytic Enzyme with a Catalytic Serine Accessible to Solvent, Nature 356(6370) (1992) 615-618.

[158] D.B. Wigley, A.R. Clarke, C.R. Dunn, D.A. Barstow, T. Atkinson, W.N. Chia, H. Muirhead, J.J. Holbrook, The Engineering of a More Thermally Stable Lactate-Dehydrogenase by Reduction of the Area of a Water-Accessible Hydrophobic Surface, Biochim Biophys Acta 916(1) (1987) 145-148.

[159] M.G. Lin, B.E. Chen, W.C. Liang, W.M. Chou, J.H. Chen, L.Y. Kuo, L.L. Lin, Site-Saturation Mutagenesis of Leucine 134 of Bacillus licheniformis Nucleotide

Exchange Factor GrpE Reveals the Importance of this Residue to the Co-chaperone Activity, Protein J 29(5) (2010) 365-372.

[160] M.T. Reetz, J.D. Carballeira, Iterative saturation mutagenesis (ISM) for rapid directed evolution of functional enzymes, Nat Protoc 2(4) (2007) 891-903.

[161] M.T. Reetz, L.W. Wang, M. Bocola, Directed evolution of enantioselective enzymes: Iterative cycles of CASTing for probing protein-sequence space, Angew Chem Int Edit 45(8) (2006) 1236-1241.

[162] K. Miyazaki, F.H. Arnold, Exploring nonnatural evolutionary pathways by saturation mutagenesis: Rapid improvement of protein function, J Mol Evol 49(6) (1999) 716-720.

[163] G.P. Horsman, A.M.F. Liu, E. Henke, U.T. Bornscheuer, R.J. Kazlauskas, Mutations in distant residues moderately increase the enantioselectivity of Pseudomonas fluorescens esterase towards methyl 3-bromo-2-methylpropanoate and ethyl 3-phenylbutyrate, Chem-Eur J 9(9) (2003) 1933-1939.

[164] M.T. Reetz, D. Kahakeaw, R. Lohmer, Addressing the numbers problem in directed evolution, Chembiochem 9(11) (2008) 1797-1804.